Informe final del proyecto: TEST DE UNIVERSALIDAD LEPTÓNICA Y EL MODELO DE PATI-SALAM

Proyecto trabajo Convocatoria Docente 2022

UNIVERSIDAD DE NARIÑO
FACULTAD DE CIENCIAS, DEPARTAMENTO DE FÍSICA
PASTO, NARIÑO
2022

Índice

1. Introducción **4**

1.1. Marco Teórico-Conceptual 4

1.2. Antecedentes 6

1.3. Objetivo general 6

2. Metodología **6**

3. Resultados **7**

3.1. Informe del artículo *Non-universal flipped trinification models with arbitrary* β [1] 7

3.1.1. Contenido fermiónico y cancelación de anomalías 7

3.1.2. Estructura de los modelos viables 7

3.1.3. Fenomenología del bosón Z' 8

3.1.4. Discusión 8

3.2. Informe sobre el artículo: *The Standard Model of Particle Physics as an effective theory from two non-universal U(1)'s* [2] 9

3.3. Informe sobre el artículo *Alternative 3-3-1 models with exotic electric charges* [3]. 11

3.4. Modelos 3-3-1 alternativos con cargas eléctricas exóticas 11

3.5. Informe sobre el artículo *A minimal axion model for mass matrices with five texture-zero* [4]. 12

3.6. Informe sobre tesis de pregrado *Test de universalidad leptónica y el modelo de Pati-Salam*, presentada por el estudiante Oscar David Rosero, bajo la dirección del profesor Eduardo Rojas. 14

4. Conclusiones generales **15**

5. Recomendaciones **16**

Informe del proyecto: Test de Universalidad leptónica y el modelo de Pati-Salam

RESUMEN

Presentamos el informe del proyecto de investigación: **Test de Universalidad Leptónica y el modelo de Pati-Salam**. Las mediciones experimentales de decaimientos semileptónicos del quark b se han desviado de las predicciones del modelo estándar (ME). Particularmente, las anomalías en los decaimientos del mesón B, que sugieren una violación en la universalidad leptónica, son quizás la evidencia directa más significativa de nueva física más allá del ME. El objeto de estudio del presente trabajo es un modelo realista que busca dar cuenta de dichas anomalías en modelos de unificación, como por ejemplo el de Pati-Salam, que es bien conocido en la literatura. **Es necesario aclarar, que aparte del dinero correspondiente a los rubros del proyecto y de las descargas por investigación, por concepto de este proyecto o del presente informe no recibí de la VIIS dinieros adicionales por bonificación.**

1. Introducción

1.1. Marco Teórico-Conceptual

Nuestro interés son las extensiones que permiten estudiar las anomalías experimentales que regularmente se presentan en el área. Nuestro programa nos permite poner a la Universidad de Nariño en contacto con desarrollos teóricos relacionados con la física del LHC *Large hadron collider*. Este experimento es el proyecto mas importante de física de altas energías en el mundo, y con nuestro grupo podemos contribuir en el análisis teórico de la física que se estudia en este laboratorio. Este trabajo permitió formar estudiantes a nivel de pregrado y publicar artículos de investigación y ponencias.

El modelo estándar (ME) proporciona una descripción de la naturaleza notablemente exitosa a nivel de partículas elementales y, hasta ahora, solo hay un puñado de indicaciones experimentales de desviaciones de sus predicciones. Quizás la evidencia directa más significativa de física más allá del ME son las anomalías recientemente observadas en las desintegraciones del mesón B [5, 6], que sugieren que la universalidad leptónica podría violarse. Suponiendo que esas anomalías no son el resultado de errores sistemáticos, se explican mejor con un leptoquark vectorial $(3,1)_{2/3}$ ó $(3,3)_{2/3}$ [1] [7, 8, 9]. Sin embargo, la construcción de modelos UV-completos – es decir, que sean viables en un marco general a energías arbitrariamente altas – que involucren tales partículas es un desafío, especialmente a la luz de las estrictas restricciones sobre la violación del sabor leptónico (VSL) de varias búsquedas experimentales.

Un intento por construir un modelo de leptoquark vectorial para las anomalías observadas en la razón $R_{K^{(*)}}$ entre los branchings de los modos de decaimiento semieptónico del mesón B con un kaón en el estado final, se realizó en [10], donde Assad, Fornal y Grinstein proponen que el leptoquark vectorial $(3,1)_{2/3}$, que explica las anomalías, podría ser el bosón gauge de una teoría como la de unificación de Pati-Salam [11]. La conclusión fue que el modelo mínimo basado en $\mathrm{SU}(4) \times \mathrm{SU}(2)_L \times \mathrm{SU}(2)_R$ no es capaz de hacer esto debido a límites estrictos en decaimientos raros del kaón y el mesón B [12, 13, 14, 15, 16, 17]. El problema subyacente en ese modelo surge de la interferencia entre corrientes leptónicas izquierdas y derechas que cambian de sabor. Fornal y sus colaboradores proponen una solución a esto: extendiendo el grupo gauge a $\mathrm{SU}(4)_L \times \mathrm{SU}(4)_R \times \mathrm{SU}(2)_L \times \mathrm{U}(1)'$ y rompiendo $\mathrm{SU}(4)_R$ a una escala alta, de modo que las corrientes leptónicas derechas con cambio de sabor se supriman.

Un planteamiento viable de tal modelo, que extiende el grupo gauge, es el tema del trabajo de Fornal, et.al. [18]. En él se demuestra que un leptoquark gauge de Pati-Salam tan liviano como 10 TeV puede explicar las anomalías $R_{K^{(*)}}$ y seguir siendo coherente con todos los límites experimentales sin introducir ninguna mezcla de quarks y leptones con nuevos fermiones. Discutiremos en detalle las limitaciones que surgen de las búsquedas de VSL y mostraremos que la ausencia de corrientes leptónicas derechas con cambio de sabor relaja los

[1] Esto es, leptoquarks vectoriales con hipercarga 2/3 y que son, triplete de SU(3) del color, singlete de $\mathrm{SU}(2)_L$, o triplete de SU(3) del color, triplete de $\mathrm{SU}(2)_L$ respectivamente.

límites considerablemente. Se espera que el modelo tenga observables que permitan distinguirlo en futuros colisionadores.

Varios modelos diferentes para las anomalías de sabor basados en la unificación de Pati-Salam han sido propuestos [19, 20, 21, 22, 23, 24, 25]. Esos modelos evaden las restricciones experimentales mezclando todos o un subconjunto de quarks y leptones del Modelo Estándar con nuevos fermiones vectoriales. Otros enfoques para explicar las anomalías del decaimiento del mesón B que involucran leptoquarks escalares o Z' en lugar de leptoquarks vectoriales también han sido propuestos (ver, por ejemplo, [26, 27, 28, 29, 30, 31, 32, 33]).

Durante la década pasada varias medidas de decaimientos semileptónicos del quark b (i.e. decaimientos en mesones livianos y pares de leptones en el estado final) se han desviado de las predicciones del ME. Tales discrepancias son conocidos colectivamente como "anomalías de sabor" y típicamente, exhiben variaciones a nivel de 2–3 σ de desviación estándar entre los resultados experimentales y las predicciones del ME. Un aspecto interesante de tales anomalías se debe al hecho de que todas ellas parecen apuntar a la presencia de violaciones en la universalidad de sabor leptónica (USL) en las interacciones que median los procesos. El año pasado, medidas de decaimientos raros $B^+ \to K^+\ell^+\ell^-$, con ℓ denotando un electrón o un muón han proporcionado evidencia adicional de rompimiento de la USL en decaimientos de quarks beauty en un sólo proceso, con una significancia de 3,1 σ, para una luminosidad acumulada de $9\,\mathrm{fb}^{-1}$ de datos de colisiones protón-protón recolectados en el LHCb [34].

El modelo de Pati-Salam es una teoría unificada basada en el grupo gauge $\mathrm{SU}(4) \times \mathrm{SU}(2)_\mathrm{L} \times \mathrm{SU}(2)_\mathrm{R}$ que extiende el ME y busca determinar el orden intrínseco subyacente en su aparente arbitrariedad. Varios modelos basados en la unificación de Pati-Salam han sido propuestos para intentar dar razón de las anomalías de sabor, algunos de ellos mezclan todos o un subconjunto de quarks y leptones del ME con nuevos fermiones vectoriales [19, 20, 21, 22, 23, 24, 25], mientras que otros introducen leptoquarks escalares o Z' en lugar de leptoquarks vectoriales [26, 27, 28, 29, 30, 31, 32, 33].

Addazi y sus colaboradores presentaron un artículo [35] que interpreta las anomalías en los decaimientos del bosón B en términos de una teoría gauge 331 extendida, agregando dos especies adicionales de leptones con cargas 331 exóticas. En contraste con los modelos 331 canónicos, las cargas gauge de las dos primeras familias de leptones difieren la una de la otra, permitiendo violación de la USL. La novedad de este artículo muestra que la temática del presente trabajo es un área de gran interés en la física actual y cuya investigación arroja resultados importantes que abren caminos a nuevas exploraciones en la frontera de nuestro actual conocimiento.

Un modelo de interés para explicar las anomalías de sabor es descrito en [18]. Tal modelo sigue el esquema de unificación de Pati-Salam, se construye a partir de las interacciones del leptoquark vectorial $(3, 1)_{2/3}$ y está basado en el grupo gauge $\mathrm{SU}(4)_\mathrm{L} \times \mathrm{SU}(4)_\mathrm{R} \times \mathrm{SU}(2)_\mathrm{L} \times \mathrm{U}(1)'$. El modelo provee una explicación realista de las anomalías de sabor sin introducir ninguna mezcla de quarks y leptones con nuevos fermiones. Este modelo es el objeto principal de estudio del presente trabajo.

1.2. Antecedentes

Los investigadores del grupo de investigación en Física de Altas Energías de la Universidad de Nariño han estudiado en trabajos pasados las anomalías de sabor. En particular el asesor del presente trabajo cuenta con varios trabajos publicados sobre el tema [36, 37, 38, 39], que acumulan más de 30 citas. En 2016 publicó, junto a sus colaboradores, un estudio sobre extensiones mínimas electrodébiles no universales al ME, un modelo que sólo requiere fermiones del modelo estándar y neutrinos derechos [39]. En un trabajo de 2019 analiza anomalías de la corriente cargada $b \to c\tau\overline{\nu}_\tau$ en un escenario general del bosón W'. En dicho trabajo no se considera ningún modelo específico de nueva física, sino que se ejecuta un análisis considerando todas las diferentes cargas quirales de los términos de interacción charm-bottom y $\tau - \nu_\tau$ con un bosón W' para explicar las anomalías [38]. En 2020 publicó un trabajo [36] donde analiza la contribución del bosón escalar a la anomalías de corriente cargada del mesón B, llevando a cabo un estudio fenomenológico del espacio de parámetros de los acoplamientos de Yukawa que acomoda las anomalías. Finalmente, en un artículo de 2021 el Doctor Rojas y sus colaboradores vuelven sobre las consecuencias de nueva física de las anomalías en mediciones de la corriente cargada $b \to c\tau\overline{\nu}_\tau$ y la corriente neutra $b\bar{b} \to \tau\overline{\tau}$, dentro de un modelo simplificado con bosones gauge masivos adicionales que se acoplan predominantemente a los leptones izquierdos de la tercera generación. Sus resultados apuntan a nuevos observables anómalos [37].

1.3. Objetivo general

Estudiar la violación de universalidad leptónica en experimentos de colisionadores y los posibles modelos de nueva física que pueden explicar estas anomalías.

2. Metodología

A continuación se presenta la metodología a seguir, la cual permitirá alcanzar los objetivos propuestos y llevar a cabo el análisis de las predicciones y establecimiento de cotas experimentales del modelo estudiado a lo largo del proyecto.

1. Revisión bibliográfica de la literatura.
2. Estudiar el artículo [18] detalladamente.
3. Análisis de χ^2 para ver si hay una discrepancia entre el experimento y el modelo teórico propuesto.
4. Escritura de los artículos. Transversal a todo el trabajo.

3. Resultados

Se publicaron cuatro artículos y se graduó el estudiante de pregrado Oscar Rosero con la tesis: Test de universalidad leptónica y el modelo de Pati-Salam https://sired.udenar.edu.co/7409/.

Un resumen de los resultados de los artículos y de la tesis de Oscar se presenta a continuación:

3.1. Informe del artículo *Non-universal flipped trinification models with arbitrary* β [1]

Se estudia una extensión del Modelo Estándar basada en la simetría de gauge

$$SU(3)_C \otimes SU(3)_L \otimes SU(3)_R \otimes U(1)_X, \tag{1}$$

la cual contiene como subgrupos tanto el modelo Left-Right simétrico como el modelo 3-3-1. Esta estructura permite construir realizaciones que heredan propiedades fenomenológicas atractivas de ambos marcos.

3.1.1. Contenido fermiónico y cancelación de anomalías

Dentro de esta simetría se derivan cuatro familias leptónicas y cuatro familias de quarks. Se analizan sus contribuciones a las anomalías gauge para un valor arbitrario del parámetro β, el cual determina la incrustación del generador electromagnético dentro de la combinación de los generadores diagonales de $SU(3)_L$, $SU(3)_R$ y $U(1)_X$.

Se calculan sistemáticamente las anomalías triangulares relevantes:

$$[SU(3)_L]^3, \quad [SU(3)_R]^3, \quad [SU(3)_C]^2U(1)_X, \quad [SU(3)_{L,R}]^2U(1)_X, \quad [U(1)_X]^3, \quad \text{y gravitacional-}U(1)_X. \tag{2}$$

Imponiendo la cancelación simultánea de todas las anomalías, se identifican los siguientes conjuntos libres de anomalías:

- Ocho combinaciones no universales con tres familias.
- Cuatro combinaciones no universales con dos familias.

3.1.2. Estructura de los modelos viables

Los conjuntos con tres familias son particularmente relevantes, pues constituyen extensiones realistas del Modelo Estándar. Estos modelos presentan:

- Universalidad en el sector leptónico.
- No universalidad en el sector de quarks.

La no universalidad quark es una característica típica de los modelos 3-3-1 y puede estar relacionada con la estructura generacional del modelo y la posible explicación del número de familias.

Por otra parte, los conjuntos con dos familias permiten la construcción de modelos con un número par de familias mayor o igual que cuatro, proporcionando flexibilidad adicional en escenarios extendidos.

3.1.3. Fenomenología del bosón Z'

La estructura gauge extendida predice la existencia de un bosón neutro adicional Z', asociado a la combinación ortogonal del grupo abeliano tras la ruptura espontánea de la simetría.

Se derivan límites experimentales provenientes de búsquedas en colisionadores para el caso particular

$$\beta = -\frac{1}{\sqrt{3}}, \tag{3}$$

considerando todas las posibles asignaciones de familias leptónicas y quark.

Los acoplamientos del Z' a los fermiones del Modelo Estándar dependen de un ángulo de mezcla libre θ, que parametriza la rotación entre los estados gauge neutros. Como consecuencia, las cotas experimentales sobre la masa del Z' presentan una fuerte dependencia funcional respecto a θ.

En particular, se observa que:

- Las restricciones del LHC no son universales.
- La masa mínima permitida del Z' varía significativamente con el valor de θ.
- Las cotas dependen de la estructura específica del sector fermiónico.

3.1.4. Discusión

El esquema

$$SU(3)_C \otimes SU(3)_L \otimes SU(3)_R \otimes U(1)_X \tag{4}$$

proporciona un marco unificado que integra naturalmente los modelos Left-Right y 3-3-1. La clasificación sistemática de configuraciones libres de anomalías demuestra la viabilidad de múltiples extensiones consistentes, incluyendo ocho realizaciones realistas con tres familias.

La fuerte dependencia de las restricciones experimentales respecto al ángulo de mezcla θ resalta la riqueza estructural del modelo y la necesidad de análisis fenomenológicos completos al confrontarlo con datos experimentales.

Este marco ofrece una plataforma prometedora para futuras investigaciones en unificación a altas energías, construcción del potencial escalar, física de neutrinos, materia oscura y posibles efectos de violación de CPT.

3.2. Informe sobre el artículo: *The Standard Model of Particle Physics as an effective theory from two non-universal U(1)'s* [2]

En el trabajo *The Standard Model of Particle Physics as an effective theory from two non-universal* $U(1)'s$ [2] se propone un marco en el cual el Modelo Estándar (SM) emerge como teoría efectiva de baja energía a partir de una extensión gauge basada en dos simetrías abelianas adicionales no universales,

$$\mathcal{G}_{\text{ext}} = SU(3)_C \otimes SU(2)_L \otimes U(1)_{X_1} \otimes U(1)_{X_2}. \tag{5}$$

En este escenario, las cargas bajo $U(1)_{X_1}$ y $U(1)_{X_2}$ son no universales en el espacio generacional, lo que permite reproducir de manera natural estructuras jerárquicas en el sector fermiónico tras la ruptura espontánea de la simetría.

Estructura gauge y generación del hipercarga

Un resultado central del trabajo es que el grupo abeliano del Modelo Estándar,

$$U(1)_Y, \tag{6}$$

surge como combinación lineal de las dos simetrías abelianas originales,

$$Y = a\, X_1 + b\, X_2, \tag{7}$$

donde los coeficientes a y b se determinan imponiendo la correcta normalización de cargas y la consistencia con los acoplamientos del SM. La combinación ortogonal corresponde a un nuevo bosón neutro pesado Z' cuya masa se genera a través del mecanismo de ruptura espontánea mediante campos escalares adicionales.

De este modo, el SM aparece como teoría efectiva tras integrar los grados de libertad pesados asociados a la ruptura de $U(1)_{X_1} \otimes U(1)_{X_2}$.

Cancelación de anomalías

Dado el carácter no universal de las cargas fermiónicas, el análisis de anomalías constituye un elemento fundamental del modelo. Se imponen las condiciones de cancelación de las anomalías triangulares relevantes:

$$[SU(3)_C]^2 U(1)_{X_i}, \quad [SU(2)_L]^2 U(1)_{X_i}, \quad [U(1)_{X_i}]^3, \quad U(1)_{X_i}\text{-gravitacional}, \tag{8}$$

así como las anomalías mixtas entre ambas simetrías abelianas.

El trabajo muestra que es posible asignar cargas no universales a las tres familias fermiónicas de manera consistente, sin necesidad de introducir contenido fermiónico exótico a baja energía. Las condiciones de cancelación restringen fuertemente las posibles asignaciones de carga, lo que dota al esquema de poder predictivo.

Estructura de Yukawa y jerarquías

Un aspecto relevante del modelo es que las simetrías $U(1)'$ no universales controlan la estructura de los términos de Yukawa efectivos. Tras la ruptura espontánea, los operadores efectivos generados pueden explicar de manera natural:

- Las jerarquías de masas fermiónicas.
- La estructura del mezclado CKM.
- La supresión de ciertos acoplamientos prohibidos a nivel renormalizable.

En este sentido, el marco actúa de forma análoga a un mecanismo de tipo Froggatt–Nielsen, pero embebido en una estructura gauge consistente y libre de anomalías.

Fenomenología del Z'

La combinación ortogonal al hipercarga da lugar a un bosón neutro adicional Z' con acoplamientos no universales a los fermiones del SM. Debido a la no universalidad generacional, pueden aparecer:

- Corrientes neutras con cambio de sabor a nivel árbol.
- Modificaciones en observables electrodébiles de precisión.
- Señales directas en búsquedas resonantes en colisionadores.

Las restricciones experimentales imponen cotas sobre la escala de ruptura de las simetrías abelianas y, por tanto, sobre la masa del Z' y sus acoplamientos efectivos.

Conclusiones

El trabajo demuestra que el Modelo Estándar puede interpretarse como teoría efectiva emergente de una estructura gauge más fundamental basada en dos $U(1)'$ no universales. La correcta reconstrucción del hipercarga, la cancelación consistente de anomalías y el control de la estructura de Yukawa muestran que el esquema es teóricamente viable y fenomenológicamente rico.

Este marco proporciona una plataforma coherente para abordar problemas abiertos del SM, tales como el origen de las jerarquías fermiónicas, posibles desviaciones en observables de sabor y la búsqueda de nueva física asociada a bosones Z' en experimentos actuales y futuros.

3.3. Informe sobre el artículo *Alternative 3-3-1 models with exotic electric charges* [3].

3.4. Modelos 3-3-1 alternativos con cargas eléctricas exóticas

En el trabajo *Alternative 3-3-1 models with exotic electric charges* [3] se realiza una clasificación sistemática de modelos basados en la simetría gauge

$$SU(3)_C \otimes SU(3)_L \otimes U(1)_X, \tag{9}$$

considerando el valor particular

$$\beta = \sqrt{3}, \tag{10}$$

el cual conduce a la aparición de fermiones con cargas eléctricas exóticas. El objetivo central del artículo es identificar todas las configuraciones fermiónicas consistentes con la cancelación de anomalías gauge y analizar sus implicaciones fenomenológicas.

Estructura de carga eléctrica

El operador de carga eléctrica en los modelos 3-3-1 está dado por

$$Q = T_3 + \beta T_8 + X, \tag{11}$$

donde T_3 y T_8 son los generadores diagonales de $SU(3)_L$ y X es la carga asociada al grupo $U(1)_X$. Para $\beta = \sqrt{3}$, algunas componentes de los tripletes y antitripletes de $SU(3)_L$ adquieren valores de carga no estándar, tales como $5/3$ o $-4/3$, dando lugar a quarks y leptones exóticos.

Cancelación de anomalías

El trabajo impone la cancelación simultánea de las anomalías gauge relevantes:

$$[SU(3)_L]^3, \quad [SU(3)_C]^2 U(1)_X, \quad [SU(3)_L]^2 U(1)_X, \quad [U(1)_X]^3, \quad \text{y gravitacional-}U(1)_X. \tag{12}$$

Debido a la naturaleza no universal de las asignaciones fermiónicas, la cancelación de anomalías ocurre entre distintas generaciones y no necesariamente dentro de cada familia individual. Esto permite una variedad de configuraciones consistentes, clasificadas sistemáticamente en [3].

No universalidad y corrientes de sabor

Una consecuencia directa de estas asignaciones no universales es la aparición de corrientes neutras con cambio de sabor (FCNC) a nivel árbol, mediadas por el nuevo bosón neutro Z'. Asimismo, pueden generarse procesos de violación de sabor leptónico cargado (CLFV), dependiendo de la estructura específica del sector leptónico.

Estas características hacen que los modelos sean altamente restrictivos desde el punto de vista fenomenológico, ya que deben satisfacer límites provenientes de mezcla de mesones neutros, decaimientos raros y observables de precisión electrodébil.

Restricciones experimentales

El modelo predice la existencia de nuevos bosones gauge, incluyendo un Z' y bosones cargados adicionales asociados a la ampliación de $SU(2)_L$ a $SU(3)_L$. Las búsquedas directas en el LHC imponen cotas inferiores sobre sus masas, particularmente a través de canales dileptónicos y dijet.

Las restricciones dependen de las asignaciones específicas de carga y del patrón de ruptura espontánea de la simetría. En ciertas configuraciones, los acoplamientos pueden suprimirse parcialmente, permitiendo regiones del espacio de parámetros compatibles con los datos actuales.

Conclusión

El análisis presentado en [3] demuestra que los modelos 3-3-1 con $\beta = \sqrt{3}$ admiten múltiples configuraciones libres de anomalías que incorporan fermiones con cargas eléctricas exóticas. La clasificación sistemática realizada proporciona un marco general para estudiar extensiones del Modelo Estándar con no universalidad generacional y rica fenomenología en el sector de sabor y en búsquedas de nueva física en colisionadores.

3.5. Informe sobre el artículo *A minimal axion model for mass matrices with five texture-zero* [4].

En el trabajo *A minimal axion model for mass matrices with five texture-zero* [4] se propone un esquema compacto que combina un **modelo axiónico mínimo** con estructuras de textura específicas en las matrices de masa fermiónicas. La motivación principal es enlazar la física del axión —como solución a la violación de CP en el sector fuerte— con patrones predictivos en los parámetros de mezcla y masas de quarks y leptones.

Estructura del modelo y simetrías

El modelo introducido en [4] se basa en la extensión del contenido del Modelo Estándar mediante:

- Un campo escalar complejo singlete que da lugar al **axión** tras la ruptura espontánea de una simetría global $U(1)_{\mathrm{PQ}}$ (Peccei–Quinn).
- Asignaciones de cargas bajo $U(1)_{\mathrm{PQ}}$ no triviales para los fermiones del Modelo Estándar.

La simetría $U(1)_{\mathrm{PQ}}$ es global y está diseñada de forma tal que el axión resultante se acopla débilmente a la materia normal, cumpliendo con las características de un **axión invisible**.

Texturas con cinco ceros en matrices de masa

Un elemento central del artículo es la **implementación de texturas con cinco ceros** en las matrices de masa fermiónicas. Se considera que estructuras con ceros posicionados de manera estratégica en la matriz pueden generar relaciones entre masas y ángulos de mezcla que reproduzcan de manera eficiente los datos experimentales.

En particular:

- Se asume una configuración de ceros para las matrices de masa de quarks y leptones que deja un número mínimo de parámetros independientes.
- Esto conduce a predicciones correlacionadas entre masas y elementos de las matrices CKM (quarks) y PMNS (neutrinos).

El análisis demuestra que **cinco ceros** es el número mínimo que permite compatibilidad con los datos actuales sin introducir grados de libertad adicionales más allá del axión.

Cancelación de anomalías y consistencia gauge

Dado que la simetría $U(1)_{\mathrm{PQ}}$ es global, el modelo evita la introducción de nuevas anomalías gauge. Sin embargo, para que la estructura de textura sea consistente con interacciones renormalizables y con la ruptura espontánea de $U(1)_{\mathrm{PQ}}$, se deben satisfacer varias restricciones:

- La ausencia de términos que rompan explícitamente $U(1)_{\mathrm{PQ}}$ a orden bajo,
- La correcta generación de términos de Yukawa efectivos después de la rotura de simetría.

El artículo demuestra que estas condiciones se pueden satisfacer de forma coherente sin necesidad de introducir fermiones exóticos adicionales ni campos vectoriales extra.

Predicciones y correlaciones

Al imponer las texturas con cinco ceros, el modelo genera predicciones concretas:

- Relaciones entre elementos de la matriz CKM y las masas de quarks cargados,
- Correlaciones entre parámetros de mezcla en el sector leptónico y las jerarquías de masa de neutrinos,
- Restricciones sobre fases CP débiles y fuertes como consecuencia del patrón de texturas.

Estas predicciones pueden confrontarse con datos experimentales actuales y futuros, constituyendo una prueba directa de la estructura propuesta.

Fenomenología del axión

El axión resultante de este modelo es del tipo "invisible", con acoplamientos suprimidos a fotones y materia normal. El trabajo estima:

- La escala de ruptura de $U(1)_{\mathrm{PQ}}$ necesaria para cumplir con límites astrofísicos y cosmológicos,
- La relación entre esta escala y los parámetros de textura que afectan las matrices de masa.

La compatibilidad con límites actuales de búsquedas de axiones, lentes gravitacionales y observaciones astrofísicas se discute en detalle, mostrando que el modelo puede ser consistente con restricciones vigentes.

Conclusiones

El artículo [4] presenta un esquema minimalista que:

1. Integra de forma coherente un axión invisible mediante una simetría Peccei–Quinn global,
2. Reproduce patrones predictivos en las matrices de masa fermiónicas mediante cinco ceros de textura,
3. Evita la introducción de nuevos grados de libertad exóticos innecesarios,
4. Confronta con éxito relaciones teóricas con datos experimentales actuales en sectores quark y leptón.

Este enfoque proporciona un marco compacto y predictivo para explorar relaciones entre la física del axión y las texturas de masas, abriendo la posibilidad de probar el modelo mediante observables de mezcla y límites de búsqueda de axiones.

3.6. Informe sobre tesis de pregrado *Test de universalidad leptónica y el modelo de Pati-Salam*, presentada por el estudiante Oscar David Rosero, bajo la dirección del profesor Eduardo Rojas.

En la tesis de pregrado de Oscar David Rosero se tomo como punto de partida el hecho de que las mediciones experimentales de los decaimientos semileptónicos del quark b han mostrado desviaciones con respecto a las predicciones del Modelo Estándar (ME). En particular, las anomalías observadas en los decaimientos de mesones B, que sugieren una posible violación de la universalidad leptónica, constituyen quizá la evidencia directa más significativa de nueva física más allá del ME hasta la fecha.

El trabajo de grado de Oscar consistió en estudiar un modelo realista capaz de dar cuenta de dichas anomalías, basado en una versión modificada del conocido modelo de unificación de Pati–Salam. En este marco, algunos de los bosones mediadores del modelo corresponden a leptoquarks vectoriales en la representación $(\mathbf{3},\mathbf{1})_{2/3}$, y la teoría se construye a partir del grupo gauge

$$SU(4)_L \times SU(4)_R \times SU(2)_L \times U(1)\,. \tag{13}$$

En el mencionado trabajo se hizo un análisis detallado del modelo, poniendo énfasis en los métodos y técnicas empleados en la construcción de modelos de nueva física en teorías de partículas. Asimismo, se lleva a cabo un estudio fenomenológico con el fin de determinar cotas sobre los acoplamientos del leptoquark a partir de decaimientos semileptónicos, utilizando como pseudo-observables los coeficientes de Wilson C_9 y C_{10}.

El trabajo de grado de Oscar fue reconocido con mención meritoria.

Parte de la continuación de este trabajo se aplicó en las publicaciónes que mencionamos en la sección de resultados. En particular, en dos artículos analizamos grupos de unificación, en *Alternative 3-3-1 models with exotic electric charges [3]* se analizó el grupo $SU(3)_C \otimes SU(3)_L \otimes U(1)_X$, y en artículo *Non-universal flipped trinification models with arbitrary* β [1], se estudió $SU(3)_C \otimes SU(3)_L \otimes SU(3)_R \otimes U(1)_X$. Estos grupos de simetría pueden ser el marco natural para algunos modelos no universales y pueden ser útiles para estudiar anomalías de sabor. Un modelo, que auque no se considera de unificación, también es no universal fue el publicado en el artículo *The Standard Model of Particle Physics as an effective theory from two non-universal U(1)'s* [2]. El boson Z' de este modelo acopla muy débilmente a las dos promeras familias de tal forma que puede evadir restricciones de colliders, sabor y de restricciones electrodébiles, tal como se mostró en la publicación.

Finalmente un trabajo muy importante sobre física del sabor es *A minimal axion model for mass matrices with five texture-zero [4]* en el que se propone reducir el problema del sabor a la elección de los valores esperados en el vacío de los dobletes de Higgs del modelo (VEVs *Vacuum expectatión values*). En este modelo estudiamos las corrientes neutras con cambio del sabor inducidas por un axión saboreado y obtuvimos las restricciones sobre el acoplamiento axión foton de nuestro modelo.

Podemos concluir que como resultado de este proyecto, la línea de física del sabor de nuestro departamento se ha fortalecido.

4. Conclusiones generales

Hemos logrado consolidar un proyecto sobre el problema del sabor en física de partículas en nuestro departamento. En este momento el estudiante de pregrado se encuentra haciendo una maestría en física de altas energías a nivel experimental en Suecia, mostrando la relevancia de contar con proyectos conectados con la física que se está haciendo en este momento en el mundo. Es muy importante resaltar que hubo varias publicaciones por encima de la exigencia mínima con la que nos habíamos comprometido, mostrando la madurez de nuestra línea de investigación.

5. Recomendaciones

Todos los objetivos del proyecto se cumplieron. Se graduo el estudiante de pregrado, hubo varias publicaciones asociadas al proyecto y varias ponencias en eventos internacionales. La recomendación es darle continuidad a este proyecto, para continuar fortaleciendo esta líea de investigación en el departamento de física de la universidad de Nariño.

Referencias

[1] R. H. Benavides, Y. Giraldo, and E. Rojas, "Non-universal flipped trinification models with arbitrary β," *Eur. Phys. J. C*, vol. 85, no. 8, p. 897, 2025.

[2] R. H. Benavides, Y. Giraldo, W. A. Ponce, O. Rodríguez, and E. Rojas, "The standard model of particle physics as an effective theory from two non-universal U (1)'s," *J. Phys. G*, vol. 52, no. 5, p. 055002, 2025.

[3] E. Suarez, R. H. Benavides, Y. Giraldo, W. A. Ponce, and E. Rojas, "Alternative 3-3-1 models with exotic electric charges," *J. Phys. G*, vol. 51, no. 3, p. 035004, 2024.

[4] Y. Giraldo, R. Martínez, E. Rojas, and J. C. Salazar, "A minimal axion model for mass matrices with five texture-zeros," *Eur. Phys. J. C*, vol. 83, no. 7, p. 638, 2023.

[5] R. Aaij *et al.*, "Test of lepton universality using $B^+ \to K^+\ell^+\ell^-$ decays," *Phys. Rev. Lett.*, vol. 113, p. 151601, 2014.

[6] R. Aaij *et al.*, "Test of lepton universality with $B^0 \to K^{*0}\ell^+\ell^-$ decays," *JHEP*, vol. 08, p. 055, 2017.

[7] R. Alonso, B. Grinstein, and J. Martin Camalich, "Lepton universality violation and lepton flavor conservation in B-meson decays," *JHEP*, vol. 10, p. 184, 2015.

[8] R. Alonso, B. Grinstein, and J. Martin Camalich, "$SU(2) \times U(1)$ gauge invariance and the shape of new physics in rare B decays," *Phys. Rev. Lett.*, vol. 113, p. 241802, 2014.

[9] N. Kosnik, "Model independent constraints on leptoquarks from $b \to s\ell^+\ell^-$ processes," *Phys. Rev. D*, vol. 86, p. 055004, 2012.

[10] N. Assad, B. Fornal, and B. Grinstein, "Baryon Number and Lepton Universality Violation in Leptoquark and Diquark Models," *Phys. Lett. B*, vol. 777, pp. 324–331, 2018.

[11] J. C. Pati and A. Salam, "Lepton Number as the Fourth Color," *Phys. Rev. D*, vol. 10, pp. 275–289, 1974. [Erratum: Phys.Rev.D 11, 703–703 (1975)].

[12] G. Valencia and S. Willenbrock, "Quark - lepton unification and rare meson decays," *Phys. Rev. D*, vol. 50, pp. 6843–6848, 1994.

[13] A. D. Smirnov, "Mass limits for scalar and gauge leptoquarks from K(L)0 —> e-+ mu+-, B0 —> e-+ tau+- decays," *Mod. Phys. Lett. A*, vol. 22, pp. 2353–2363, 2007.

[14] A. D. Smirnov, "Contributions of gauge and scalar leptoquarks to K0(L) —> l(i)+ l(j)- and B0 —> l(i)+ l(j)- decay and constraints on leptoquark masses from the decays K0(L) —> e-+ mu+- and B0 —> e-+ tau+-," *Phys. Atom. Nucl.*, vol. 71, pp. 1470–1480, 2008.

[15] M. Carpentier and S. Davidson, "Constraints on two-lepton, two quark operators," *Eur. Phys. J. C*, vol. 70, pp. 1071–1090, 2010.

[16] A. V. Kuznetsov, N. V. Mikheev, and A. V. Serghienko, "The third type of fermion mixing in the lepton and quark interactions with leptoquarks," *Int. J. Mod. Phys. A*, vol. 27, p. 1250062, 2012.

[17] A. D. Smirnov, "Vector leptoquark mass limits and branching ratios of $K_L^0, B^0, B_s \to l_i^+ l_j^-$ decays with account of fermion mixing in leptoquark currents," *Mod. Phys. Lett. A*, vol. 33, p. 1850019, 2018.

[18] B. Fornal, S. A. Gadam, and B. Grinstein, "Left-Right SU(4) Vector Leptoquark Model for Flavor Anomalies," *Phys. Rev. D*, vol. 99, no. 5, p. 055025, 2019.

[19] L. Di Luzio, A. Greljo, and M. Nardecchia, "Gauge leptoquark as the origin of B-physics anomalies," *Phys. Rev. D*, vol. 96, no. 11, p. 115011, 2017.

[20] L. Calibbi, A. Crivellin, and T. Li, "Model of vector leptoquarks in view of the B-physics anomalies," *Phys. Rev. D*, vol. 98, no. 11, p. 115002, 2018.

[21] M. Bordone, C. Cornella, J. Fuentes-Martin, and G. Isidori, "A three-site gauge model for flavor hierarchies and flavor anomalies," *Phys. Lett. B*, vol. 779, pp. 317–323, 2018.

[22] R. Barbieri and A. Tesi, "B-decay anomalies in Pati-Salam SU(4)," *Eur. Phys. J. C*, vol. 78, no. 3, p. 193, 2018.

[23] M. Blanke and A. Crivellin, "B Meson Anomalies in a Pati-Salam Model within the Randall-Sundrum Background," *Phys. Rev. Lett.*, vol. 121, no. 1, p. 011801, 2018.

[24] A. Greljo and B. A. Stefanek, "Third family quark–lepton unification at the TeV scale," *Phys. Lett. B*, vol. 782, pp. 131–138, 2018.

[25] S. Balaji, R. Foot, and M. A. Schmidt, "Chiral SU(4) explanation of the $b \to s$ anomalies," *Phys. Rev. D*, vol. 99, no. 1, p. 015029, 2019.

[26] D. Marzocca, "Addressing the B-physics anomalies in a fundamental Composite Higgs Model," *JHEP*, vol. 07, p. 121, 2018.

[27] U. Aydemir, D. Minic, C. Sun, and T. Takeuchi, "B-decay anomalies and scalar leptoquarks in unified Pati-Salam models from noncommutative geometry," *JHEP*, vol. 09, p. 117, 2018.

[28] D. Bečirević, I. Doršner, S. Fajfer, N. Košnik, D. A. Faroughy, and O. Sumensari, "Scalar leptoquarks from grand unified theories to accommodate the B-physics anomalies," *Phys. Rev. D*, vol. 98, no. 5, p. 055003, 2018.

[29] D. Guadagnoli, M. Reboud, and O. Sumensari, "A gauged horizontal $SU(2)$ symmetry and $R_{K^{(*)}}$," *JHEP*, vol. 11, p. 163, 2018.

[30] S.-P. Li, X.-Q. Li, Y.-D. Yang, and X. Zhang, "$R_{D^{(*)}}, R_{K^{(*)}}$ and neutrino mass in the 2HDM-III with right-handed neutrinos," *JHEP*, vol. 09, p. 149, 2018.

[31] T. Faber, M. Hudec, M. Malinský, P. Meinzinger, W. Porod, and F. Staub, "A unified leptoquark model confronted with lepton non-universality in B-meson decays," *Phys. Lett. B*, vol. 787, pp. 159–166, 2018.

[32] J. Heeck and D. Teresi, "Pati-Salam explanations of the B-meson anomalies," *JHEP*, vol. 12, p. 103, 2018.

[33] B. C. Allanach and J. Davighi, "Third family hypercharge model for $R_{K^{(*)}}$ and aspects of the fermion mass problem," *JHEP*, vol. 12, p. 075, 2018.

[34] R. Aaij *et al.*, "Test of lepton universality in beauty-quark decays," 3 2021.

[35] A. Addazi, G. Ricciardi, S. Scarlatella, R. Srivastava, and J. W. F. Valle, "An old theme for new data: Interpreting recent B anomaly data within an extended 331 gauge theory," 1 2022.

[36] J. Cardozo, J. H. Muñoz, N. Quintero, and E. Rojas, "Analysing the charged scalar boson contribution to the charged-current B meson anomalies," *J. Phys. G*, vol. 48, no. 3, p. 035001, 2021.

[37] C. H. García-Duque, J. H. Muñoz, N. Quintero, and E. Rojas, "Extra gauge bosons and lepton flavor universality violation in Υ and B meson decays," *Phys. Rev. D*, vol. 103, no. 7, p. 073003, 2021.

[38] J. D. Gómez, N. Quintero, and E. Rojas, "Charged current $b \to c\tau\bar{\nu}_\tau$ anomalies in a general W' boson scenario," *Phys. Rev. D*, vol. 100, no. 9, p. 093003, 2019.

[39] R. Benavides, L. A. Muñoz, W. A. Ponce, O. Rodríguez, and E. Rojas, "Minimal nonuniversal electroweak extensions of the standard model: A chiral multiparameter solution," *Phys. Rev. D*, vol. 95, no. 11, p. 115018, 2017.

Eur. Phys. J. C (2025) 85:897
https://doi.org/10.1140/epjc/s10052-025-14633-9

THE EUROPEAN PHYSICAL JOURNAL C

Regular Article -Theoretical Physics

Non-universal flipped trinification models with arbitrary β

Richard H. Benavides[1,a], **Yithsbey Giraldo**[2,b], **Eduardo Rojas**[2,c]

[1] Facultad de Ciencias Exactas y Aplicadas, Institución Universitaria ITM, Calle 73 N 76 A -354 Vía al Volador, Medellín, Colombia
[2] Departamento de Física, Universidad de Nariño, Calle 18 Carrera 50, A.A. 1175, San Juan de Pasto, Colombia

Received: 25 June 2025 / Accepted: 9 August 2025

Abstract We explore the recently proposed gauge symmetry $SU(3)_C \otimes SU(3)_L \otimes SU(3)_R \otimes U(1)_X$, which naturally embeds both the Left-Right symmetric model and the 3-3-1 model as subgroups. Within this unified framework, we propose four families of leptons and quarks. A detailed analysis of their contributions to gauge anomaly cancellation is carried out for a general value of the parameter β. From this analysis, eight non-universal anomaly-free three-family models and four non-universal two-family anomaly free sets were identified. The three-family models offer realistic extensions of the Standard Model, retaining several appealing features of the 3-3-1 models, while the two-family sets provide flexibility for constructing models with even numbers of families. We also report LHC bounds on the Z' mass for the particular case $\beta = -1/\sqrt{3}$, considering all possible combinations of lepton and quark families. These limits exhibit a strong dependence on the mixing parameter θ, which enters the couplings of Standard Model fermions to the Z' boson.

1 Introduction

The Standard Model (SM) does not fully explain why electric charge is quantized, that is, why all observed charges are integer multiples of $e/3$. Anomaly cancellation imposes certain restrictions on hypercharges, but these are not sufficient to uniquely determine the SM charges, even adding right-handed neutrinos [1,2]. So, the standard lore says that it may be necessary to embed the SM into a larger symmetry group to address this issue [3,4].

An extension that has been studied recently in the literature is flipped-trinification (FT) [5–9], which is based on the $SU(3)_C \otimes SU(3)_L \otimes SU(3)_R \otimes U(1)_X$ (3-3-3-1) gauge group; this class of models can explain the number of families of the Standard Model as 3-3-1 models do [10–14], and the origin of parity violation as it happens in the Left-Right models (LR) [3,15]. This class of models is also suitable for explaining dark-matter stability.

The left-right symmetric models are among the simplest extensions of the SM. This class of models represents an ideal theoretical framework for understanding the origin of parity violation in gauge theories, neutrino masses, and dark matter. Similarly, 3-3-1 models have been used for many years to explain neutrino masses and dark matter. Additionally, they can provide a relation between the number of families and the number of colors [12]. FT manages to integrate in a single model the advantages of the LR and the 3-3-1 models, creating a theoretical framework that includes two of the most motivated extensions of the SM.

By a suitable choice of the Higgs sector, it is possible to break the trinification gauge group to $SU(3)_C \otimes SU(2)_L \otimes U(1)_{L8+R8} \otimes U(1)_R \otimes U(1)_X$ [1] We provide a classification of the viable models that can be derived from this symmetry, subject to certain assumptions.

In Sect. 2, we construct all possible families for models based on this symmetry and calculate their contribution to the anomalies. From these results, we obtain several non-universal 3-3-3-1 models. In Sect. 4 we calculate the Z' electroweak charges. In Sect. 5, we compute and summarize the collider constraints for all combinations of quark and lepton families considered in our analysis.

[a] e-mail: richardbenavides@itm.edu.co
[b] e-mail: yithsbey@gmail.com (corresponding author)
[c] e-mail: eduro4000@gmail.com

[1] Where the generator of $U(1)_{L8+R8}$ in dimension 3 is given by $\frac{1}{2}\left(\lambda^8(f_L) + \lambda^8(f_R)\right)$, with $\lambda^a(f)$ is the representation of the $SU(3)$ group in the fermions f.

Published online: 24 August 2025

2 Quark and lepton families

In this section, we construct sets of fermions that include at least one SM quark or lepton family. These sets also contain exotic particles, as will be discussed below. Each family must have at least one quark and one lepton triplet to accommodate a left quark doublet and a lepton doublet from the Standard Model. It is also necessary to have $SU(2)_L$ singlets to accommodate the right-handed components of the charged particles. In $SU(3)_L$ for each 3_L triplet, there exists the conjugate representation 3_L^*, and in both triplets it is possible to accommodate the left doublets of the Standard Model. Due to $SU(3)_R$, there also exist right 3_R triplets and their respective conjugate representations 3_R^*, so that it is possible to put the right-handed singlets of the Standard Model in these triplets. The charge operator is given by

$$Q = T_{3L} + Y = T_{3L} + T_{3R} + \beta\,(T_{8L} + T_{8R}) + X\mathbf{1}, \qquad (1)$$

where $T_{aL,R} = \frac{1}{2}\lambda^a_{L,R}$ with $\lambda^a_{L,R} = \lambda^a P_{L,R}$, such that the λ^a's are the Gell–Mann matrices. By treating the charge q of the third component of the lepton triplet as a free parameter, we determine the values of β and X from the relation $Q = \mathrm{diag}(0, -1, q)$, such that $X = \frac{q-1}{3}$ and

$$\beta = -\frac{1+2q}{\sqrt{3}}.$$

It is important to use the same value of β for all fermion representations to maintain a unique adjoint representation. In our case, this is not an issue, since the electric charge is given by $q = -\frac{1+\sqrt{3}\beta}{2}$. In similar way we can obtain the charges of the conjugated representations from $Q^{\mathrm{conj}}_{L,R} = -\frac{1}{2}\lambda^3_{L,R} - \frac{\beta}{2}\lambda^8_{L,R} + X_{L,R}\mathbf{1}$. For the lepton triplet, with $X = -\frac{q+2}{3}$, we have $Q^{\mathrm{conj}}_{L,R} = \mathrm{diag}(-1, 0, -1-q)$. Similar results hold for the quark triplet with $X = \frac{q+1}{3}$, $Q_{L,R} = \mathrm{diag}(2/3, -1/3, q + \frac{2}{3})$ and $Q^{\mathrm{conj}}_{L,R} = \mathrm{diag}(-1/3, +2/3, -\frac{1}{3} - q)$ with $X = -\frac{q}{3}$.

From these considerations, we derive four viable families of S_{Qi} quarks and four of S_{Li} leptons, which are listed below.

2.1 Families in the lepton sector

The first generation of leptons is assigned to the $\mathbf{3}_L$ and $\mathbf{3}_R$ representations. Owing to the imposed left-right (L-R) symmetry, the $U(1)_X$ charge is identical for both representations.

$$S_{L1} = \begin{pmatrix} \nu_L \\ e_L \\ E^q_L \end{pmatrix}, \begin{pmatrix} \nu_R \\ e_R \\ E^q_R \end{pmatrix}.$$

In $S_{L1} = \mathbf{3}_L \cup \mathbf{3}_R$, the left-handed SM lepton doublets are embedded in $(1, 3, 1, \frac{q-1}{3})$ and the right-handed SM lepton components in $(1, 1, 3, \frac{q-1}{3})$.

$$S_{L2} = \begin{pmatrix} \nu_L \\ e_L \\ E^q_L \end{pmatrix}, \begin{pmatrix} e_R \\ \nu_R \\ E^{-q-1}_R \end{pmatrix}, E^q_R, E^{-q-1}_L.$$

For $S_{L2} = \mathbf{3}_L \cup \mathbf{3}^*_R \cup \mathbf{1}_R \cup \mathbf{1}_L$, the SM left-handed lepton doublets are embedded in $(1, 3, 1, \frac{q-1}{3})$, the right-handed leptons are in $(1, 1, 3^*, -\frac{q+2}{3})$, and the chirality flipped components of the third element of the triplets in $(1, 1, 1, q)$ and $(1, 1, 1, -q-1)$, respectively.
For $q = -\frac{1}{2}$ (which is equivalent to $\beta = 0$), the third components of the left- and right-handed triplets have the same electric charge, eliminating the need to introduce singlets.

$$S_{L3} = \begin{pmatrix} e_L \\ \nu_L \\ E^{-q-1}_L \end{pmatrix}, \quad \begin{pmatrix} \nu_R \\ e_R \\ E^q_R \end{pmatrix}, \quad E^{-q-1}_R, \quad E^q_L.$$

For $S_{L3} = \mathbf{3}^*_L \cup \mathbf{3}_R \cup \mathbf{1}_R \cup \mathbf{1}_L$, the SM left-handed lepton doublets are embedded in $(1, 3^*, 1, -\frac{q+2}{3})$, the right-handed lepton in $(1, 1, 3, \frac{q-1}{3})$ and the chirality flipped components of the third element of the triplets in $(1, 1, 1, -q-1)$ and $(1, 1, 1, q)$ with $q \neq -\frac{1}{2}$.

$$S_{L4} = \begin{pmatrix} e_L \\ \nu_L \\ E^{-q-1}_L \end{pmatrix}, \begin{pmatrix} e_R \\ \nu_R \\ E^{-q-1}_R \end{pmatrix}.$$

For $S_{L4} = \mathbf{3}^*_L \cup \mathbf{3}^*_R$, the SM left-handed lepton doublets are embedded in $(1, 3^*, 1, -\frac{q+2}{3})$ and the right-handed leptons in $(1, 1, 3^*, -\frac{q+2}{3})$.

2.2 Families in the quark sector

Proceeding in the same way as in the case of leptons, we have:

$$S_{Q1} = \begin{pmatrix} u_L \\ d_L \\ Q^{q+2/3}_L \end{pmatrix}, \quad \begin{pmatrix} u_R \\ d_R \\ Q^{q+2/3}_R \end{pmatrix}.$$

For $S_{Q1} = \mathbf{3}_L \cup \mathbf{3}_R$, the SM left-handed quark doublets are embedded in $(3, 3, 1, \frac{q+1}{3})$ and the right-handed quarks in $(3, 1, 3, \frac{q+1}{3})$.

$$S_{Q2} = \begin{pmatrix} u_L \\ d_L \\ Q^{q+2/3}_L \end{pmatrix}, \begin{pmatrix} d_R \\ u_R \\ Q^{-q-1/3}_R \end{pmatrix}, Q^{q+2/3}_R, Q^{-q-1/3}_L.$$

For $S_{Q2} = \mathbf{3}_L \cup \mathbf{3}^*_R \cup \mathbf{1}_R \cup \mathbf{1}_L$, the SM left-handed quark doublets are embedded in $(3, 3, 1, \frac{q+1}{3})$, the right-handed quarks in $(3, 1, 3^*, -\frac{q}{3})$ and the chirally flipped third components of the quark triplets in $(3, 1, 1, q + 2/3)$, $(3, 1, 1, -q - 1/3)$, with $q \neq -\frac{1}{2}$.

$$S_{Q3} = \begin{pmatrix} d_L \\ u_L \\ Q^{-q-1/3}_L \end{pmatrix}, \begin{pmatrix} u_R \\ d_R \\ Q^{q+2/3}_R \end{pmatrix}, Q^{-q-1/3}_R, Q^{q+2/3}_L.$$

For $S_{Q3} = \mathbf{3}_L^* \cup \mathbf{3}_R \cup \mathbf{1}_R \cup \mathbf{1}_L$, the SM left-handed quark doublets are embedded in $(3, 3^*, 1, -\frac{q}{3})$, the right-handed quarks in $(3, 1, 3, \frac{q+1}{3})$ and the chirally flipped third components of the quark triplets in $(3, 1, 1, -q - 1/3)$ and $(3, 1, 1, q + 2/3)$, with $q \neq -\frac{1}{2}$.

$$S_{Q4} = \begin{pmatrix} d_L \\ u_L \\ Q_L^{-q-1/3} \end{pmatrix}, \quad \begin{pmatrix} d_R \\ u_R \\ Q_R^{-q-1/3} \end{pmatrix}.$$

For $S_{Q4} = \mathbf{3}_L^* \cup \mathbf{3}_R^*$, the SM left-handed quark doublets are embedded in $(3, 3^*, 1, -\frac{q}{3})$, the right-handed quarks in $(3, 1, 3^*, -\frac{q}{3})$.

3 Irreducible anomaly-free sets

By combining the families of quarks S_{Qi} and leptons S_{Li}, according to Table 1, it is possible to construct eight three-generation models that produce anomaly-free particle spectra. The corresponding eight three-family models are:

$$\begin{aligned}
M_1 &: 3S_{L4} + S_{Q1} + S_{Q2} + S_{Q3} \\
M_2 &: 3S_{L4} + 2S_{Q1} + S_{Q4} \\
M_3 &: 3S_{L3} + 2S_{Q2} + S_{Q3} \\
M_4 &: 3S_{L3} + S_{Q1} + S_{Q2} + S_{Q4} \\
M_5 &: 3S_{L2} + S_{Q2} + 2S_{Q3} \\
M_6 &: 3S_{L2} + S_{Q1} + S_{Q3} + S_{Q4} \\
M_7 &: 3S_{L1} + S_{Q2} + S_{Q3} + S_{Q4} \\
M_8 &: 3S_{L1} + S_{Q1} + 2S_{Q4}.
\end{aligned}$$

It is also possible to construct anomaly-free sets containing two generations, which may serve as building blocks for models with an even number of generations, such as four, six, and so on. However, since these models do not account for the observed three families in the SM, they have only been sparsely explored in the literature. However, it is important to note that models that incorporate additional generations can play a significant role in various phenomenological contexts. The irreducible anomaly-free sets of two families are:

$$\begin{aligned}
&S_{L2} + S_{L3} + S_{Q2} + S_{Q3} \\
&S_{L2} + S_{L3} + S_{Q1} + S_{Q4} \\
&S_{L1} + S_{L4} + S_{Q2} + S_{Q3} \\
&S_{L1} + S_{L4} + S_{Q1} + S_{Q4}.
\end{aligned}$$

By introducing two such sets, a four-family model emerges. Three of these families align with those of the Standard Model, while the fourth is considered exotic. There exists extensive literature on top-prime models (see [16] and references therein), encompassing both theoretical frameworks and phenomenological analyses.

3.1 Embeddings

As shown by the previous results, models based on irreducible sets of three families exhibit universality in the lepton sector. In contrast, in the quark sector, universality holds for at most two families. Therefore, we restrict our analysis to embeddings in the quark sector, identifying the two universal families with the first and second generations of the Standard Model (Table 2).

4 Electroweak Z' charges

From the charge operator (1) we can obtain the corresponding low-energy gauge group $G = SU(3)_C \otimes SU(2)_L \otimes SU(2)_R \otimes U(1)_{8L+8R} \otimes U(1)_X$. The neutral current Lagrangian for these models is:

$$\begin{aligned}
-\mathcal{L}_{NC} &= g_L J_{3L\mu} A_{3L}^{\mu} + g_L \left(J_{8L\mu} + J_{8R\mu}\right) A_8^{\mu} \\
&\quad + g_X J_{X\mu} A_X^{\mu} + g_R J_{3R\mu} A_{3R}^{\mu}, \\
&= g_L J_{3L\mu} A_{3L}^{\mu} + g' J_{Y\mu} B^{\mu} \\
&\quad + g_{Z'} J_{Z'\mu} Z'^{\mu} + g_{Z''} J_{Z''\mu} Z''^{\mu}.
\end{aligned} \tag{2}$$

By means of an orthogonal matrix we can rotate from the left-right basis of the Neutral Current (NC) vector bosons to the (B, Z') basis i.e.,

$$\begin{pmatrix} A_{3L}^{\mu} \\ A_8^{\mu} \\ A_X^{\mu} \\ A_{3R}^{\mu} \end{pmatrix} = \mathcal{O} \begin{pmatrix} A_{3L}^{\mu} \\ B^{\mu} \\ Z'^{\mu} \\ Z''^{\mu} \end{pmatrix} = \begin{pmatrix} 1 & 0 & 0 & 0 \\ 0 & O_{11} & O_{12} & O_{13} \\ 0 & O_{21} & O_{22} & O_{23} \\ 0 & O_{31} & O_{32} & O_{33} \end{pmatrix} \begin{pmatrix} A_{3L}^{\mu} \\ B^{\mu} \\ Z'^{\mu} \\ Z''^{\mu} \end{pmatrix}, \tag{3}$$

In order to keep invariant the Lagrangian, the currents must transform with the same orthogonal matrix

$$g_Y J_Y^{\mu} = g_L J_8^{\mu} O_{11} + g_X J_X^{\mu} O_{21} + g_R J_R^{\mu} O_{31}, \tag{4}$$

$$g_{Z'} J_{Z'}^{\mu} = g_L J_8^{\mu} O_{12} + g_X J_X^{\mu} O_{22} + g_R J_R^{\mu} O_{32}, \tag{5}$$

$$g_{Z''} J_{Z''}^{\mu} = g_L J_8^{\mu} O_{13} + g_X J_X^{\mu} O_{23} + g_R J_R^{\mu} O_{33}. \tag{6}$$

From the charge operator, we have

$$Y = \beta \left(T_{8L} + T_{8R}\right) + T_{3R} + X\mathbf{1}. \tag{7}$$

It is also well known that $Y = T_{3R} + \frac{1}{2}(B - L)$, such that $\frac{1}{2}(B-L) = \beta \left(T_{8L} + T_{8R}\right) + X\mathbf{1}$. Which implies the relation

$$J_Y = \beta \left(J_{8L} + J_{8R}\right) + J_{3R} + J_X. \tag{8}$$

By comparing these expressions we obtain

$$\frac{g_L}{g_Y} O_{11} = \beta, \qquad \frac{g_X}{g_Y} O_{21} = 1, \qquad \frac{g_R}{g_Y} O_{31} = 1. \tag{9}$$

Table 1 Contribution to the anomalies from each quark family (S_{Qi}) and lepton family (S_{Li}) in 3-3-3-1 models

Anomalies	S_{L1}	S_{L2}	S_{L3}	S_{L4}	S_{Q1}	S_{Q2}	S_{Q3}	S_{Q4}
$[SU(3)_C]^2 \otimes U(1)_X$	0	0	0	0	0	0	0	0
$[SU(3)_L]^2 \otimes U(1)_X$	$\frac{q-1}{3}$	$\frac{q-1}{3}$	$-\frac{(q+2)}{3}$	$-\frac{(q+2)}{3}$	$1+q$	$1+q$	$-q$	$-q$
$[SU(3)_R]^2 \otimes U(1)_X$	$\frac{q-1}{3}$	$-\frac{(q+2)}{3}$	$\frac{q-1}{3}$	$-\frac{(q+2)}{3}$	$1+q$	$-q$	$1+q$	$-q$
$[\text{Grav}]^2 \otimes U(1)_X$	0	0	0	0	0	0	0	0
$[U(1)_X]^3$	0	$-\frac{2}{9}(1+2q)^3$	$\frac{2}{9}(1+2q)^3$	0	0	$-\frac{2}{3}(1+2q)^3$	$\frac{2}{3}(1+2q)^3$	0
$[SU(3)_L]^3$ and $[SU(3)_R]^3$	2	0	0	-2	6	0	0	-6

Table 2 Embeddings of the Standard Model quarks within each family are shown. The superscript denotes the quark content of each family. The lepton sector is universal and does not require an explicit embedding. A check mark indicates that a configuration with at least two families (2+1) sharing identical Z' charges is possible. LHC constraints are reported only for embeddings where identical Z' charges can be assigned to the first two families. In models with three non-universal quark families, Flavor-Changing Neutral Currents (FCNC) arise between the first two generations, in conflict with experimental constraints. In all cases, the models exhibit universality in the lepton sector. ED stands for Embedding Dependent. In these cases, the lower limit depends on which families are identified with the first generation of the SM

Model	Lepton content	SM quark embeddings	2 + 1	FCNC	LHC-lower limit (TeV)
M_1	$3S_{L4}$	$S_{Q_1} + S_{Q_2} + S_{Q_3}$	×	✓	ED
M_2	$3S_{L4}$	$2S_{Q_1}^{ud,cs} + S_{Q_4}^{tb}$	✓	×	4.3
M_3	$3S_{L3}$	$2S_{Q_2}^{ud,cs} + S_{Q_3}^{tb}$	✓	×	4
M_4	$3S_{L3}$	$S_{Q_1} + S_{Q_2} + S_{Q_4}$	×	✓	ED
M_5	$3S_{L2}$	$2S_{Q_3}^{ud,cs} + S_{Q_2}^{tb}$	✓	×	4.5
M_6	$3S_{L2}$	$S_{Q_1} + S_{Q_3} + S_{Q_4}$	×	✓	ED
M_7	$3S_{L1}$	$S_{Q_2} + S_{Q_3} + S_{Q_4}$	×	✓	ED
M_8	$3S_{L1}$	$2S_{Q_4}^{ud,cs} + S_{Q_1}^{tb}$	✓	×	4.3

As is well known, an orthogonal matrix satisfies $O_{ij}O_{jk}^T = \delta_{ik}$. For $i = k = 1$ we have $O_{1j}O_{j1}^T = O_{1j}O_{1j} = O_{11}^2 + O_{12}^2 + O_{13}^2 = 1$, such that

$$\left(\frac{\beta}{g_L}\right)^2 + \left(\frac{1}{g_X}\right)^2 + \left(\frac{1}{g_R}\right)^2 = \frac{1}{g_Y^2}. \tag{10}$$

Let us now consider an explicit representation for the orthogonal matrix $\mathcal{O}$ in terms of three angles ω, ϕ and θ, which are allowed to take values in the $[-\pi, \pi)$ interval. For convenience we choose

$$\mathcal{O} = \begin{pmatrix} 1 & 0 & 0 & 0 \\ 0 & \cos\omega & -\sin\omega & 0 \\ 0 & \sin\omega & \cos\omega & 0 \\ 0 & 0 & 0 & 1 \end{pmatrix} \begin{pmatrix} 1 & 0 & 0 & 0 \\ 0 & \cos\phi & 0 & -\sin\phi \\ 0 & 0 & 1 & 0 \\ 0 & \sin\phi & 0 & \cos\phi \end{pmatrix} \begin{pmatrix} 1 & 0 & 0 & 0 \\ 0 & 1 & 0 & 0 \\ 0 & 0 & \cos\theta & -\sin\theta \\ 0 & 0 & \sin\theta & \cos\theta \end{pmatrix}.$$

From Eq. (9) we obtain

$$\cos\phi\cos\omega = \frac{\beta g_Y}{g_L}, \quad \cos\phi\sin\omega = \frac{g_Y}{g_X}, \quad \sin\phi = \frac{g_Y}{g_R},$$

From this relation we obtain

$$\cos\phi = \hat{\alpha}_R \frac{g_Y}{g_R}, \quad \cos\omega = \frac{\beta g_R}{\hat{\alpha}_R g_L}, \quad \sin\omega = \frac{g_R}{\hat{\alpha}_R g_X}.$$

Here $\hat{\alpha}_R = g_R\sqrt{\frac{\beta^2}{g_L^2} + \frac{1}{g_X^2}} = \sqrt{\frac{g_R^2}{g_L^2}\cot^2\theta_W - 1}$. The typical left-right gauge coupling is $g_L = g_R = 0.652$. By assuming

$$\begin{aligned} J_{Z'} &= \sum_f \bar{f}\left(\epsilon_L^{Z'}(f)P_L + \epsilon_R^{Z'}(f)P_R\right) f, \\ J_{8L} + J_{8R} &= \sum_f \bar{f}\left(\epsilon_L^{8}(f)P_L + \epsilon_R^{8}(f)P_R\right) f, \\ J_{3R} &= \sum_f \bar{f}\epsilon_R^{8}(f)P_R f, \\ J_X &= \sum_f \bar{f}\left(X_L(f)P_L + X_R(f)P_R\right) f, \end{aligned} \tag{11}$$

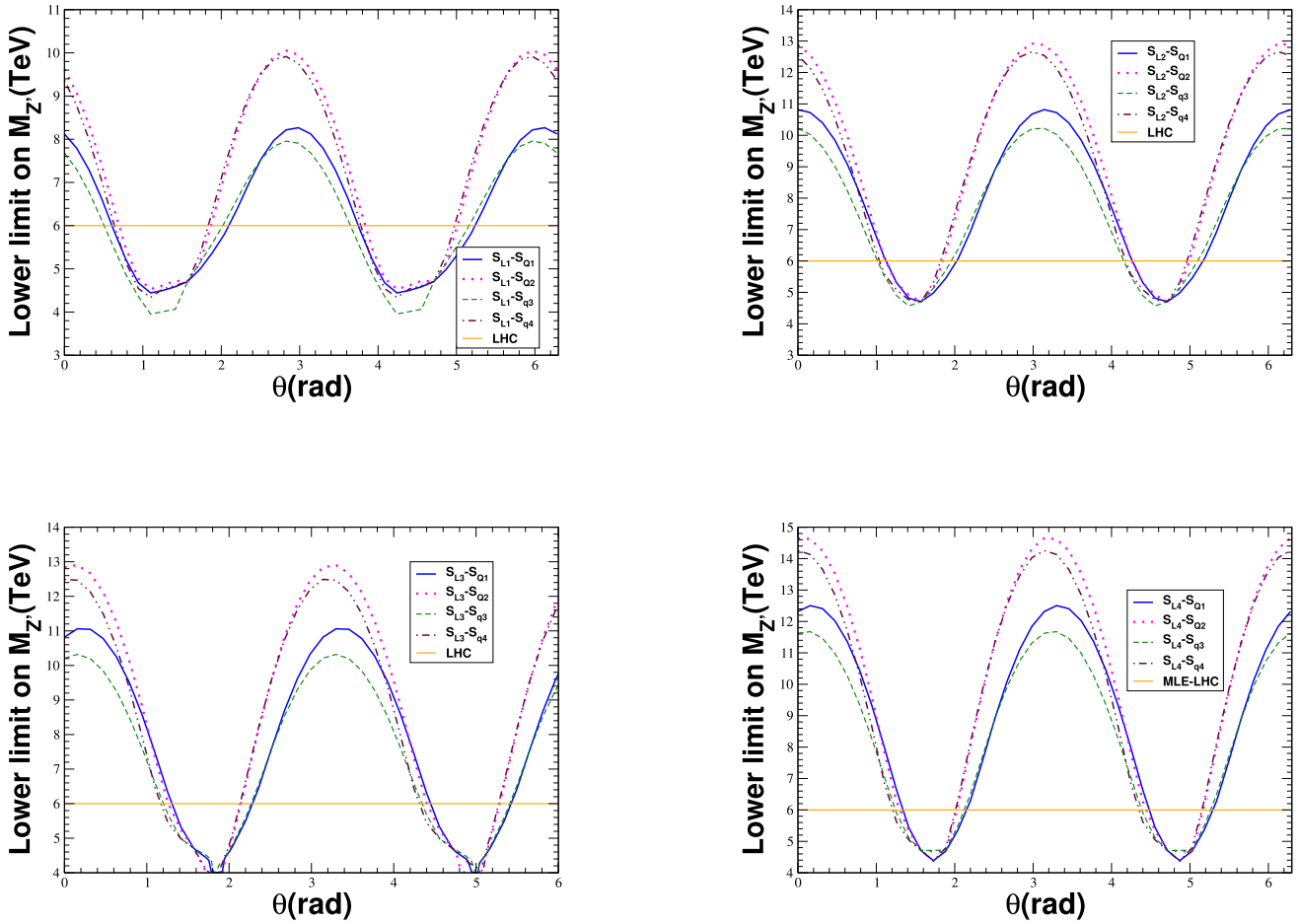

Fig. 1 Left: Lower limit on the Z' mass. We obtain these limits from the 95% CL upper limits on the fiducial Z' production cross section times the $Z' \to \ell^+\ell^-$ branching [17]. The continuous yellow line labeled LHC refers to the highest Z' mass for which the ATLAS Collaboration has reported upper limits on the production cross section. Restrictions for Z' masses above 6 TeV are assumed to be projected limits. They are obtained assuming that the projected upper limit for the cross section in this region cannot exceed the ATLAS limit at 6 TeV (The general trend of the upper limits on the cross section is to decrease with the mass of the Z'.) Below this value, the ATLAS restrictions apply. $S_{Lj} - S_{Qi}$ indicates the chosen set of fermions for the Z' charges of the first two families in the SM, with $i, j = 1, 2, 3, 4$. The corresponding Z' charges are shown in Appendix A

where we define $\epsilon^a_{L,R}$ as the corresponding chiral charges associated with the gauge group generators $T^a_{L,R} = \frac{1}{2}\lambda^a$, with λ^a the Gell–Mann matrices. Replacing these expressions in Eq. (5) and using the elements of the rotation matrix $\mathcal{O}$ we get the Z' chiral charges:

$$g_{Z'}\epsilon^{Z'}_{L,R} = A_{L,R}\cos\theta + B_{L,R}\sin\theta, \tag{12}$$

$$g_{Z''}\epsilon^{Z''}_{L,R} = -A_{L,R}\sin\theta + B_{L,R}\cos\theta, \tag{13}$$

and θ is an angle of the rotation matrix $\mathcal{O}$ which can take any value between $-\pi$ and π and

$$A_L = \frac{g_R}{\hat{\alpha}_R}\left(\beta\frac{g_X}{g_L}X_L - \frac{g_L}{g_X}\epsilon^8_L\right), \tag{14}$$

$$A_R = \frac{g_R}{\hat{\alpha}_R}\left(\beta\frac{g_X}{g_L}X_R - \frac{g_L}{g_X}\epsilon^8_R\right), \tag{15}$$

$$B_L = -g_Y\frac{\beta\epsilon^8_L + X_L}{\hat{\alpha}_R}, \tag{16}$$

$$B_R = g_Y\left(-\frac{\beta\epsilon^8_R + X_R}{\hat{\alpha}_R} + \hat{\alpha}_R\epsilon^3_R\right). \tag{17}$$

In these expressions, to reproduce the SM charges it is necessary to take into account that $\beta(\epsilon^8_L + \epsilon^8_R) + X = \frac{1}{2}(B-L)$, which is equivalent to $\beta\epsilon^8_{L,R} + X_{L,R} = \frac{1}{2}(B-L)$. For exact left-right symmetry we have $g_L = g_R$, replacing these identities in $A_{L,R}$ and $B_{L,R}$ we obtain the following.

$$A_{L,R} = \frac{g_L}{\hat{\alpha}_R}\left[\left(\frac{1}{z} + z\right)X_{L,R} - \frac{z}{2}(B-L)\right], \tag{18}$$

$$B_L = -\, g_Y \frac{B-L}{2\hat{\alpha}_R}, \tag{19}$$

$$B_R = g_Y \left(-\frac{B-L}{2\hat{\alpha}_R} + \hat{\alpha}_R \epsilon_R^3 \right). \tag{20}$$

Here $z = \frac{g_L}{\beta g_X} = \frac{1}{\beta}\sqrt{\cot^2\theta_W - \beta^2 - 1} = \frac{1}{\beta}\sqrt{\hat{\alpha}_R^2 - \beta^2}$. Under the previous assumptions with $\sin^2\theta_W = 0.23120$ (here, we use the value for the weak mixing angle in the $\overline{\text{MS}}$ scheme) we get $\hat{\alpha}_R = \sqrt{\cot^2\theta_W - 1}$. To avoid imaginary couplings, we require: $\beta < \hat{\alpha}_R \approx 1.525$, this condition rules out the notable case $\beta = \sqrt{3}$. From these expressions, we obtain the chiral charges for the lepton and quark families. These charges are reported in Appendix A.

5 Low energy and collider constraints

To establish lower bounds on the Z' mass, we analyze results from searches for high-mass resonances decaying into dielectron and dimuon final states, focusing on the mass range 250 GeV to 6 TeV [17]. These searches were performed using data collected by the ATLAS experiment during Run 2 of the Large Hadron Collider, corresponding to an integrated luminosity of 139 fb^{-1} at a center-of-mass energy of $\sqrt{s} =$ 13 TeV. The ATLAS Collaboration reported 95% confidence level upper limits on the fiducial cross section times branching ratio, under various assumptions for the resonance width. For typical E_6-motivated couplings, these results translate into lower mass limits of approximately 4.5 TeV.

In Fig. 1, the lower limits on the Z' mass are shown. To derive the constraints, we determine the value of the Z' mass for which the QCD-predicted cross section matches the experimental upper limit on the differential cross section. To derive these limits, it is customary to assume that the masses of exotic fermions and right-handed neutrinos are effectively infinite. For a detailed description of the procedure and the corresponding theoretical expressions, we refer the reader to the references [18–20]. This approach applies for Z' masses in the range 250 GeV to 6 TeV. Figure 1 presents values of $M_{Z'}$ beyond 6 TeV. These should not be interpreted as lower bounds on the Z' mass but rather as projections. The projections are obtained under the assumption that the upper limit on the cross section for $M_{Z'} > 6$ TeV remains below the current upper limit at 6 TeV. This assumption is well-motivated, as reduced background contributions are expected at higher masses, consistent with the typical behavior of exclusion limits in this regime.

6 Conclusions

We have explored the extended gauge symmetry $SU(3)_C \otimes SU(3)_L \otimes SU(3)_R \otimes U(1)_X$, which naturally embeds both the Left-Right and 3-3-1 models as subgroups. This embedding enables the construction of models that inherit the appealing features of these established frameworks.

Within this symmetry, we derived four lepton families and four quark families, and analyzed their contributions to gauge anomalies, as summarized in Table 1. From these results, several anomaly-free sets of fermions were identified, as detailed in Sect. 3. In total, we reported eight three-family and four two-family anomaly-free combinations for an arbitrary β. The three-family anomaly-free ensembles are especially interesting, as they represent realistic extensions of the SM. These models are non-universal in the quark sector and universal in the lepton sector, inheriting many of the appealing features of the 3-3-1 models. The two-family sets are useful for constructing models with an even number of families greater than or equal to four, offering flexibility in anomaly-free model building.

Finally, we derive constraints on the Z' mass, accounting for the presence of a free parameter θ (a mixing angle) in the couplings to SM fermions. Our analysis reveals that collider bounds exhibit a strong dependence on the value of this parameter. These constraints were evaluated for all possible combinations of quark and lepton families, as illustrated in Fig. 1.

Future work could investigate the high-energy unification of these models and their consequences for low-energy phenomenology. By introducing a suitable scalar potential, they may also serve as promising frameworks to study dark matter, neutrino properties, and CPT violation.

Acknowledgements We thank W. A. Ponce for developing the formalism that underpins this work and for introducing us to this fascinating topic. RB, ER, and YG acknowledge additional financial support from Minciencias CD82315 CT ICETEX 2021-1080. This research was partially supported by the *Vicerrectoría de Investigaciones e Interacción Social* (VIIS) de la Universidad de Nariño, project numbers 2686, 2679, 3130, 3594 and 3595.

Data Availability Statement This manuscript has no associated data. [Author's comment: Data sharing not applicable to this article as no datasets were generated or analysed during the current study.]

Code Availability Statement This manuscript has no associated code/software. [Author's comment: Code/Software sharing not applicable to this article as no code/software was generated or analysed during the current study.]

Funded by SCOAP[3].

Appendix A: Z' charges

From Eq. (12), one can derive the Z' charges associated with each fermion family. The Z' charges for the Standard Model fields are presented in Tables 3, 4, 5, 6, 7, 8, 9, 10.

Table 3 Z' chiral charges for the SM quarks when they are embedded in S_{L1}. Here $\hat{\alpha}_R = \sqrt{\cot^2\theta_W - 1}$ and $z = \frac{1}{\beta}\sqrt{\hat{\alpha}_R^2 - \beta^2}$

S_{L1}: $\ell^T = (\nu_L, e_L) \subset \left(3, 3, 1, \frac{q-1}{3}\right)$, $(\nu_R, e_R) \subset \left(3, 3, 1, \frac{q-1}{3}\right)$		
Fields	$g_{Z'}\epsilon_L^{Z'}$	$g_{Z'}\epsilon_R^{Z'}$
ν_L	$\frac{g_Y}{2}\left[\frac{1}{\hat{\alpha}_R}\right]s_\theta + \frac{g_L}{\hat{\alpha}_R}\left[\frac{z}{2} + \frac{q-1}{3}(z+\frac{1}{z})\right]c_\theta$	$\frac{g_Y}{2}\left[\frac{1}{\hat{\alpha}_R} + \hat{\alpha}_R\right]s_\theta + \frac{g_L}{\hat{\alpha}_R}\left[\frac{z}{2} + \frac{q-1}{3}(z+\frac{1}{z})\right]c_\theta$
e	$\frac{g_Y}{2}\left[\frac{1}{\hat{\alpha}_R}\right]s_\theta + \frac{g_L}{\hat{\alpha}_R}\left[\frac{z}{2} + \frac{q-1}{3}(z+\frac{1}{z})\right]c_\theta$	$\frac{g_Y}{2}\left[\frac{1}{\hat{\alpha}_R} - \hat{\alpha}_R\right]s_\theta + \frac{g_L}{\hat{\alpha}_R}\left[\frac{z}{2} + \frac{q-1}{3}(z+\frac{1}{z})\right]c_\theta$

Table 4 Z' chiral charges for the SM quarks when they are embedded in S_{L2}. Here $\hat{\alpha}_R = \sqrt{\cot^2\theta_W - 1}$ and $z = \frac{1}{\beta}\sqrt{\hat{\alpha}_R^2 - \beta^2}$

S_{L2}: $\ell^T = (\nu_L, e_L) \subset \left(3, 3, 1, \frac{q-1}{3}\right)$, $(\nu_R, e_R) \subset \left(3, 3^*, 1, -\frac{q+2}{3}\right)$		
Fields	$g_{Z'}\epsilon_L^{Z'}$	$g_{Z'}\epsilon_R^{Z'}$
ν_L	$\frac{g_Y}{2}\left[\frac{1}{\hat{\alpha}_R}\right]s_\theta + \frac{g_L}{\hat{\alpha}_R}\left[\frac{z}{2} + \frac{q-1}{3}(z+\frac{1}{z})\right]c_\theta$	$\frac{g_Y}{2}\left[\frac{1}{\hat{\alpha}_R} + \hat{\alpha}_R\right]s_\theta + \frac{g_L}{\hat{\alpha}_R}\left[\frac{z}{2} - \frac{2+q}{3}(z+\frac{1}{z})\right]c_\theta$
e	$\frac{g_Y}{2}\left[\hat{\alpha}_R\right]s_\theta + \frac{g_L}{\hat{\alpha}_R}\left[\frac{z}{2} + \frac{q-1}{3}(z+\frac{1}{z})\right]c_\theta$	$\frac{g_Y}{2}\left[\frac{1}{\hat{\alpha}_R} - \hat{\alpha}_R\right]s_\theta + \frac{g_L}{\hat{\alpha}_R}\left[\frac{z}{2} - \frac{2+q}{3}(z+\frac{1}{z})\right]c_\theta$

Table 5 Z' chiral charges for the SM quarks when they are embedded in S_{L3}. Here $\hat{\alpha}_R = \sqrt{\cot^2\theta_W - 1}$ and $z = \frac{1}{\beta}\sqrt{\hat{\alpha}_R^2 - \beta^2}$

S_{L3}: $\ell^T = (\nu_L, e_L) \subset \left(3, 3^*, 1, -\frac{q+2}{3}\right)$, $(\nu_R, e_R) \subset \left(3, 3, 1, \frac{q-1}{3}\right)$		
Fields	$g_{Z'}\epsilon_L^{Z'}$	$g_{Z'}\epsilon_R^{Z'}$
ν_L	$\frac{g_Y}{2}\left[\frac{1}{\hat{\alpha}_R}\right]s_\theta + \frac{g_L}{\hat{\alpha}_R}\left[\frac{z}{2} - \frac{2+q}{3}(z+\frac{1}{z})\right]c_\theta$	$\frac{g_Y}{2}\left[\frac{1}{\hat{\alpha}_R} + \hat{\alpha}_R\right]s_\theta + \frac{g_L}{\hat{\alpha}_R}\left[\frac{z}{2} + \frac{q-1}{3}(z+\frac{1}{z})\right]c_\theta$
e	$\frac{g_Y}{2}\left[\frac{1}{\hat{\alpha}_R}\right]s_\theta + \frac{g_L}{\hat{\alpha}_R}\left[\frac{z}{2} - \frac{2+q}{3}(z+\frac{1}{z})\right]c_\theta$	$\frac{g_Y}{2}\left[\frac{1}{\hat{\alpha}_R} - \hat{\alpha}_R\right]s_\theta + \frac{g_L}{\hat{\alpha}_R}\left[\frac{z}{2} + \frac{q-1}{3}(z+\frac{1}{z})\right]c_\theta$

Table 6 Z' chiral charges for the SM quarks when they are embedded in S_{L4}. Here $\hat{\alpha}_R = \sqrt{\cot^2\theta_W - 1}$ and $z = \frac{1}{\beta}\sqrt{\hat{\alpha}_R^2 - \beta^2}$

S_{L4}: $\ell^T = (\nu_L, e_L) \subset \left(3, 3^*, 1, -\frac{q+2}{3}\right)$, $(\nu_R, e_R) \subset \left(3, 3^*, 1, -\frac{q+2}{3}\right)$		
Fields	$g_{Z'}\epsilon_L^{Z'}$	$g_{Z'}\epsilon_R^{Z'}$
ν_L	$\frac{g_Y}{2}\left[\frac{1}{\hat{\alpha}_R}\right]s_\theta + \frac{g_L}{\hat{\alpha}_R}\left[\frac{z}{2} - \frac{2+q}{3}(z+\frac{1}{z})\right]c_\theta$	$\frac{g_Y}{2}\left[\frac{1}{\hat{\alpha}_R} + \hat{\alpha}_R\right]s_\theta + \frac{g_L}{\hat{\alpha}_R}\left[\frac{z}{2} - \frac{2+q}{3}(z+\frac{1}{z})\right]c_\theta$
e	$\frac{g_Y}{2}\left[\frac{1}{\hat{\alpha}_R}\right]s_\theta + \frac{g_L}{\hat{\alpha}_R}\left[\frac{z}{2} - \frac{2+q}{3}(z+\frac{1}{z})\right]c_\theta$	$\frac{g_Y}{2}\left[\hat{\alpha}_R - \frac{1}{\hat{\alpha}_R}\right]s_\theta + \frac{g_L}{\hat{\alpha}_R}\left[\frac{z}{2} - \frac{2+q}{3}(z+\frac{1}{z})\right]c_\theta$

Table 7 Z' chiral charges for the SM quarks when they are embedded in S_{Q1}. Here $\hat{\alpha}_R = \sqrt{\cot^2\theta_W - 1}$ and $z = \frac{1}{\beta}\sqrt{\hat{\alpha}_R^2 - \beta^2}$

S_{Q1}: $q^T = (u_L, d_L) \subset \left(3, 3, 1, \frac{q+1}{3}\right)$, $(u_R, d_R) \subset \left(3, 3, 1, \frac{q+1}{3}\right)$		
Fields	$g_{Z'}\epsilon_L^{Z'}$	$g_{Z'}\epsilon_R^{Z'}$
u	$-g_Y\left[\frac{1}{6\hat{\alpha}_R}\right]s_\theta + \frac{g_L}{3\hat{\alpha}_R}\left[-\frac{z}{2} + (1+q)(z+\frac{1}{z})\right]c_\theta$	$-g_Y\left[\frac{1}{6\hat{\alpha}_R} - \frac{\hat{\alpha}_R}{2}\right]s_\theta + \frac{g_L}{3\hat{\alpha}_R}\left[-\frac{z}{2} + (1+q)(z+\frac{1}{z})\right]c_\theta$
d	$-g_Y\left[\frac{1}{6\hat{\alpha}_R}\right]s_\theta + \frac{g_L}{3\hat{\alpha}_R}\left[-\frac{z}{2} + (1+q)(z+\frac{1}{z})\right]c_\theta$	$-g_Y\left[\frac{1}{6\hat{\alpha}_R} + \frac{\hat{\alpha}_R}{2}\right]s_\theta + \frac{g_L}{3\hat{\alpha}_R}\left[-\frac{z}{2} + (1+q)(z+\frac{1}{z})\right]c_\theta$

Table 8 Z' chiral charges for the SM quarks when they are embedded in S_{Q2}. Here $\hat{\alpha}_R = \sqrt{\cot^2\theta_W - 1}$ and $z = \frac{1}{\beta}\sqrt{\hat{\alpha}_R^2 - \beta^2}$

S_{Q2}: $q^T = (u_L, d_L) \subset \left(3, 3, 1, \frac{q+1}{3}\right)$, $(u_R, d_R) \subset \left(3, 3^*, 1, -\frac{q}{3}\right)$		
Fields	$g_{Z'}\epsilon_L^{Z'}$	$g_{Z'}\epsilon_R^{Z'}$
u	$-\frac{g_Y}{6\hat{\alpha}_R}s_\theta + \frac{g_L}{3\hat{\alpha}_R}\left[-\frac{z}{2} + (1+q)(z+\frac{1}{z})\right]c_\theta$	$-g_Y\left[\frac{1}{6\hat{\alpha}_R} - \frac{\hat{\alpha}_R}{2}\right]s_\theta - \frac{g_L}{3\hat{\alpha}_R}\left[\frac{z}{2} + q(z+\frac{1}{z})\right]c_\theta$
d	$-\frac{g_Y}{6\hat{\alpha}_R}s_\theta + \frac{g_L}{3\hat{\alpha}_R}\left[-\frac{z}{2} + (1+q)(z+\frac{1}{z})\right]c_\theta$	$-g_Y\left[\frac{\hat{\alpha}_R}{2} + \frac{1}{6\hat{\alpha}_R}\right]s_\theta - \frac{g_L}{3\hat{\alpha}_R}\left[\frac{z}{2} + q(z+\frac{1}{z})\right]c_\theta$

Table 9 Z' chiral charges for the SM quarks when they are embedded in S_{Q3}. Here $\hat{\alpha}_R = \sqrt{\cot^2\theta_W - 1}$ and $z = \frac{1}{\beta}\sqrt{\hat{\alpha}_R^2 - \beta^2}$

S_{Q3}: $q^T = (u_L, d_L) \subset \left(3, 3^*, 1, -\frac{q}{3}\right)$, $(u_R, d_R) \subset \left(3, 3, 1, \frac{1+q}{3}\right)$		
Fields	$g_{Z'}\epsilon_L^{Z'}$	$g_{Z'}\epsilon_R^{Z'}$
u	$-\frac{g_Y}{6\hat{\alpha}_R}s_\theta - \frac{g_L}{3\hat{\alpha}_R}\left[\frac{z}{2} + q(z+\frac{1}{z})\right]c_\theta$	$g_Y\left[\frac{\hat{\alpha}_R}{2} - \frac{1}{6\hat{\alpha}_R}\right]s_\theta + \frac{g_L}{3\hat{\alpha}_R}\left[-\frac{z}{2} + (1+q)(z+\frac{1}{z})\right]c_\theta$
d	$-\frac{g_Y}{6\hat{\alpha}_R}s_\theta - \frac{g_L}{3\hat{\alpha}_R}\left[\frac{z}{2} + q(z+\frac{1}{z})\right]c_\theta$	$-g_Y\left[\frac{\hat{\alpha}_R}{2} + \frac{1}{6\hat{\alpha}_R}\right]s_\theta + \frac{g_L}{3\hat{\alpha}_R}\left[-\frac{z}{2} + (1+q)(z+\frac{1}{z})\right]c_\theta$

Table 10 Z' chiral charges for the SM quarks when they are embedded in S_{Q4}.Here $\hat{\alpha}_R = \sqrt{\cot^2\theta_W - 1}$ and $z = \frac{1}{\beta}\sqrt{\hat{\alpha}_R^2 - \beta^2}$

S_{Q4}: $q^T = (u_L, d_L) \subset \left(3, 3^*, 1, -\frac{q}{3}\right)$, $(u_R, d_R) \subset \left(3, 3^*, 1, -\frac{q}{3}\right)$		
Fields	$g_{Z'}\epsilon_L^{Z'}$	$g_{Z'}\epsilon_R^{Z'}$
u	$-\frac{g_Y}{6\hat{\alpha}_R}s_\theta - \frac{g_L}{3\hat{\alpha}_R}\left[\frac{z}{2} + q(z+\frac{1}{z})\right]c_\theta$	$g_Y\left[\frac{\hat{\alpha}_R}{2} - \frac{1}{6\hat{\alpha}_R}\right]s_\theta - \frac{g_L}{3\hat{\alpha}_R}\left[\frac{z}{2} + q(z+\frac{1}{z})\right]c_\theta$
d	$-\frac{1}{6\hat{\alpha}_R}s_\theta - \frac{g_L}{3\hat{\alpha}_R}\left[\frac{z}{2} + q(z+\frac{1}{z})\right]c_\theta$	$-g_Y\left[\frac{\hat{\alpha}_R}{2} + \frac{1}{6\hat{\alpha}_R}\right]s_\theta - \frac{g_L}{3\hat{\alpha}_R}\left[\frac{z}{2} + q(z+\frac{1}{z})\right]c_\theta$

References

1. R. Foot, H. Lew, R.R. Volkas, Electric charge quantization. J. Phys. G **19**, 361 (1993) [Erratum: J. Phys. G 19, 1067 (1993)]. https://doi.org/10.1088/0954-3899/19/3/005. arXiv:hep-ph/9209259
2. M. Nowakowski, A. Pilaftsis, A note on charge quantization through anomaly cancellation. Phys. Rev. D **48**, 259 (1993). https://doi.org/10.1103/PhysRevD.48.259. arXiv:hep-ph/9304312
3. J.C. Pati, A. Salam, Lepton number as the fourth color. Phys. Rev. D **10**, 275 (1974) [Erratum: Phys. Rev. D 11, 703–703 (1975)]. https://doi.org/10.1103/PhysRevD.10.275
4. H. Georgi, S.L. Glashow, Unity of all elementary particle forces. Phys. Rev. Lett. **32**, 438 (1974). https://doi.org/10.1103/PhysRevLett.32.438
5. M. Reig, J.W.F. Valle, C.A. Vaquera-Araujo, Unifying left-right symmetry and 331 electroweak theories. Phys. Lett. B **766**, 35 (2017). https://doi.org/10.1016/j.physletb.2016.12.049. arXiv:1611.02066 [hep-ph]
6. C. Hati, S. Patra, M. Reig, J.W.F. Valle, C.A. Vaquera-Araujo, Towards gauge coupling unification in left-right symmetric $SU(3)_c \times SU(3)_L \times SU(3)_R \times U(1)_X$ theories. Phys. Rev. D **96**, 015004 (2017). https://doi.org/10.1103/PhysRevD.96.015004. arXiv:1703.09647 [hep-ph]
7. P.V. Dong, D.T. Huong, F.S. Queiroz, J.W.F. Valle, C.A. Vaquera-Araujo, The dark side of flipped trinification. JHEP **04**, 143. https://doi.org/10.1007/JHEP04(2018)143. arXiv:1710.06951 [hep-ph]
8. D.T. Huong, P.V. Dong, N.T. Duy, N.T. Nhuan, L.D. Thien, Investigation of dark matter in the 3-2-3-1 model. Phys. Rev. D **98**, 055033 (2018). https://doi.org/10.1103/PhysRevD.98.055033. arXiv:1802.10402 [hep-ph]
9. D.N. Dinh, D.T. Huong, N.T. Duy, N.T. Nhuan, L.D. Thien, P. Van Dong, Flavor changing in the flipped trinification. Phys. Rev. D **99**, 055005 (2019). https://doi.org/10.1103/PhysRevD.99.055005. arXiv:1901.07969 [hep-ph]
10. M. Singer, J.W.F. Valle, J. Schechter, Canonical neutral current predictions from the weak electromagnetic gauge group SU(3) X u(1). Phys. Rev. D **22**, 738 (1980). https://doi.org/10.1103/PhysRevD.22.738
11. F. Pisano, V. Pleitez, An SU(3) x U(1) model for electroweak interactions. Phys. Rev. D **46**, 410 (1992). https://doi.org/10.1103/PhysRevD.46.410. arXiv:hep-ph/9206242
12. P.H. Frampton, Chiral dilepton model and the flavor question. Phys. Rev. Lett. **69**, 2889 (1992). https://doi.org/10.1103/PhysRevLett.69.2889
13. R.H. Benavides, Y. Giraldo, L. Muñoz, W.A. Ponce, E. Rojas, Systematic study of the $SU(3)_c \otimes SU(3)_L \otimes U(1)_X$ local gauge symmetry. J. Phys. G **49**, 105007 (2022). https://doi.org/10.1088/1361-6471/ac894a. arXiv:2111.02563 [hep-ph]
14. E. Suarez, R.H. Benavides, Y. Giraldo, W.A. Ponce, E. Rojas, Alternative 3-3-1 models with exotic electric charges. J. Phys. G **51**, 035004 (2024). https://doi.org/10.1088/1361-6471/ad1e21. arXiv:2307.15826 [hep-ph]
15. R.N. Mohapatra, J.C. Pati, Left-right gauge symmetry and an isoconjugate model of CP violation. Phys. Rev. D **11**, 566 (1975). https://doi.org/10.1103/PhysRevD.11.566
16. R. Franceschini, Physics beyond the standard model associated with the top quark. Annu. Rev. Nucl. Part. Sci. **73**, 397 (2023). https://doi.org/10.1146/annurev-nucl-102020-011427. arXiv:2301.04407 [hep-ph]
17. G. Aad et al. [ATLAS], Search for high-mass dilepton resonances using 139 fb^{-1} of pp collision data collected at $\sqrt{s}$ =13 TeV with

the ATLAS detector. Phys. Lett. B **796**, 68 (2019). https://doi.org/10.1016/j.physletb.2019.07.016. arXiv:1903.06248 [hep-ex]
18. J. Erler, P. Langacker, S. Munir, E. Rojas, Z' bosons at colliders: a Bayesian viewpoint. JHEP **11**, 076. https://doi.org/10.1007/JHEP11(2011)076. arXiv:1103.2659 [hep-ph]
19. C. Salazar, R.H. Benavides, W.A. Ponce, E. Rojas, LHC constraints on 3-3-1 models. JHEP **07**, 096. https://doi.org/10.1007/JHEP07(2015)096. arXiv:1503.03519 [hep-ph]
20. R.H. Benavides, L. Muñoz, W.A. Ponce, O. Rodríguez, E. Rojas, Electroweak couplings and LHC constraints on alternative Z' models in E_6. Int. J. Mod. Phys. A **33**, 1850206 (2018). https://doi.org/10.1142/S0217751X18502068. arXiv:1801.10595 [hep-ph]

Eur. Phys. J. C (2023) 83:638
https://doi.org/10.1140/epjc/s10052-023-11808-0

THE EUROPEAN PHYSICAL JOURNAL C

Regular Article - Theoretical Physics

A minimal axion model for mass matrices with five texture-zeros

Yithsbey Giraldo[1,a], **R. Martinez**[2,b], **Eduardo Rojas**[1,c], **Juan C. Salazar**[1,d]

[1] Departamento de Física, Universidad de Nariño, A.A. 1175 San Juan de Pasto, Colombia
[2] Departamento de Física, Universidad Nacional de Colombia, Ciudad Universitaria, K.45 No. 26-85, Bogota D.C., Colombia

Received: 24 April 2023 / Accepted: 5 July 2023

Abstract A model with fermion and scalar fields charged under a Peccei–Queen (PQ) symmetry is proposed. The PQ charges are chosen in such a way that they can reproduce mass matrices with five texture zeros, which can generate the fermion masses, the CKM matrix, and the PMNS matrix of the Standard Model (SM). To obtain this result, at least 4 Higgs doublets are needed. As we will see in the manuscript this is a highly non-trivial result since the texture zeros of the mass matrices impose a large number of restrictions. This model shows a route to understand the different scales of the SM by extending it with a multi-Higgs sector and an additional PQ symmetry. Since the PQ charges are not universal, the model predicts flavor-changing neutral currents (FCNC) at the tree level, a feature that constitutes the main source of restrictions on the parameter space. We report the allowed regions by lepton decays and compare them with those coming from the semileptonic decays $K^{\pm} \longrightarrow \pi \bar{\nu} \nu$. We also show the excluded regions and the projected bounds of future experiments for the axion–photon coupling as a function of the axion mass and compare it with the parameter space of our model.

1 Introduction

The discovery of the Higgs with a mass of 125 GeV, by the ATLAS [1] and CMS [2] collaborations, is very important because it provides experimental support for spontaneous symmetry breaking, which is the mechanism that explains the origin of the masses of fermions and gauge bosons. Additionally, it opens up the possibility of new physics in the scalar sector, such as the two Higgs doublet model [3–7], models with additional singlet scalar fields [8–10], or scalar fields that could be candidates for Dark Matter [11–14]. On the other hand, in the Standard Model (SM) [15–17], symmetry breaking generates a coupling of the Higgs to fermions, proportional to their masses, which is consistent with experimental data. However, there are several orders of magnitude between the fermion mass hierarchies that cannot be explained within the context of the SM. Six masses must be defined for the up and down quarks, three Cabibbo-Kobayashi-Maskawa (CKM) mixing angles, and a complex phase that involves CP violation. On the other hand, in the lepton sector, there are three masses for charged leptons, two squared mass differences for neutrinos, three mixing angles, and a complex phase that involves CP violation in the lepton sector. In this case, it is necessary to determine the mass of the lightest neutrino and the character of neutrinos, whether they are Dirac or Majorana fermions.

In the Davis experiment [18], which was designed to detect solar neutrinos, a deficiency in the solar neutrino flux was first observed. According to the results of Bahcall, only one-third of solar neutrinos would reach the Earth [19]. Neutrino oscillation was first proposed by Pontecorvo [20], and the precise mechanism of solar neutrino oscillations was proposed by Mikheyev, Smirnov, and Wolfenstein, involving a resonant enhancement of neutrino oscillations due to matter effects [21,22]. These observations have been confirmed by many experiments from four different sources: solar neutrinos as in Homestake [18], SAGE [18], GALLEX & GNO [23,24], SNO [25], Borexino [26,27] and Super-Kamiokande [28,29] experiments, atmospheric neutrinos as in IceCube [30], neutrinos from reactors as KamLAND [31], CHOOZ [32], Palo Verde [33], Daya Bay [34], RENO [35] and SBL [36], and from accelerators as in MINOS [37], T2K [38] and NOνA [39]. Neutrino oscillations depend on squared mass differences. On the other hand, the lightest neutrino mass has not been determined yet, but from cosmological considerations, none of the neutrino masses can exceed 0.3 eV, which implies

[a] e-mail: yithsbey@gmail.com
[b] e-mail: remartinezm@unal.edu.co
[c] e-mail: eduro4000@gmail.com
[d] e-mail: jusala@gmail.com (corresponding author)

Published online: 19 July 2023

that the neutrino masses are much smaller than the charged fermion masses. However, unlike quarks and charged leptons, in the SM the neutrinos are massless, which is explained by assuming that neutrinos are left-handed. Therefore, the discovery of neutrino masses implies new physics beyond the SM. By adding right-handed neutrinos, the Higgs mechanism of the SM can give neutrinos the same type of mass acquired by charged leptons and quarks. It is possible to add right-handed neutrinos ν_R to the SM, as long as they do not participate in weak interactions. With the presence of right-handed neutrinos, it would be possible to generate Dirac masses m_D, similar to those of charged leptons and quarks. In principle, it is also possible to give Majorana masses to left-handed neutrinos, and similarly, right-handed neutrinos can have Majorana masses M_R. For a very large M_R, it would give effective Majorana masses for left-handed neutrinos as $m_{\text{eff}} \approx m_D^2/M_R$. The presence of large Majorana masses allows to explain the tiny neutrino masses compared to the charged fermion masses [38]. To explain the smallness of neutrino masses, there are three types of seesaw mechanisms in the literature: type I with three electroweak neutrinos and three heavy right-handed neutrinos, type II [40,41], type III [42], and inverse seesaw [43,44]. One way to explain the fermion mass hierarchies and the CKM and PMNS mixing angles is through zeros in the Yukawa couplings of fermions (this is known as texture-zeros or simply textures of the mass matrices, and these zeros are usually chosen by hand). It is common in the literature to consider Fritzsch-type textures [45,46], or similar [47–52], for the neutrino and charged lepton mass matrices.

There is no theory that provides values for the entries of the Yukawa Lagrangian, and consequently, there is no a first-principle explanation for the masses and their large differences in the SM. The mass hierarchy between fermions is unnatural because it requires Yukawa constants that differ by many orders of magnitude; this feature is known as the flavor problem or flavor puzzle [53–57]. In this direction, a way that has been explored in the literature is to propose a sector with multiple scalar doublets along with discrete symmetries [58,59], to reduce the number of Yukawa couplings, or equivalently, by introducing texture-zeros in the mass matrices [60–65]. It is also possible to consider global symmetry groups that prohibit certain Yukawas, which somehow generate the texture-zeros mentioned [53–57]. Another way of obtaining these textures is through horizontal gauge symmetries, with the assignment of quantum numbers to the fermion sector, which can break the universality of the SM [62,66–81]. This gauge symmetry generates textures that produce flavor changes in the neutral currents and that, in principle, could be seen in future colliders. There are models with electroweak extensions of the SM such as $SO(14)$, $SU(9)$, 3-3-1, $U(1)_X$, etc. [82–97] that attempt to explain the flavor and the mass hierarchy problem of the SM. Another mechanism to generate textures in the Yukawa Lagrangian is through additional discrete or global symmetries. Some groups that have been used in the literature are: S_3, A_4, Δ_{27}, Z_2, etc. [98–110]. The simplest symmetries are of abelian type, which can be used to impose texture-zeros in the mass matrices to make them predictive. On the other hand, given fermion mass matrices with texture-zeros, it is possible to find an extended scalar sector so that the texture-zeros can be generated from abelian symmetries [58,59].

Due to the fact that there are three up-type quarks and three down-type quarks, the mass operators are 3×3 complex matrices with 36 degrees of freedom. If we consider these operators to be Hermitian [111–113], the number of free parameters reduces to 18, which cannot be fully determined from the 10 available physical quantities, namely masses and mixing angles [114]. This provides freedom to reduce the number of free parameters in the matrices and search for matrix structures with zeros that provide eigenvalues and mixing angles consistent with the masses and mixing matrices of the fermions. One way to find zeros in the mass matrices that is automatically consistent with experimental data is based on weak basis transformations (WBT) for quarks and leptons [112,113,115,116]. Fritzsch proposed an ansatz with six zeros [117,118,118–122], but the value of $|V_{ub}/V_{cb}| \approx 0.06$ is too small compared to the experimental value $|V_{ub}/V_{cb}|_{exp} \approx 0.09$ [123]. For this reason, the use of 4 and 5 zero-textures was proposed [111,112,122,124–127]. References [111,113] showed that matrices with five zero-textures could reproduce the mass hierarchy and mixing angles of the CKM matrix.

The strong CP problem arises from the fact that the QCD Lagrangian has a non-perturbative term ("θ-term") that explicitly violates CP in strong interactions. On the other hand, the possible connection between the strong CP problem and flavor problems was first mentioned in [128], and in later works [129–133]. Some recent studies and further references in the same direction are found in [59,129,134–146]. Peccei and Quinn proposed a solution to the strong CP problem [147,148], where it is assumed that the SM has an additional global chiral symmetry $U(1)$, which is spontaneously broken at a large energy scale f_a. One consequence of this breaking is the existence of a particle called the axion, which is the Goldstone boson of the broken $U(1)_{PQ}$ symmetry [149,150]. Due to the fact that the PQ symmetry is not exact at the quantum level, as a result of a chiral anomaly, the axion is massive and its mass (see Appendix D) is given by:

$$m_a = \frac{f_\pi m_\pi}{f_a}\frac{\sqrt{z}}{1+z} \approx 6\mu eV\left(\frac{10^{12}GeV}{f_a}\right), \tag{1}$$

where $z = 0.56$ is assumed for the up and down quark mass ratio, while $f_\pi \approx 92$ MeV and $m_\pi = 135$ MeV are the pion decay constant and mass, respectively.

The effective couplings of axions to ordinary particles are inversely proportional to f_a, and also depend on the model. It was originally thought that the PQ symmetry breaking occurred at the electroweak scale, but experiments have ruled this out. The mass of the axion and its coupling to matter and radiation scale as $1/f_a$, making its direct detection extremely difficult. The combined limits from unsuccessful searches in nuclear and particle physics experiments and from stellar evolution imply that $f_a \geq 3 \times 10^9$ GeV [151]. Furthermore, there is an upper limit of $f_a \leq 10^{12}$GeV that comes from cosmology, since light axions are produced in abundance during the QCD phase transition [152–156]. Hence, these models are generically referred to as "invisible" axion models and remain phenomenologically viable. There are two classes of invisible axion models in the literature: KSVZ (Kim, Shifman, Vainshtein, and Zakharov) [151,157] and DFSZ (Dine, Fischler, Srednicki, and Zhitnitsky) [158,159]. The main difference between KSVZ-type and DFSZ-type axions is that the former do not couple to ordinary quarks and leptons at tree level, but instead require an exotic quark that ensures a nonzero QCD anomaly to generate CP violation. Depending on the assumed value of f_a, the existence of axions could have interesting consequences in astrophysics and cosmology. The emission of axions produced in stellar plasma through their coupling to photons, electrons, and nucleons would provide a new mechanism for energy loss in stars. This could accelerate the evolutionary process of stars and, therefore, shorten their lifespan. Axions can also exist as primordial cosmic relics produced copiously in early times and could be candidates for dark matter. From numerous laboratory experiments and astrophysical observations, together with the cosmological requirement that the contribution to the mass density of the Universe from relic axions does not saturate the Universe. In post-inflationary scenarios, these constraints restrict the allowed values of the axion mass to a range of of [160] 10^{-5} eV $< m_a < 10^{-4}$ eV. One source of axions would be the Sun, which, coupled to two photons, could be produced through the Primakoff conversion of thermal photons in the electric and magnetic fields of the solar plasma. The limits are primarily useful for complementing the arguments of stellar energy loss [161] and the searches for solar axions by CAST at CERN [162] and the Tokyo axion helioscope [163].

The axion–photon coupling (see Appendix D) can be calculated in chiral perturbation theory as [147,148].

$$g_{a\gamma} = -\frac{\alpha}{2\pi f_a}\left(\frac{E}{N} - \frac{2}{3}\frac{z+4}{z+1}\right). \tag{2}$$

This coupling and the axion mass are related to each other through the relation E/N, which depends on the model and can be tested in experiments.

The strongest limits on the axion-electron coupling are derived from observations of stars with a dense core, where bremsstrahlung is very effective. These conditions are realized in White Dwarfs and Red Giant Stars, where the evolution of a White Dwarf is a cooling process by photon radiation and neutrino emission, with the possible addition of new energy loss channels such as axions. Current numerical analysis suggest a limit of $g_{ae} \leq 2.8 \times 10^{-13}$ [160]. In particular, using data from the Sloan Digital Sky Survey (SDSS) and SuperCOSMOS Sky Survey (SCSS) [164], they showed that the axion-electron coupling is approximately 1.4×10^{-13}. In a more recent analysis of the data in Ref. [164] by interpreting anomalous cooling observations in White Dwarfs and Red Giant Stars as a consequence of additional cooling channels induced by axions, the axion-electron coupling is determined to lie within the 2 σ confidence interval $g_{ae} = 1.5^{+0.6}_{-0.9} \times 10^{-13}$ (95% CL) [165,166]. The two groups studying the axion-electron coupling are M5 [161] and M3 [167]. Their combination yields the limit $g_{ae} = 1.6^{+0.29}_{-0.34} \times 10^{-13}$. For a recent and comprehensive review of axion physics, see [160].

This document is organized as follows: In Sect. 2, we review the textures for the quark and lepton mass matrices that will be used in this work. We also write the real parameters of these matrices in terms of the masses of the SM fermions and two free parameters. In Sect. 3, we present the particle content of our model and the necessary PQ charges to generate the mass matrix textures presented in Sect. 2. In Sect. 4, we adjust the Yukawa couplings to obtain the masses of the charged leptons and neutrinos. It is important to note that we cannot use the VEVs to adjust the lepton masses, as these were already adjusted to reproduce the quark masses. It is also important to note that by using a seesaw mechanism, we can avoid adjusting the Yukawas, however, that is not our purpose in the present work. In Sect. 5, we show the Lagrangian of our model. In Sect. 6, we present some constraints in the parameter space, as well as projected constraints for upcoming experimental results, both for experiments under construction and in the data-taking phase.

2 The five texture-zero mass matrices

The reason for dealing with texture zeros in the Standard Model (SM) and its extensions is to simplify as much as possible the number of free parameters that allow us to see relationships between masses and mixings present in these models. The Yukawa Lagrangian is responsible for giving mass to SM fermions after spontaneous symmetry breaking. A first simplification, without losing generality, is to consider that the fermion mass matrices are Hermitian, so the number of free parameters for each sector of quarks and leptons is reduced to 18, but there is still an excess of parameters to reproduce the experimental data provided in the literature. Due to the lack of a model to make predictions, discrete symmetries can be used to prohibit some components in the

Yukawa matrix, generating the so-called texture zeros for the mass matrices. In many works, instead of proposing discrete symmetries, texture zeros are proposed as practical and direct alternatives. The advantage of this approach is that it is possible to choose each mass matrix in an optimal way for the analytical treatment of the problem, and at the same time adjust the mixing angles and the masses of the fermions.

2.1 Quark sector

We should keep in mind that six-zero textures in the SM have already been discarded because their predictions are outside the experimental ranges allowed; but, five-zero textures for quark mass matrices is a viable possibility [55,115,168–171]. Specifically, we chose the following five-zero textures because they fit well with experimental quark masses and mixing parameters [111,113,172]:

$$M^U = \begin{pmatrix} 0 & 0 & C_u \\ 0 & A_u & B_u \\ C_u^* & B_u^* & D_u \end{pmatrix}, \qquad M^D = \begin{pmatrix} 0 & C_d & 0 \\ C_d^* & 0 & B_d \\ 0 & B_d^* & A_d \end{pmatrix}. \tag{3}$$

In addition, the phases in M^D can be removed by a weak basis transformation (WBT) [111,112,116], so that they are absorbed by the off-diagonal terms in M^U. In this way, the mass matrices (3) can be rewritten as:

$$M^U = \begin{pmatrix} 0 & 0 & |C_u|e^{i\phi_{C_u}} \\ 0 & A_u & |B_u|e^{i\phi_{B_u}} \\ |C_u|e^{-i\phi_{C_u}} & |B_u|e^{-i\phi_{B_u}} & D_u \end{pmatrix}, \qquad M^D = \begin{pmatrix} 0 & |C_d| & 0 \\ |C_d| & 0 & |B_d| \\ 0 & |B_d| & A_d \end{pmatrix}, \tag{4}$$

By applying the trace and the determinant to the mass matrices (4), before and after the diagonalization process, the free real parameters of M^U and M^D can be written in terms of their masses:

$$D_u = m_u - m_c + m_t - A_u, \tag{5a}$$

$$|B_u| = \sqrt{\frac{(A_u - m_u)(A_u + m_c)(m_t - A_u)}{A_u}}, \tag{5b}$$

$$|C_u| = \sqrt{\frac{m_u\, m_c\, m_t}{A_u}}, \tag{5c}$$

$$A_d = m_d - m_s + m_b, \tag{5d}$$

$$|B_d| = \sqrt{\frac{(m_b - m_s)(m_d + m_b)(m_s - m_d)}{m_d - m_s + m_b}}, \tag{5e}$$

$$|C_d| = \sqrt{\frac{m_d\, m_s\, m_b}{m_d - m_s + m_b}}. \tag{5f}$$

A possibility that works very well is to consider the second generation of quark masses to be negative, i.e., with eigenvalues $-m_c$ and $-m_s$. And A_u is a free parameter, whose value, determined by the quark mass hierarchy, must be in the following range:

$$m_u \leq A_u \leq m_t. \tag{6}$$

The exact analytical procedure for diagonalizing the mass matrices (4) is indicated in Appendix C.

2.2 Lepton sector

In this work, we will consider Dirac neutrinos. This is achieved, in part, by extending the SM with right-handed neutrinos. In this way, we can carry out a treatment similar to that of the quark sector, that is, the mass matrices of the lepton sector can be considered Hermitian and the weak basis transformation (WBT) can be applied [111,112]. In the literature, work has been done considering various texture-zeros for the Dirac mass matrices of the lepton sector [53,173–184]. In our treatment, we are going to consider the following five-zero texture model studied in the paper [126], which can accurately reproduce the Pontecorvo–Maki–Nakagawa–Sakata (PMNS) mixing matrix V_{PMNS} (mixing angles and the CP violating phase), the charged lepton masses, and the squared mass differences in the normal mass ordering.

$$M^N = \begin{pmatrix} 0 & |C_\nu|e^{ic_\nu} & 0 \\ |C_\nu|e^{-ic_\nu} & E_\nu & |B_\nu|e^{ib_\nu} \\ 0 & |B_\nu|e^{-ib_\nu} & A_\nu \end{pmatrix}, \qquad M^E = \begin{pmatrix} 0 & |C_\ell| & 0 \\ |C_\ell| & 0 & |B_\ell| \\ 0 & |B_\ell| & A_\ell \end{pmatrix}. \tag{7}$$

Without loss of generality, by using a WBT, the phases of the charged lepton mass matrix, M^E, can be absorbed into the entries C_ν and B_ν of the neutrino mass matrix, M^N. Similarly, as was done in the case of the quark sector, the parameters present in the mass matrices of the lepton sector (7) can be expressed in terms of the masses of the charged leptons m_e, m_μ and m_τ and the masses of the neutrinos m_1, m_2 and m_3, in the normal ordering ($m_1 < m_2 < m_3$):

$$A_\ell = m_e - m_\mu + m_\tau, \tag{8a}$$

$$|B_\ell| = \sqrt{\frac{(m_\tau - m_\mu)(m_e + m_\tau)(m_\mu - m_e)}{m_e - m_\mu + m_\tau}}, \tag{8b}$$

$$|C_\ell| = \sqrt{\frac{m_e m_\mu m_\tau}{m_e - m_\mu + m_\tau}}, \tag{8c}$$

$$E_\nu = m_1 - m_2 + m_3 - A_\nu, \tag{8d}$$

$$|B_\nu| = \sqrt{\frac{(A_\nu - m_1)(A_\nu + m_2)(m_3 - A_\nu)}{A_\nu}}, \tag{8e}$$

$$|C_\nu| = \sqrt{\frac{m_1 m_2 m_3}{A_\nu}}, \tag{8f}$$

where the values of the masses and the parameter A_ν are given in Table 5. Furthermore, for the adjustment of the mass matrices (7) it is very convenient to assume that the eigenvalues associated with the masses of the second family, $-m_2$ and $-m_\mu$, are negative quantities. The exact diagonalizing matrices of the mass matrices (7) are shown in Appendix C, Eqs. (49), (50) and (51).

3 PQ symmetry and the minimal particle content

3.1 Yukawa Lagrangian and the PQ symmetry

The texture-zeros of the mass matrices defined in the Eqs. (4) and (7) can be generated by imposing a Peccei–Queen symmetry $U(1)_{PQ}$ on the Lagrangian model, Eq. (9) [59,185,186]. As will be explained below, the minimal Lagrangian that allows us to implement this symmetry is given by [58,187]

$$\begin{aligned}\mathcal{L}_{\rm LO} \supset\ & (D_\mu \Phi^\alpha)^\dagger D^\mu \Phi^\alpha + \sum_\psi i\bar{\psi}\gamma^\mu D_\mu \psi + \sum_{i=1}^{2}(D_\mu S_i)^\dagger D^\mu S_i \\ & - \Big(\bar{q}_{Li}\, y_{ij}^{D\alpha}\Phi^\alpha d_{Rj} + \bar{q}_{Li}\, y_{ij}^{U\alpha}\tilde{\Phi}^\alpha u_{Rj} \\ & + \bar{\ell}_{Li}\, y_{ij}^{E\alpha}\Phi^\alpha e_{Rj} + \bar{\ell}_{Li}\, y_{ij}^{N\alpha}\tilde{\Phi}^\alpha \nu_{Rj} + \text{h.c}\Big) \\ & + (\lambda_Q \bar{Q}_R Q_L S_2 + \text{h.c}) - V(\Phi, S_1, S_2)\,. \end{aligned} \tag{9}$$

As it was shown in Ref. [58], at least four Higgs doublets are required to generate the quark mass textures, therefore $\alpha = 1,2,3,4$. In (9) i, j are family indices (there is an implicit sum over repeated indices). The superscripts U, D, E, N refer to up-type quarks, down-type quarks, electron-like and neutrino-like fermions, respectively; and $D_\mu = \partial_\mu + i\Gamma_\mu$ is the covariant derivative in the SM. The scalar potential $V(\Phi, S_1, S_2)$ is shown in appendix A (for further details, see Ref. [58]). In Eq. (9) ψ stands for the SM fermion fields plus the heavy quark Q (see Tables 1 and 2). As it is shown in Table 2 the PQ charges of the heavy quark can be chosen in such a way that only the interaction with the scalar singlet S_2 is allowed. We assign $Q_{\rm PQ}$ charges for the left-handed quark doublets (q_L): x_{q_i}, right-handed up-type quark singlets (u_R): x_{u_i}, right-handed down-type quark singlets (d_R): x_{d_i}, left-handed lepton doublets (ℓ_L): x_{ℓ_i}, right-handed charged leptons (e_R): x_{e_i} and right-handed Dirac neutrinos (ν_R): x_{ν_i} for each family ($i = 1,2,3$). We follow a similar notation for the scalar doublets, x_{ϕ_α} ($\alpha = 1,2,3,4$), and the scalar singlets $x_{S_{1,2}}$.

In this work, the PQ charges assigned to the quark sector and the scalar sector, as well as the VEVs assigned to the scalar doublets, will be the same as those assigned in [58] (Tables 1 and 2), and we will adjust the PQ charges of the lepton sector to reproduce the texture-zeros given in Eq. (7). To forbid a given entry in the lepton mass matrices, the corresponding sum of PQ charges must be different from zero, so that we can obtain texture-zeros by imposing the following conditions:

$$M^N = \begin{pmatrix} 0 & x & 0 \\ x & x & x \\ 0 & x & x \end{pmatrix} \longrightarrow \begin{pmatrix} S_{11}^{N\alpha} \neq 0 & S_{12}^{N\alpha} = 0 & S_{13}^{N\alpha} \neq 0 \\ S_{21}^{N\alpha} = 0 & S_{22}^{N\alpha} = 0 & S_{23}^{N\alpha} = 0 \\ S_{31}^{N\alpha} \neq 0 & S_{32}^{N\alpha} = 0 & S_{33}^{N\alpha} = 0 \end{pmatrix}, \tag{10}$$

$$M^E = \begin{pmatrix} 0 & x & 0 \\ x & 0 & x \\ 0 & x & x \end{pmatrix} \longrightarrow \begin{pmatrix} S_{11}^{E\alpha} \neq 0 & S_{12}^{E\alpha} = 0 & S_{13}^{E\alpha} \neq 0 \\ S_{21}^{E\alpha} = 0 & S_{22}^{E\alpha} \neq 0 & S_{23}^{E\alpha} = 0 \\ S_{31}^{E\alpha} \neq 0 & S_{32}^{E\alpha} = 0 & S_{33}^{E\alpha} = 0 \end{pmatrix}, \tag{11}$$

where $S_{ij}^{N\alpha} = (-x_{\ell_i} + x_{\nu_j} - x_{\phi_\alpha})$ and $S_{ij}^{E\alpha} = (-x_{\ell_i} + x_{e_j} + x_{\phi_\alpha})$.

Since the PQ charges of the Higgs doublets ($\alpha = 1,2,3,4$) are already given, the possible solutions of (10) and (11) are strongly constrained. Table 1 provides a solution for the PQ charges of the lepton sector.

In our model we include two scalar singlets S_1 and S_2 that break the global symmetry $U(1)_{PQ}$. The QCD anomaly of the PQ charges is

$$N = 2\sum_i^3 x_{q_i} - \sum_i^3 x_{u_i} - \sum_i^3 x_{d_i} + A_Q\,, \tag{12}$$

where $A_Q = x_{QL} - x_{QR}$ is the contribution to the anomaly of the heavy quark Q, which is a singlet under the electroweak gauge group, with left (right) Peccei-Quinn charges $x_{QL,R}$, respectively. We can write the charges as a function of N (since N must be different from zero), such that

$$s_1 = \frac{N}{9}\hat{s}_1, \qquad s_2 = \frac{N}{9}\left(\epsilon + \hat{s}_1\right), \quad \text{with} \quad \epsilon = 1 - \frac{A_Q}{N}\,, \tag{13}$$

where $\hat{s}_1$ and ϵ are arbitrary real numbers. To solve the strong CP problem with $N \neq 0$ and simultaneously generate the texture-zeros in the mass matrices, it is necessary to maintain $\epsilon = \frac{9(s_2 - s_1)}{N} \neq 0$. With these definitions for Flavor-Changing Neutral Currents (FCNC) observables, the relevant parameters are $\hat{s}_1$ and ϵ. This parameterization is quite convenient (for those cases where the parameters α_q and α_ℓ are not relevant) because by fixing N and f_a, we can vary $\hat{s}_1$ and ϵ for a fixed $\Lambda_{\rm PQ} = f_a N$ in such a way that the parameter space naturally reduces to two dimensions.

Table 1 Particle content. The subindex $i = 1, 2, 3$ stand for the family number in the interaction basis. Columns 6–8 are the Peccei-Quinn charges, Q_{PQ}, for each family of quarks and leptons in the SM. s_1, s_2 and α are real parameters, with $s_1 \neq s_2$

Particles	Spin	$SU(3)_C$	$SU(2)_L$	$U(1)_Y$	$U_{\rm PQ}(i=1)$	$U_{\rm PQ}(i=2)$	$U_{\rm PQ}(i=3)$	$Q_{\rm PQ}$
q_{Li}	1/2	3	2	1/6	$-2s_1+2s_2+\alpha_q$	$-s_1+s_2+\alpha_q$	α_q	x_{q_i}
u_{Ri}	1/2	3	1	2/3	$s_1+\alpha_q$	$s_2+\alpha_q$	$-s_1+2s_2+\alpha_q$	x_{u_i}
d_{Ri}	1/2	3	1	$-1/3$	$2s_1-3s_2+\alpha_q$	$s_1-2s_2+\alpha_q$	$-s_2+\alpha_q$	x_{d_i}
ℓ_{Li}	1/2	1	2	$-1/2$	$-2s_1+2s_2+\alpha_\ell$	$-s_1+s_2+\alpha_\ell$	α_ℓ	x_{ℓ_i}
e_{Ri}	1/2	1	1	-1	$2s_1-3s_2+\alpha_\ell$	$s_1-2s_2+\alpha_\ell$	$-s_2+\alpha_\ell$	x_{e_i}
ν_{Ri}	1/2	1	1	0	$-4s_1+5s_2+\alpha_\ell$	$-s_1+2s_2+\alpha_\ell$	$s_2+\alpha_\ell$	x_{ν_i}

Table 2 Beyond the SM fields and their respective PQ charges. The parameters s_1, s_2 are reals, with $s_1 \neq s_2$ and $x_{Q_R} \neq x_{Q_L}$

Particles	Spin	$SU(3)_C$	$SU(2)_L$	$U(1)_Y$	$U_{\rm PQ}$	$Q_{\rm PQ}$
Φ_1	0	1	2	1/2	s_1	x_{ϕ_1}
Φ_2	0	1	2	1/2	s_2	x_{ϕ_2}
Φ_3	0	1	2	1/2	$-s_1+2s_2$	x_{ϕ_3}
Φ_4	0	1	2	1/2	$-3s_1+4s_2$	x_{ϕ_4}
Q_L	1/2	3	1	0	x_{Q_L}	x_{Q_L}
Q_R	1/2	3	1	0	x_{Q_R}	x_{Q_R}
S_1	0	1	1	0	s_1-s_2	x_{S_1}
S_2	0	1	1	0	$x_{Q_R}-x_{Q_L}$	x_{S_2}

4 Naturalness of Yukawa couplings

4.1 The mass matrices in the quark sector

In Ref. [58], it was shown that to generate five texture zeros in the quark mass matrices (3), as a consequence of a PQ symmetry, it is necessary to include at least four scalar doublets in the model. After spontaneous symmetry breaking, the quark sector mass matrices take on the following form:

$$M^U = \hat{v}_\alpha y_{ij}^{U\alpha} = \begin{pmatrix} 0 & 0 & y_{13}^{U1}\hat{v}_1 \\ 0 & y_{22}^{U1}\hat{v}_1 & y_{23}^{U2}\hat{v}_2 \\ y_{13}^{U1*}\hat{v}_1 & y_{23}^{U2*}\hat{v}_2 & y_{33}^{U3}\hat{v}_3 \end{pmatrix},$$
$$M^D = \hat{v}_\alpha y_{ij}^{D\alpha} = \begin{pmatrix} 0 & |y_{12}^{D4}|\hat{v}_4 & 0 \\ |y_{12}^{D4}|\hat{v}_4 & 0 & |y_{23}^{D3}|\hat{v}_3 \\ 0 & |y_{23}^{D3}|\hat{v}_3 & y_{33}^{D2}\hat{v}_2 \end{pmatrix}, \quad (14)$$

where the $\hat{v}_i$ are defined in terms of the vacuum expectation values, $\hat{v}_i = v_i/\sqrt{2}$. In [58] it was shown that the five-texture zeros (4) are flexible enough to set the quark Yukawa couplings close to 1 for most of them (except for y_{23}^{U2}, y_{23}^{D3} and y_{13}^{U1}), in this way we obtain:

$$\hat{v}_1 = 1.71\,\text{GeV}, \qquad \hat{v}_2 = 2.91\,\text{GeV},$$
$$\hat{v}_3 = 174.085\,\text{GeV}, \qquad \hat{v}_4 = 13.3\,\text{MeV}. \quad (15)$$

As we can see, the hermiticity of the mass matrices is not fully achieved, but it is good to impose it for several reasons: (i) In the SM and its extensions, in which the right chirality fields are singlets under $SU(2)$, the mass matrices can be assumed Hermitian without losing generality, (ii) the previous fact allows us to consider Hermitian mass matrices, even after imposing an additional PQ symmetry in the model, (iii) we can implement the WBT method [111], and (iv) there is an extensive literature on physically viable Hermitian mass matrices. It is important to noticing that the mass matrices in Eq. (14) are Hermitian.

4.2 The mass matrices in the lepton sector

We can obtain the lepton mass matrices by starting from the Yukawa Lagrangian (9), which is invariant under the Peccei-Quinn $U(1)_{PQ}$ symmetry, and taking into account the Yukawa parameters and expectation values (15). After the spontaneous symmetry breaking, the mass matrices for neutral and charged leptons are given respectively by [126,188]:

$$M^N = \hat{v}_\alpha y_{ij}^{N\alpha} = \begin{pmatrix} 0 & y_{12}^{N1}\hat{v}_1 & 0 \\ y_{21}^{N4}\hat{v}_4 & y_{22}^{N2}\hat{v}_2 & y_{23}^{N1}\hat{v}_1 \\ 0 & y_{32}^{N3}\hat{v}_3 & y_{33}^{N2}\hat{v}_2 \end{pmatrix}, \quad (16)$$
$$M^E = \hat{v}_\alpha y_{ij}^{E\alpha} = \begin{pmatrix} 0 & |y_{12}^{E4}|\hat{v}_4 & 0 \\ |y_{12}^{E4}|\hat{v}_4 & 0 & |y_{23}^{E3}|\hat{v}_3 \\ 0 & |y_{23}^{E3}|\hat{v}_3 & y_{33}^{E2}\hat{v}_2 \end{pmatrix}. \quad (17)$$

As we previously mentioned, at least four Higgs doublets are needed to obtain the five texture-zeros for the chosen quark

mass matrices. Our goal in this work is to keep the same number of Higgs doublets and their respective PQ charges to generate the mass matrices and texture zeros for the lepton sector, Eq. (7). To get an Hermitian mass matrix M^N, it is necessary to impose $y_{21}^{N4}/y_{12}^{N1*} = \hat{v}_1/\hat{v}_4$ and $y_{32}^{N3}/y_{23}^{N1*} = \hat{v}_1/\hat{v}_3$, requiring that the diagonal elements be real, i.e., $y_{22}^{N2} = y_{22}^{N2*}$ and $y_{33}^{N2} = y_{33}^{N2*}$. On the other hand, to obtain a symmetric mass matrix, M^E, for the charged leptons, it is sufficient to assume that the Yukawa couplings are Hermitian. Through these choices it is possible to avoid additional Higgs doublets.

Based on the results of Table 5, Appendix C, and the relationships established in (8), we find the following values for the Yukawa couplings of the lepton sector:

$$
\begin{aligned}
|y_{12}^{E4}| &= 0.569582, & |y_{23}^{E3}| &= 0.00248291,\\
y_{33}^{E2} &= 0.574472, & |y_{12}^{N1}| &= 4.74362 \times 10^{-6},\\
|y_{21}^{N4}| &= 0.000609894, & y_{22}^{N2} &= 6.68808 \times 10^{-6},\\
|y_{23}^{N1}| &= 0.0000159881, & |y_{32}^{N3}| &= 1.57047 \times 10^{-7},\\
y_{33}^{N2} &= 8.65364 \times 10^{-6}.
\end{aligned}
$$

To reproduce the neutrino masses quoted in [126], in the SM is required a Yukawa coupling around 10^{-14}. In our case, the smallest Yukawa coupling is 10^{-7}, which significantly reduces the fine-tuning in comparison to that given by the SM.

5 The effective Lagrangian

The strongest constraints on non-universal PQ charges come from the FCNC. To determine these constraints, we start by writing the most general next-to-leading order (NLO) effective Lagrangian as [189,190]:

$$
\mathcal{L}_{\rm NLO} = c_{a\Phi^\alpha} O_{a\Phi^\alpha} + c_1 \frac{\alpha_1}{8\pi} O_B + c_2 \frac{\alpha_2}{8\pi} O_W + c_3 \frac{\alpha_3}{8\pi} O_G, \tag{18}
$$

$c_{a\Phi^\alpha}$ and $c_{1,2,3}$ are Wilson coefficients; $\alpha_{1,2,3} = \frac{g_{1,2,3}^2}{4\pi}$, where $g_{1,2,3}$ are the coupling strengths of the electroweak and strong interactions in the interaction basis; and the Wilson operators are:

$$
\begin{aligned}
O_{a\Phi} &= i \frac{\partial^\mu a}{\Lambda_{\rm PQ}} \left((D_\mu \Phi^\alpha)^\dagger \Phi^\alpha - \Phi^{\alpha\dagger} (D_\mu \Phi^\alpha) \right),\\
O_B &= -\frac{a}{\Lambda_{\rm PQ}} B_{\mu\nu} \tilde{B}^{\mu\nu},\\
O_W &= -\frac{a}{\Lambda_{\rm PQ}} W_{\mu\nu}^a \tilde{W}^{a\mu\nu},\\
O_G &= -\frac{a}{\Lambda_{\rm PQ}} G_{\mu\nu}^a \tilde{G}^{a\mu\nu},
\end{aligned} \tag{19}
$$

where B, W^a and G^a correspond to the gauge fields associated with the SM gauge groups $U(1)_Y$, $SU(2)_L$ and $SU(3)_C$, respectively. a is the axion field which corresponds to the CP odd component of S_1. It is possible to redefine the fields by multiplying by a phase

$$
\begin{aligned}
\Phi^\alpha &\longrightarrow e^{i \frac{x_{\Phi^\alpha}}{\Lambda_{\rm PQ}} a} \Phi^\alpha,\\
\psi_L &\longrightarrow e^{i \frac{x_{\psi_L}}{\Lambda_{\rm PQ}} a} \psi_L,\\
\psi_R &\longrightarrow e^{i \frac{x_{\psi_R}}{\Lambda_{\rm PQ}} a} \psi_R,\\
S_i &\longrightarrow e^{i \frac{x_{S_i}}{\Lambda_{\rm PQ}} a} S_i.
\end{aligned} \tag{20}
$$

In this expression, x_ψ corresponds to the PQ charges of the SM fermions, i.e., $\{x_{\psi_{L,R}}\} = \{x_{q_i}, x_{u_i}, x_{d_i}, x_{l_i}, x_{e_i}, x_{\nu_i}\}$ and $\{x_{\Phi^\alpha}\}$ are the PQ charges of the Higgs doublets $\{\Phi^\alpha\}$. Replacing these definitions in the kinetic terms of Eq. (9), we obtain new contributions to the effective Lagrangian Eq. (18) (the NLO contributions in the non-derivative terms cancel out). The leading order (LO) terms in $\Lambda_{\rm PQ}^{-1}$ can be written as [187,189]:

$$
\mathcal{L}_{\rm NLO} \longrightarrow \mathcal{L}_{\rm NLO} + \Delta\mathcal{L}_{\rm NLO}, \tag{21}
$$

where

$$
\Delta\mathcal{L}_{\rm NLO} = \Delta\mathcal{L}_{K^\Phi} + \Delta\mathcal{L}_{K^\psi} + \Delta\mathcal{L}_{K^S} + \Delta\mathcal{L}(F_{\mu\nu}), \tag{22}
$$

with

$$
\begin{aligned}
\Delta\mathcal{L}_{K^\Phi} &= i x_{\Phi^\alpha} \frac{\partial^\mu a}{\Lambda_{\rm PQ}} \left[(D_\mu \Phi^\alpha)^\dagger \Phi^\alpha - \Phi^{\alpha\dagger} (D_\mu \Phi^\alpha) \right],\\
\Delta\mathcal{L}_{K^\psi} &= \frac{\partial_\mu a}{2\Lambda_{\rm PQ}} \sum_\psi (x_{\psi_L} - x_{\psi_R}) \bar{\psi} \gamma^\mu \gamma^5 \psi\\
&\quad - (x_{\psi_L} + x_{\psi_R}) \bar{\psi} \gamma^\mu \psi,\\
\Delta\mathcal{L}_{K^S} &= i x_{S_i} \frac{\partial^\mu a}{\Lambda_{\rm PQ}} \left[(D_\mu S_i)^\dagger S_i - S_i^\dagger (D_\mu S_i) \right] + \text{h.c}.
\end{aligned} \tag{23}
$$

The field redefinitions (20) induce a modification in the measure of the functional path integral whose effects can be obtained from the divergence of the axial-vector current: $J_\mu^{PQ5} = \sum_\psi (x_{\psi_L} - x_{\psi_R}) \bar{\psi} \gamma_\mu \gamma^5 \psi$ [191],

$$
\begin{aligned}
\partial^\mu J_\mu^{PQ5} &= \sum_\psi 2 i m_\psi (x_{\psi_L} - x_{\psi_R}) \bar{\psi} \gamma^5 \psi\\
&\quad - \sum_\psi (x_{\psi_L} - x_{\psi_R}) \frac{\alpha_1 Y^2(\psi)}{2\pi} B_{\mu\nu} \tilde{B}^{\mu\nu}
\end{aligned}
$$

$$- \sum_{SU(2)_L \text{doublets}} x_{\psi_L} \frac{\alpha_2}{4\pi} W^a_{\mu\nu} \tilde{W}^{a\mu\nu} - \sum_{SU(3)\text{triplets}} (x_{\psi_L} - x_{\psi_R}) \frac{\alpha_3}{4\pi} G^a_{\mu\nu} \tilde{G}^{a\mu\nu}, \tag{24}$$

where the hypercharge is normalized by $Q = T_{3L} + Y$. The relation (24) is an on-shell relation, which is consistent with the momentum of an on-shell axion.

Substituting this result into $\mathcal{L}_{K^\psi} = \frac{\partial^\mu a}{2\Lambda_{\rm PQ}} J^{PQ5}_\mu = -\frac{a}{2\Lambda_{\rm PQ}} \partial^\mu J^{PQ5}_\mu$ we obtain new contributions to the leading-order Wilson coefficients [192]

$$\begin{aligned} c_1 &\longrightarrow c_1 - \frac{1}{3}\Sigma q + \frac{8}{3}\Sigma u + \frac{2}{3}\Sigma d - \Sigma \ell + 2\Sigma e, \\ c_2 &\longrightarrow c_2 - 3\Sigma q - \Sigma \ell, \\ c_3 &\longrightarrow c_3 - 2\Sigma q + \Sigma u + \Sigma d - A_Q, \end{aligned} \tag{25}$$

where $\Sigma q \equiv x_{q_1} + x_{q_2} + x_{q_3}$. The corresponding NLO Lagrangian is

$$\begin{aligned} \Delta\mathcal{L}(F_{\mu\nu}) = &\frac{a}{\Lambda_{\rm PQ}} \frac{\alpha_1}{8\pi} B_{\mu\nu} \tilde{B}^{\mu\nu} \left(\frac{1}{3}\Sigma q - \frac{8}{3}\Sigma u - \frac{2}{3}\Sigma d + \Sigma \ell - 2\Sigma e \right) \\ &+ \frac{a}{\Lambda_{\rm PQ}} \frac{\alpha_2}{8\pi} W^a_{\mu\nu} \tilde{W}^{a\mu\nu} \left(3\Sigma q + \Sigma \ell\right) \\ &+ \frac{a}{\Lambda_{\rm PQ}} \frac{\alpha_3}{8\pi} G^a_{\mu\nu} \tilde{G}^{a\mu\nu} \left(2\Sigma q - \Sigma u - \Sigma d + A_Q\right). \end{aligned} \tag{26}$$

It is convenient to define $c_3^{\rm eff} = c_3 - 2\Sigma q + \Sigma u + \Sigma d - A_Q = -N$. In our case, $c_i = 0$ and the only contributions to $c_i^{\rm eff}$ come from the anomaly. It is customary to define $\Lambda_{\rm PQ} = f_a |c_3^{\rm eff}|$ to include the factor $c_3^{\rm eff}$ in the normalization of the PQ charges. From now on, we will assume that all the PQ charges are normalized in this way, so that x_ψ corresponds to $x_\psi / c_3^{\rm eff}$. For normalized charges, $c_3^{\rm eff} = 1$, therefore, we still maintain the general form despite writing all the expressions in terms of the effective scale f_a.

The scalar fields and their PQ charges are the same as in the Ref. [58], so the scalar potential $V(\Phi, S)$ is identical to that of the mentioned reference. With the VEVs and couplings given in [58], the model reproduces the mass of the SM Higgs, while the masses of the exotic scalars are above the TeV scale. This potential has the appropriate number of Goldstone bosons to give masses to the SM gauge bosons Z^0, $W^\pm$ and has an extra field that can be identified with the axion a.

6 Low energy constraints

6.1 Flavor changing neutral currents

Due to the non-universal PQ charges in our model, a tree-level analysis of flavor-changing neutral currents is necessary. As mentioned in Ref. [160], the strongest limits on the axion-quark FCNC couplings come from meson decays in light mesons and missing energy.

The decays $K^\pm \to \pi^\pm a$ provide the tightest limits (NA62 Collaboration [193]) for the axion mass [160]. Currently the most restrictive limits come from the semileptonic decays of kaons $K^\pm \to \pi^\pm \bar{\nu}\nu$ and leptons $\ell_1 \to \ell_2$+missing energy. From the term $\Delta\mathcal{L}_{K^\psi}$, we obtain the vector and axial couplings for a multi-Higgs sector model, as shown in Refs. [58,160]

$$\Delta\mathcal{L}_{K^\psi} = -\partial_\mu a \bar{f}_i \gamma^\mu \left(g^V_{af_if_j} + \gamma^5 g^A_{af_if_j} \right) f_j, \tag{27}$$

where

$$g^{V,A}_{af_if_j} = \frac{1}{2 f_a c_3^{\rm eff}} \Delta^{Fij}_{V,A}, \tag{28}$$

where:

$$\Delta^{Fij}_{V,A} = \Delta^{Fij}_{RR}(d) \pm \Delta^{Fij}_{LL}(q), \tag{29}$$

with $\Delta^{Fij}_{LL}(q) = \left(U^F_L x_q \, U^{F\dagger}_L \right)^{ij}$ and $\Delta^{Fij}_{RR}(d) = \left(U^F_R x_d \, U^{F\dagger}_R \right)^{ij}$. In these expressions, F stands for U, D, N or E and the $U^F_{L,R}$ are de diagonalizing matrices (see Appendix C). In Eq. (28), we normalize the charges using $c_3^{\rm eff}$, as explained in the last paragraph of Sect. 5 (in other references $|c_3^{\rm eff}| = |N|$ is considered, corresponding to the $SU(3) \times U(1)_{PQ}$ anomaly). The branching ratio for lepton decays $\ell_i \to \ell_j a$ is given by [134]

$$\text{Br}(\ell_1 \to \ell_2 a) = \frac{m^3_{\ell_1}}{16\pi \Gamma(\ell_1)} \left(1 - \frac{m^2_{\ell_2}}{m^2_{\ell_1}} \right)^3 |g_{a\ell_1\ell_2}|^2,$$

in this expression, the vector and axial couplings contribute in the same way

$$|g_{a\ell_1\ell_2}|^2 = |g^V_{a\ell_1\ell_2}|^2 + |g^A_{a\ell_1\ell_2}|^2.$$

where m is the mass of the leptons and $\Gamma(\ell_i)$ is the total decay width of the particle ℓ_j.

For the lepton decay $\ell_i \to \ell_j a \gamma$, we can relate this branching ratio to the branching ratio of the process without the photon in the final state, according to the expression:

$$\text{Br}(\ell_1 \to \ell_2 a \gamma) = \left(\frac{\alpha}{2\pi} \int dx \, dy f(x, y) \right) \text{Br}(\ell_1 \to \ell_2 a),$$

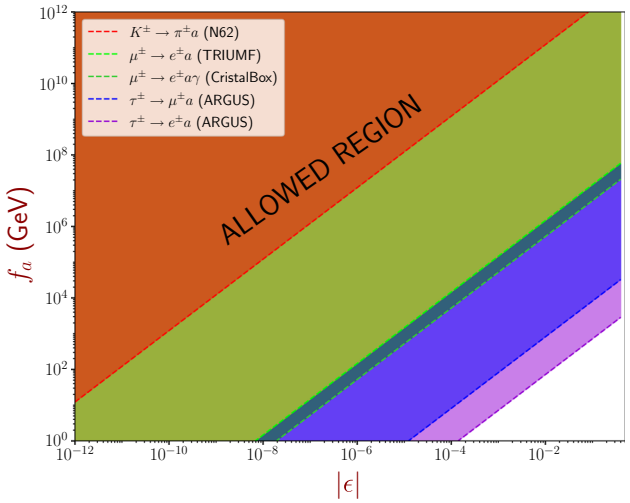

Fig. 1 Allowed regions by lepton decays. For the down-type quarks and charged leptons the non-universal part of the PQ charges just depend on the diference $s_2 - s_1 = N\epsilon/9$, hence the flavor-changing neutral-current couplings (the off diagonal elements) just depend on ϵ

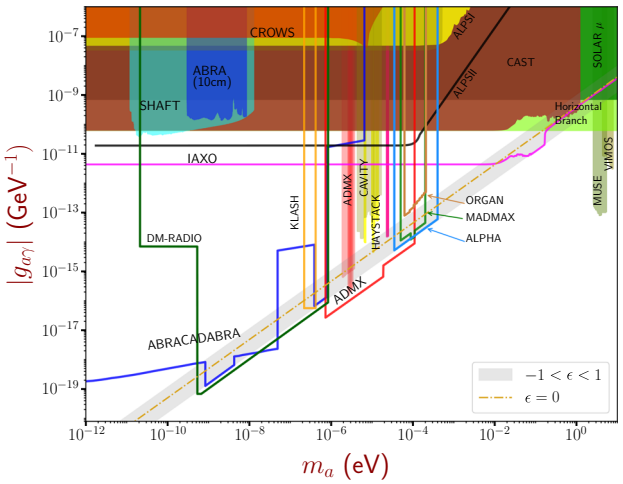

Fig. 2 The excluded parameter space by various experiments corresponds to the colored regions, the dashed-lines correspond to the projected bounds of coming experiments looking for axion signals [199]. The gray region corresponds to the parameter space scanned by our model

where α is the fine structure constant, and the function:

$$f(x, y) = \frac{(1-x)(2-y-xy)}{y^2(x+y-1)} \tag{30}$$

depends on the mass and the energies $x = 2E_{\ell_2}/m_{\ell_1}$ and $y = 2E_\gamma/m_{\ell_1}$. For the lepton decay $\mu \to e\,a\,\gamma$, the constraints come from the Crystal Box experiment [194], with cut energies $E_\gamma, E_e > 30\,\text{MeV}, \theta_{e\gamma} > 140°$, where:

$$\cos\theta_{e\gamma} = 1 + \frac{2(1-x-y)}{xy}, \tag{31}$$

so that $\int dx\,dy f(x, y) \approx 0.011$ (Table 3).

In our model, there is a natural alignment between the Φ_3 (which is quite similar to H_1 in the Georgi basis [198]) and the standard model Higgs boson as a consequence of the large suppression of the VEVs of the scalar doublets v_i, with $i = 1, 2, 4$, respect to v_3, the VEV of Φ_3. To some extent, this alignment avoids FCNC involving the SM Higgs boson [198]; however, after alignment, there are other sources of FCNC associated with the additional scalar doublets, which cannot be avoided by any means; however, as argued in Ref. [58] they are suppressed by a factor $1/M^4$ (where $M > 1\text{TeV}$ is the mass of the exotic scalar doublets), and therefore, our model avoids these potential sources of FCNC in agreement with the general argument presented in [198].

From astrophysical considerations we have: bounds from black holes superradiance and the SN 1987A upper limit on the neutron electric dipole moment, which, when combined, impose a constraint on the axion decay constant in the range [160] (see Fig. 1): $0.8 \times 10^6\text{GeV} \leq f_a \leq 2.8 \times 10^{17}\text{GeV}$.

6.2 Constraints on the axion–photon coupling

There are several experiments designed to look for exotic particles. The sources studied in the search for axions are: the solar axion flux (helioscopes experiments), dark matter halo (haloscopes experiments), and axions produced in the laboratory.

Among the experiments with the potential to search for evidence of axions in regions that cover areas within the limits established by the parameters of our model are: DM-Radio [200], KLASH [201,202], ADMX [203], ALPHA [204], MADMAX [205], IAXO [206,207] and ABRACADABRA [208]. Similarly, some experiments have already ruled out regions established by the parameters of our model, among which are: ADMX [209–211], CAST [212,213], CAPP [214–216], HAYSTACK [217,218], Solar ν [219], Horizontal Branch [220], MUSE [221] and VIMOS [222]

7 Discussion and conclusions

We have presented a model in which the fermion and scalar fields are charged under a $U(1)_{PQ}$ Peccei-Quinn symmetry. A recent work [58] showed that at least four Higgs doublets are required to generate Hermitian mass matrices in the quark sector with five texture-zeros, reproducing the quark masses, the mixing angles, and the CP-violating phase of the CKM mixing matrix. In this work, we show that using the same number of Higgs doublets, without changing the PQ charges in the quark and Higgs sectors, it is possible to generate Hermitian mass matrices in the lepton sector that reproduce the neutrino mass-squared differences in the normal mass

Table 3 These inequalities come from the window for new physics in the branching ratio uncertainty of the meson decay in a pair $\bar{\nu}\nu$

Collaboration	Upper bound
N62 collaboration [193]	$\mathcal{B}\left(K^+ \to \pi^+ a\right) < (10.6^{+4.0}_{-3.4}\big\vert_{stat} \pm 0.9_{syst}) \times 10^{-11}$
TRIUMF [195]	$\mathcal{B}\left(\mu^+ \to e^+ a\right) < 2.6 \times 10^{-6}$
Crystal Box [196]	$\mathcal{B}\left(\mu^+ \to e^+ \gamma a\right) < 1.1 \times 10^{-9}$
ARGUS [197]	$\mathcal{B}\left(\tau^+ \to e^+ a\right) < 1.5 \times 10^{-2}$
ARGUS [197]	$\mathcal{B}\left(\tau^+ \to \mu^+ a\right) < 2.6 \times 10^{-2}$

ordering, the mixing angles, and the CP-violating phase of the PMNS mixing matrix. This result is quite non-trivial as we maintain the same four Higgs doublets required in the quark sector to generate a different texture pattern in the lepton sector. When compared to the SM, our model has almost all Yukawa couplings close to 1 in the quark sector. In the neutrino sector, the smallest Yukawa coupling is of the order of 1.6×10^{-7}, which is seven orders of magnitude larger than the corresponding Yukawa coupling in the SM, so it requires less fine-tuning than the SM.

The polar decomposition theorem [223,224] allows any matrix to be written as the product of a Hermitian matrix and a unitary matrix. In the SM and in theories where the right-handed fermion fields are singlets under the gauge group, it is possible to absorb the unitary matrix into the right-handed fields by redefining them; from this procedure, we can write any mass matrix as a Hermitian matrix. In our work, we assume that the mass matrices are Hermitian in the interaction space, this hypothesis has been used in previous studies on textures [55,111,115,225–227], and it is quite useful for studying the flavor problem. In our work, we have normalized the PQ charges with the QCD anomaly $-N$ in such a way that by keeping the parameter $\epsilon \neq 0$, we obtain the textures of the mass matrices, addressing the flavor and strong CP problems simultaneously.

If nature is not fine-tuned in a more fundamental high-energy theory, we expect that, eventually, it will be possible to find a texture that allows us to obtain all the scales of the SM from the VEVs of a Higgs sector with a minimal scalar content without the need to adjust the Yukawa couplings.

In our analysis, we report the constraints from lepton decays and compare them with the constraints from the search for neutrino pairs in charged Kaon decays $K^{\pm} \longrightarrow \pi^{\pm}\bar{\nu}\nu$. The results are shown in Fig. 1, where the allowed region in the parameter space generated by ϵ and the axion decay constant f_a is displayed. This figure shows that the strongest constraints come from the semileptonic meson decay $K^{\pm} \to \pi\nu\bar{\nu}$. It is important to note that the lepton decays do not further constrain the parameter space of our model (compared to the region excluded by the meson decay). We also show the excluded regions for the axion–photon coupling as a function of the axion mass; these results are summarized in Fig. 2; the gray region corresponds to the parameter space of our model in the interval $-1 < \epsilon < 1$.

In this article, we have demonstrated that with four Higgs doublets, it is possible to fit the textures of the mass matrices, both in the lepton and quark sectors. These matrices generate the masses and the mixing matrices for quarks and leptons within the experimentally reported values in the literature. The introduction these doublets improves the fine-tuning problem of the Yukawa couplings and shows that this approach is a viable way to tackle the flavor problem. We hope to improve our results in future work by using the See-saw mechanism in the lepton sector.

Acknowledgements We thank Financial support from "Patrimonio Autónomo Fondo Nacional de Financiamiento para la Ciencia, la Tecnología y la Innovación, Francisco José de Caldas". This research was partly supported by the "Vicerrectoría de Investigaciones e Interacción Social VIIS de la Universidad de Nariño", project numbers 1928, 2172, 2686, 2693 and 2679. E.R and Y.G. acknowledge additional financial support from Minciencias CD 82315 CT ICETEX 2021-1080.

Data Availability Statement This manuscript has no associated data or the data will not be deposited. [Authors' comment: The article is self-contained, and that experimental data have been taken from published articles and correctly referenced].

Funded by SCOAP^3. SCOAP^3 supports the goals of the International Year of Basic Sciences for Sustainable Development.

Appendix A: The mass operator matrices

The most general Yukawa Lagrangian for the interaction of four Higgs doublets Φ_α with the SM fermions is given by

$$\mathcal{L} = -\bar{q}'^{i}_{L}\Phi_\alpha y^{D\alpha}_{ij} d'^{j}_{R} - \bar{q}'^{i}_{L}\tilde{\Phi}_\alpha y^{U\alpha}_{ij} u'^{j}_{R} - \bar{\ell}'^{i}_{L}\Phi_\alpha y^{E\alpha}_{ij} e'^{j}_{R}$$

$$- \bar{\ell}_L'^i \tilde{\Phi}_\alpha y_{ij}^{N\alpha} \nu_R'^j + \text{h.c}, \tag{32}$$

where a sum is assumed on repeated indices. Here i, j run over $1, 2, 3$ and α over $1, 2, 3, 4$. The Higgs boson doublet fields are parameterized as follows:

$$\Phi_\alpha = \begin{pmatrix} \phi_\alpha^+ \\ \frac{v_\alpha + h_\alpha + i\eta_\alpha}{\sqrt{2}} \end{pmatrix}, \qquad \tilde{\Phi}_\alpha = i\sigma_2 \Phi_\alpha^*. \tag{33}$$

Similar to the two Higgs doublet model [228] we rotate the Higgs fields to the (generalized) Georgi basis, that is,

$$\begin{pmatrix} H_1 \\ H_2 \\ H_3 \\ H_4 \end{pmatrix} = R_1(\beta_1) R_2(\beta_2) R_3(\beta_3) \begin{pmatrix} \Phi_1 \\ \Phi_2 \\ \Phi_3 \\ \Phi_4 \end{pmatrix} \equiv R_{\beta\alpha} \Phi_\alpha, \tag{34}$$

where the orthogonal matrices

$$R_1(\beta_1) = \begin{pmatrix} \cos\beta_1 & \sin\beta_1 & 0 & 0 \\ -\sin\beta_1 & \cos\beta_1 & 0 & 0 \\ 0 & 0 & 1 & 0 \\ 0 & 0 & 0 & 1 \end{pmatrix}, \tag{35a}$$

$$R_2(\beta_2) = \begin{pmatrix} 1 & 0 & 0 & 0 \\ 0 & \cos\beta_2 & \sin\beta_2 & 0 \\ 0 & -\sin\beta_2 & \cos\beta_2 & 0 \\ 0 & 0 & 0 & 1 \end{pmatrix}, \tag{35b}$$

$$R_3(\beta_3) = \begin{pmatrix} 1 & 0 & 0 & 0 \\ 0 & 1 & 0 & 0 \\ 0 & 0 & \cos\beta_3 & \sin\beta_3 \\ 0 & 0 & -\sin\beta_3 & \cos\beta_3 \end{pmatrix}, \tag{35c}$$

where $\tan\beta_1 = \frac{\sqrt{v_2^2+v_3^2+v_4^2}}{v_1}$, $\tan\beta_2 = \frac{\sqrt{v_3^2+v_4^2}}{v_2}$ and $\tan\beta_3 = \frac{v_4}{v_3}$, and $H_\beta = (H_\beta^+, (H_\beta^0 + i H_\beta^{\text{odd}})/\sqrt{2})^{\text{T}}$. This basis is chosen in such a way that only the neutral component of H_1 acquires a vacuum expectation value

$$\begin{aligned} &\langle H_1^0 \rangle = \sqrt{v_1^2 + v_2^2 + v_3^2 + v_4^2} \equiv v, \\ &\langle H_2^0 \rangle = 0, \quad \langle H_3^0 \rangle = 0, \quad \langle H_4^0 \rangle = 0. \end{aligned} \tag{36}$$

In this way $\Phi_\alpha y_{ij}^{F\alpha} = y_{ij}^{F\alpha} R_{\alpha\beta}^T R_{\beta\gamma} \Phi_\gamma = \mathcal{Y}_{ij}^{F\beta} H_\beta$, and $F = U, D, N, E$; where we have defined

$$\mathcal{Y}_{ij}^{F\beta} = R_{\beta\alpha} y_{ij}^{F\alpha}. \tag{37}$$

With these definitions, Eq. (32) becomes

$$\begin{aligned} \mathcal{L} = &- \bar{q}_L'^i H_\beta \mathcal{Y}_{ij}^{D\beta} d_R'^j - \bar{q}_L'^i \tilde{H}_\beta \mathcal{Y}_{ij}^{U\beta} u_R'^j - \bar{\ell}_L'^i H_\beta \mathcal{Y}_{ij}^{E\beta} e_R'^j \\ &- \bar{\ell}_L'^i \tilde{H}_\beta \mathcal{Y}_{ij}^{N\beta} \nu_R'^j + \text{h.c}. \end{aligned} \tag{38}$$

It is necessary to rotate to the fermion mass eigenstates, i.e.,

$$f_{L,R} = U_{L,R}^F f_{L,R}', \tag{39}$$

where the diagonalization matrices $U_{L,R}$ are defined below, in Appendix C. From the Lagrangian for the charged currents

$$\begin{aligned} \mathcal{L}_{CC} &= -\frac{g}{\sqrt{2}} \bar{u}_{Li}' \gamma^\mu d_{Li}' W^+ - \frac{g}{\sqrt{2}} \bar{e}_{Li}' \gamma^\mu \nu_{Li}' W^- + \text{h.c} \\ &= -\frac{g}{\sqrt{2}} \bar{u}_{Li} \gamma^\mu \left(V_{\text{CKM}}\right)_{ij} d_{Lj} W^+ \\ &\quad - \frac{g}{\sqrt{2}} \bar{e}_{Li} \gamma^\mu \left(V_{\text{PMNS}}\right)_{ij} \nu_{Lj} W^- + \text{h.c}, \end{aligned} \tag{40}$$

it is possible to obtain the CKM ($V_{\text{CKM}} = U_L^U U_L^{D\dagger}$) and PMNS ($V_{\text{PMNS}} = U_L^E U_L^{\nu\dagger}$) mixing matrices by rotating to the fermion mass eigenstates. In particular, we are interested in the coupling of the axial neutral current to the axion in the mass eigenstates.

$$\begin{aligned} \mathcal{L}_{H^0} &= -\frac{1}{\sqrt{2}} \bar{d}_L'^i H_\beta^0 \mathcal{Y}_{ij}^{D\beta} d_R'^j - \frac{1}{\sqrt{2}} \bar{u}_L'^i H_\beta^{0*} \mathcal{Y}_{ij}^{U\beta} u_R'^j \\ &\quad - \frac{1}{\sqrt{2}} \bar{e}_L'^i H_\beta^0 \mathcal{Y}_{ij}^{E\beta} e_R'^j - \frac{1}{\sqrt{2}} \bar{\nu}_L'^i H_\beta^{0*} \mathcal{Y}_{ij}^{N\beta} \nu_R'^j + \text{h.c}, \\ &= -\frac{1}{\sqrt{2}} \bar{d}_L^i H_\beta^0 Y_{ij}^{D\beta} d_R^j - \frac{1}{\sqrt{2}} \bar{u}_L^i H_\beta^{0*} Y_{ij}^{U\beta} u_R^j \\ &\quad - \frac{1}{\sqrt{2}} \bar{e}_L^i H_\beta^0 Y_{ij}^{E\beta} e_R^j - \frac{1}{\sqrt{2}} \bar{\nu}_L^i H_\beta^{0*} Y_{ij}^{N\beta} \nu_R^j + \text{h.c}, \end{aligned}$$

where $Y_{ij}^{F\beta} = \left(U_L^F \mathcal{Y}^{F\beta} U_R^{F\dagger}\right)_{ij}$. In these expressions the mass functions in the interaction basis are:

$$\begin{aligned} M_{ij}^D &= \frac{v}{\sqrt{2}} \mathcal{Y}_{ij}^{D1}, \qquad M_{ij}^U = \frac{v}{\sqrt{2}} \mathcal{Y}_{ij}^{U1}, \\ M_{ij}^E &= \frac{v}{\sqrt{2}} \mathcal{Y}_{ij}^{E1}, \qquad M_{ij}^N = \frac{v}{\sqrt{2}} \mathcal{Y}_{ij}^{N1}, \end{aligned} \tag{41}$$

where $v = \langle H_1^0 \rangle$ is the Higgs vacuum expectation value.

Appendix B: Scalar potential

As studied in [58], the scalar sector requires four scalar doublets ϕ^α to reproduce the mass textures of the fermion sector correctly, and two scalar singlets S_1 and S_2 that break the PQ symmetry while generating a phenomenologically viable scalar mass spectrum. The S_2 singlet also gives mass to the heavy quark. The most general potential allowed by the PQ symmetry according to the charges established in Table 2 is:

$$V(\Phi, S_i) = \sum_{i=1}^4 \mu_i^2 \Phi_i^\dagger \Phi_i + \sum_{k=1}^2 \mu_{S_k}^2 S_k^* S_k + \sum_{i=1}^4 \lambda_i \left(\Phi_i^\dagger \Phi_i\right)^2$$

$$
\begin{aligned}
&+\sum_{k=1}^{2}\lambda_{s_k}\left(S_k^* S_k\right)^2+\sum_{i=1}^{4}\sum_{k=1}^{2}\lambda_{is_k}\left(\Phi_i^\dagger\Phi_i\right)\left(S_k^* S_k\right)\\
&+\underbrace{\sum_{i,\,j\,=1}^{4}}_{i<j}\left(\lambda_{ij}\left(\Phi_i^\dagger\Phi_i\right)\left(\Phi_j^\dagger\Phi_j\right)+J_{ij}\left(\Phi_i^\dagger\Phi_j\right)\left(\Phi_j^\dagger\Phi_i\right)\right)\\
&+\lambda_{s_1s_2}\left(S_1^* S_1\right)\left(S_2^* S_2\right)\\
&+K_1\left(\left(\Phi_1^\dagger\Phi_2\right)\left(\Phi_3^\dagger\Phi_2\right)+h.c.\right)\\
&+K_2\left(\left(\Phi_3^\dagger\Phi_4\right)\left(\Phi_3^\dagger\Phi_1\right)+h.c.\right)\\
&+F_1\left(\left(\Phi_2^\dagger\Phi_3\right)S_1+h.c.\right)\\
&+F_2\left(\left(\Phi_1^\dagger\Phi_2\right)S_1+h.c.\right)\\
&+\frac{1}{2}\left(m_{\zeta_{S_2}}\right)^2_{\rm SB}\zeta_{S_2}^2+\frac{1}{2}\left(m_{\xi_{S_2}}\right)^2_{\rm SB}\xi_{S_2}^2. \qquad (42)
\end{aligned}
$$

where the terms proportional to F_i are allowed by the particular choice of PQ charges and these couplings F_i have units of mass. After spontaneous symmetry breaking (SSB), the four Higgs doublets acquire VEVs that give mass to all the SM particles. The scalar doublets and singlets are written as follows:

$$
\begin{aligned}
\Phi_\alpha &= \begin{pmatrix}\phi_\alpha^+\\ \frac{v_\alpha+h_\alpha+i\eta_\alpha}{\sqrt{2}}\end{pmatrix}, \qquad \tilde{\Phi}_\alpha = i\sigma_2\Phi_\alpha^*, \alpha=1,2,3,4,\\
S_i &= \frac{v_{S_i}+\xi_{S_i}+i\zeta_{S_i}}{\sqrt{2}}; \qquad i=1,2, \qquad (43)
\end{aligned}
$$

where the VEVs satisfy the following hierarchy: $v_4 \ll v_1, v_2 \ll v_3 \ll v_{S_1} \sim v_{S_2}$. The scalar singlets S_1 and S_2 break the PQ symmetry at the high energy scale given by $v_{s_1} \approx v_{s_2}$. The last two terms in Eq. (42) correspond to the soft-breaking masses of the imaginary and the real parts of S_2, which are generated at one loop in the Coleman-Weinberg potential from the interaction term $\lambda_Q S_2 \bar{Q}_R Q_L + \text{h.c.}$ Additionally, we choose numerical values for the parameters of the potential (42) in order to obtain a scalar sector mass spectrum consistent with the existing phenomenology. The values of these parameters are:

$$
\begin{aligned}
\lambda_1 &= \lambda_2=\lambda_4=\lambda_{s_1}=\lambda_{s_2}=\lambda_{s_1s_2}=1,\\
\lambda_3 &= 0.463\\
\lambda_{ij} &= 1 \text{ for any } i,\, j,\\
\lambda_{js_1} &= \lambda_{js_2}=1 \text{ for any } j,\\
J_{12} &= J_{13}=J_{23}=J_{24}=-1, \quad \text{otherwise } J_{ij}=1,\\
K_1 &= K_2=-1,\\
F_1 &= F_2=-1\text{GeV}. \qquad (44)
\end{aligned}
$$

In particular, the value of λ_3 adjusts the SM Higgs mass. The v_i are determined from the SM fermion masses and the quark mass matrix textures, Eq. (15). The VEV v_{s_1} remains a free parameter; however, this parameter is important for the axion physics due to the relationship [165],

$$
f_a = \frac{v_{s_1}}{2N}. \qquad (45)
$$

In our calculations we took $v_{s_1} \approx v_{s_2} \approx 10^6$GeV. It is important to emphasize that in our model, f_a can take arbitrary values; nevertheless, a small f_a restricts ϵ (Eq. 13) to values close to zero. Taking into account all these considerations, including Eq. (44), the scalar mass spetrum (in GeV) is:

$$
\begin{aligned}
\text{CP even} &= \{1.73\times10^6,\, 1.\times10^6,\, 6.54\times10^3,\, 1.97\times10^3,\\
&\quad 1.09\times10^3,\, 125\},\\
\text{CP odd} &= \{6.54\times10^3,\, 1.97\times10^3,\, 1.09\times10^3,\, 0,\, 0,\, m_{\zeta_{S_2}}\},\\
\text{Charged fields} &= \{6.54\times10^3,\, 1.97\times10^3,\, 1.11\times10^3,\, 0\}. \qquad (46)
\end{aligned}
$$

The mass spectrum of the scalar fields is above the TeVs scale, except for the SM Higgs, which is at 125 GeV. The pseudoscalar sector (CP odd fields) have two massless eigenstates, the axion field and the Goldstone boson which is absorbed by the longitudinal component of the SM Z boson. A similar result is obtained in the charged sector, where it is possible to identify the two Goldstone bosons required to give mass to the SM $W^\pm$ fields.

Appendix C: diagonalization matrices

To compare with physical quantities, it is necessary to rotate fields to the mass eigenstates, i.e., $f_{L,R} = U^F_{L,R} f'_{L,R}$, where the prime symbol stands for the interaction basis. In our formalism the quark mass matrices are Hermitian, so the right- and left-handed diagonalizing matrices are identical; additionally, we establish that the eigenvalues of the second family of quarks are negative in order to generate texture-zeros in some diagonal terms of the mass matrices, as indicated in [112]. This sign is taken into account by introducing the identity matrix written as $I_2 I_2 = 1$ with $I_2 = \text{diag}(1,-1,1)$, i.e.,

$$
\begin{aligned}
M^F_{ij} &= \left(U^{F\dagger}\lambda^F U^F\right)_{ij} = \left(U_L^{F\dagger} m^F U_R^F\right)_{ij}\\
&= \frac{v}{\sqrt{2}}\mathcal{Y}^{F1}_{ij} = \frac{v}{\sqrt{2}} R_{1\alpha} y^{F\alpha}_{ij}, \qquad (47)
\end{aligned}
$$

where $\mathcal{Y}^{F\beta}_{ij}$ and $R_{\alpha\beta}$ were defined in Appendix A, $\lambda^{U,D} = \text{diag}(m_{u,d}, -m_{c,s}, m_{t,b})$ and $m^{U,D} = \text{diag}(m_{u,d}, m_{c,s}, m_{t,b})$, with similar definitions in the lepton sector, i.e., $\lambda^{N,E} = \text{diag}(m_{1,e}, -m_{2,\mu}, m_{3,\tau})$, $m^{N,E} = \text{diag}(m_{1,e}, m_{2,\mu}, m_{3,\tau})$, and

$$
U^F_L = U^F, \quad U^F_R = I_2 U^F, \qquad (48)
$$

where the U^F diagonalization matrices are defined below. It is important to stress that the texture-zeros pattern in the

matrix $\mathcal{Y}^{F1}_{ij}$ are identical to those in the original Yukawa couplings $y^{F\alpha}_{ij}$, since the sum over α does not mix the i, j indices. In fact, according to Eqs. (14) and (17), $M^F = \frac{v_\alpha}{\sqrt{2}} y^{F\alpha}_{ij} = \frac{v}{\sqrt{2}} R_{1\alpha} y^{F\alpha}_{ij}$, therefore $R_{1\alpha} = \frac{v_\alpha}{v}$. The diagonalization matrices are:

$$U^{U\dagger} = \begin{pmatrix} e^{i(\phi_{C_u}+\theta_{1u})}\sqrt{\frac{m_c m_t (A_u-m_u)}{A_u(m_c+m_u)(m_t-m_u)}} & -e^{i(\phi_{C_u}+\theta_{2u})}\sqrt{\frac{(A_u+m_c)m_t m_u}{A_u(m_c+m_t)(m_c+m_u)}} & e^{i(\phi_{C_u}+\theta_{3u})}\sqrt{\frac{m_c(m_t-A_u)m_u}{A_u(m_c+m_t)(m_t-m_u)}} \\ -e^{i(\phi_{B_u}+\theta_{1u})}\sqrt{\frac{(A_u+m_c)(m_t-A_u)m_u}{A_u(m_c+m_u)(m_t-m_u)}} & -e^{i(\phi_{B_u}+\theta_{2u})}\sqrt{\frac{m_c(m_t-A_u)(A_u-m_u)}{A_u(m_c+m_t)(m_c+m_u)}} & e^{i(\phi_{B_u}+\theta_{3u})}\sqrt{\frac{(A_u+m_c)m_t(A_u-m_u)}{A_u(m_c+m_t)(m_t-m_u)}} \\ e^{i\theta_{1u}}\sqrt{\frac{m_u(A_u-m_u)}{(m_c+m_u)(m_t-m_u)}} & e^{i\theta_{2u}}\sqrt{\frac{m_c(A_u+m_c)}{(m_c+m_t)(m_c+m_u)}} & e^{i\theta_{3u}}\sqrt{\frac{m_t(m_t-A_u)}{(m_c+m_t)(m_t-m_u)}} \end{pmatrix}, \quad (49)$$

$$U^{D\dagger} = \begin{pmatrix} e^{i\theta_{1d}}\sqrt{\frac{m_b(m_b-m_s)m_s}{(m_b-m_d)(m_d+m_s)(m_b+m_d-m_s)}} & -e^{i\theta_{2d}}\sqrt{\frac{m_b(m_b+m_d)m_d}{(m_d+m_s)(m_b+m_d-m_s)(m_b+m_s)}} & \sqrt{\frac{m_d(m_s-m_d)m_s}{(m_b-m_d)(m_b+m_d-m_s)(m_b+m_s)}} \\ e^{i\theta_{1d}}\sqrt{\frac{m_d(m_b-m_s)}{(m_b-m_d)(m_d+m_s)}} & e^{i\theta_{2d}}\sqrt{\frac{(m_b+m_d)m_s}{(m_d+m_s)(m_b+m_s)}} & \sqrt{\frac{m_b(m_s-m_d)}{(m_b-m_d)(m_b+m_s)}} \\ -e^{i\theta_{1d}}\sqrt{\frac{m_d(m_b+m_d)(m_s-m_d)}{(m_b-m_d)(m_d+m_s)(m_b+m_d-m_s)}} & -e^{i\theta_{2d}}\sqrt{\frac{(m_b-m_s)m_s(m_s-m_d)}{(m_d+m_s)(m_b+m_d-m_s)(m_b+m_s)}} & \sqrt{\frac{m_b(m_b+m_d)(m_b-m_s)}{(m_b-m_d)(m_b+m_d-m_s)(m_b+m_s)}} \end{pmatrix}, \quad (50)$$

where θ_{1u}, θ_{2u}, θ_{3u}, θ_{1d} and θ_{2d} are arbitrary phases (a third phase for the diagonalization matrix (50) can be absorbed by the remaining phases) that are useful for conforming to the $V_{\rm CKM} = U^U_L\, U^{D\dagger}_L$ matrix convention. Taking as input the SM parameters at the Z pole, the best fit values are given in Table 4.

Similarly, in the lepton sector, the diagonalization matrices of the mass matrices (7) are:

$$U^{N\dagger} = \begin{pmatrix} e^{i(\theta_{1\nu}+c_\nu)}\sqrt{\frac{m_2 m_3 (A_\nu-m_1)}{A_\nu(m_2+m_1)(m_3-m_1)}} & -e^{i(\theta_{2\nu}+c_\nu)}\sqrt{\frac{m_1 m_3 (m_2+A_\nu)}{A_\nu(m_2+m_1)(m_3+m_2)}} & e^{i(\theta_{3\nu}+c_\nu)}\sqrt{\frac{m_1 m_2 (m_3-A_\nu)}{A_\nu(m_3-m_1)(m_3+m_2)}} \\ e^{i\theta_{1\nu}}\sqrt{\frac{m_1(A_\nu-m_1)}{(m_1+m_2)(m_3-m_1)}} & e^{i\theta_{2\nu}}\sqrt{\frac{m_2(A_\nu+m_2)}{(m_2+m_1)(m_3+m_2)}} & e^{i\theta_{3\nu}}\sqrt{\frac{m_3(m_3-A_\nu)}{(m_3-m_1)(m_3+m_2)}} \\ -e^{i(\theta_{1\nu}-b_\nu)}\sqrt{\frac{m_1(A_\nu+m_2)(m_3-A_\nu)}{A_\nu(m_1+m_2)(m_3-m_1)}} & -e^{i(\theta_{2\nu}-b_\nu)}\sqrt{\frac{m_2(A_\nu-m_1)(m_3-A_\nu)}{A_\nu(m_2+m_1)(m_3+m_2)}} & e^{i(\theta_{3\nu}-b_\nu)}\sqrt{\frac{m_3(A_\nu-m_1)(A_\nu+m_2)}{A_\nu(m_3-m_1)(m_3+m_2)}} \end{pmatrix},$$

$$U^{E\dagger} = \begin{pmatrix} e^{i\theta_{1\ell}}\sqrt{\frac{m_\mu m_\tau (m_\tau-m_\mu)}{(m_e-m_\mu+m_\tau)(m_\mu+m_e)(m_\tau-m_e)}} & -e^{i\theta_{2\ell}}\sqrt{\frac{m_e m_\tau (m_e+m_\tau)}{(m_e-m_\mu+m_\tau)(m_\mu+m_e)(m_\tau+m_\mu)}} & \sqrt{\frac{m_e m_\mu (m_\mu-m_e)}{(m_e-m_\mu+m_\tau)(m_\tau-m_e)(m_\tau+m_\mu)}} \\ e^{i\theta_{1\ell}}\sqrt{\frac{m_e(m_\tau-m_\mu)}{(m_\mu+m_e)(m_\tau-m_e)}} & e^{i\theta_{2\ell}}\sqrt{\frac{m_\mu(m_e+m_\tau)}{(m_\mu+m_e)(m_\tau+m_\mu)}} & \sqrt{\frac{m_\tau(m_\mu-m_e)}{(m_\tau-m_e)(m_\tau+m_\mu)}} \\ -e^{i\theta_{1\ell}}\sqrt{\frac{m_e(m_e+m_\tau)(m_\mu-m_e)}{(m_e-m_\mu+m_\tau)(m_\mu+m_e)(m_\tau-m_e)}} & -e^{i\theta_{2\ell}}\sqrt{\frac{m_\mu(m_\tau-m_\mu)(m_\mu-m_e)}{(m_e-m_\mu+m_\tau)(m_\mu+m_e)(m_\tau+m_\mu)}} & \sqrt{\frac{m_\tau(m_\tau-m_\mu)(m_e+m_\tau)}{(m_e-m_\mu+m_\tau)(m_\tau-m_e)(m_\tau+m_\mu)}} \end{pmatrix}, \quad (51)$$

where $\theta_{1\ell}$, $\theta_{2\ell}$, $\theta_{1\nu}$, $\theta_{2\nu}$, $\theta_{3\nu}$ are necessary phases in order to adjust to the established convention for the PMNS mixing matrix [229] [1]; and c_ν and b_ν are the phases of C_ν and B_ν in the neutral mass matrix M^N in Eq. (7). The best fit values for these quantities are shown in Table 5.

Appendix D: Axion decay into photons

In the SM, $B^\mu = \cos\theta_W A^\mu - \sin\theta_W Z^\mu$ and $W^{3\mu} = \sin\theta_W A^\mu + \cos\theta_W Z^\mu$, where A^μ and Z^μ are the SM fields for the photon and Z gauge bosons, replacing these expresions in Eq. (26) we obtain

$$\begin{aligned} \mathcal{L} \supset & -c_1^{\rm eff}\frac{\alpha_1}{8\pi}\frac{a}{\Lambda_{\rm PQ}} B_{\mu\nu}\tilde{B}^{\mu\nu} - c_2^{\rm eff}\frac{\alpha_2}{8\pi}\frac{a}{\Lambda_{\rm PQ}} W^3_{\mu\nu}\tilde{W}^{3\mu\nu} \\ = & -\frac{\alpha}{8\pi}(c_1^{\rm eff}+c_2^{\rm eff})\frac{a}{\Lambda_{\rm PQ}} F_{\mu\nu}\tilde{F}^{\mu\nu} \\ & - \frac{\alpha}{8\pi c_W^2 s_W^2}(s_W^4 c_1^{\rm eff} + c_W^4 c_2^{\rm eff})\frac{a}{f_a} Z_{\mu\nu}\tilde{Z}^{\mu\nu} \\ & - \frac{2\alpha}{8\pi c_W s_W}(c_W^2 c_2^{\rm eff} - c_W^2 c_1^{\rm eff})\frac{a}{\Lambda_{\rm PQ}} F_{\mu\nu}\tilde{Z}^{\mu\nu} \\ = & \, e^2 C_{\gamma\gamma}\frac{a}{\Lambda_{\rm PQ}} F_{\mu\nu}\tilde{F}^{\mu\nu} + \frac{e^2 C_{ZZ}}{c_W^2 s_W^2}\frac{a}{\Lambda_{\rm PQ}} Z_{\mu\nu}\tilde{Z}^{\mu\nu} \\ & + \frac{2e^2 C_{\gamma Z}}{c_W s_W}\frac{a}{\Lambda_{\rm PQ}} F_{\mu\nu}\tilde{Z}^{\mu\nu} \end{aligned} \quad (52)$$

$$c_1^{\rm eff} = c_1 - \frac{1}{3}\Sigma q + \frac{8}{3}\Sigma u + \frac{2}{3}\Sigma d - \Sigma l + 2\Sigma e \quad (53)$$

$$c_2^{\rm eff} = c_2 - 3\Sigma q - \Sigma l \quad (54)$$

where $\Sigma f \equiv f_1 + f_2 + f_3$ is the sum of the PQ charges of the three families. There are similar definitions for the interaction of the axion with the gluons

$$-c_3^{\rm eff}\frac{\alpha_3}{8\pi}\frac{a}{\Lambda_{\rm PQ}} G^a_{\mu\nu}\tilde{G}^{a\mu\nu} = g_s^2 C_{GG}\frac{a}{\Lambda_{\rm PQ}} G^a_{\mu\nu}\tilde{G}^{a\mu\nu}, \quad (55)$$

[1] NuFIT collaboration (http://www.nu-fit.org/?q=node/211) (with SK atmospheric data).

Table 4 Best-fit point of the mass matrix parameters with respect to experimental data for the masses and mixing angles of the quark sector at the Z pole

θ_{1u}	θ_{2u}	θ_{3u}	θ_{1d}	θ_{2d}	ϕ_{C_u}	ϕ_{B_u}
−2.84403	1.85606	−0.00461668	1.93013	−0.976639	−1.49697	0.301461
A_u	m_u	m_c	m_t	m_d	m_s	m_b
1690.29 MeV	1.2684 MeV	633.197 MeV	171268 MeV	3.14751 MeV	56.1169 MeV	2910.01 MeV

Table 5 Best fit values

$\theta_{1\ell}$	$\theta_{2\ell}$	$\theta_{1\nu}$	$\theta_{2\nu}$	$\theta_{3\nu}$	c_ν	b_ν
0.154895	2.01797	−0.835504	2.21169	1.81786	1.01608	2.03726
A_ν (eV)	m_e (MeV)	m_μ (MeV)	m_τ (MeV)	m_1 (eV)	m_2 (eV)	m_3 (eV)
0.0251821	0.5109989461	105.6583745	1776.86	0.00353647	0.00929552	0.0504034

where $c_3^{\text{eff}} = c_3 - 2\Sigma q + \Sigma u + \Sigma d - A_Q$, in our particular case $c_i = 0$. In axion phenomenology, it is usual to define

$$C_{\gamma\gamma}=-\frac{1}{32\pi^2}(c_1^{\text{eff}}+c_2^{\text{eff}}),\ C_{ZZ}=-\frac{1}{32\pi^2}(s_W^4 c_1^{\text{eff}}+c_W^4 c_2^{\text{eff}}),$$
$$C_{\gamma Z}=-\frac{1}{32\pi^2}(c_W^2 c_2^{\text{eff}}-c_W^2 c_1^{\text{eff}}),\quad C_{GG}=-\frac{1}{32\pi^2}c_3^{\text{eff}}. \tag{56}$$

The decay widths of an axion decaying in two photons and a Z decaying in an axion and a photon are [191]

$$\Gamma(a\to\gamma\gamma)=\frac{4\pi\alpha^2 m_a^3}{\Lambda_{\text{PQ}}^2}|C_{\gamma\gamma}^{\text{eff}}|^2,$$
$$\Gamma(Z\to\gamma a)=\frac{8\pi\alpha(m_Z)m_Z^3}{3s_W^2c_W^2\Lambda_{\text{PQ}}^2}|C_{\gamma Z}^{\text{eff}}|^2\left(1-\frac{m_a^2}{m_Z^2}\right)^3. \tag{57}$$

Another possible decay channel of the axion in two photons is due to the mixing between the axion and the pion since the latter can decay in two photons, this decay mode generates an additional correction that only depends on the couplings of the axion to the gluons [230]

$$C_{\gamma\gamma}^{\text{eff}}=-\frac{c_3^{\text{eff}}}{32\pi^2}\left(\frac{c_1^{\text{eff}}+c_2^{\text{eff}}}{c_3^{\text{eff}}}-2.03\right),$$
$$C_{\gamma Z}^{\text{eff}}=-\frac{c_3^{\text{eff}}}{32\pi^2}\left(\frac{c_W^2c_2^{\text{eff}}-c_W^2c_1^{\text{eff}}}{c_3^{\text{eff}}}-0.74/2\right). \tag{58}$$

It is usual to define $\Lambda_{\text{PQ}} = |c_3^{\text{eff}}| f_a$.

$$\frac{E}{N}=\frac{c_1^{\text{eff}}+c_2^{\text{eff}}}{c_3^{\text{eff}}}. \tag{59}$$

The axion–photon interaction is given by

$$g_{a\gamma\gamma}=\frac{4e^2C_{\gamma\gamma}^{\text{eff}}}{\Lambda_{PQ}}=-\frac{\alpha}{2\pi f_a}\left(\frac{E}{N}-2.03\right) \tag{60}$$

where $\alpha=\frac{e^2}{4\pi}$. Due to the gluon-axion interaction, the axion gets a mass term, which is described at low energies as an axion–pion interaction [231]

$$m_a=5.7(7)\mu eV\left(\frac{10^{12}\text{GeV}}{f_a}\right). \tag{61}$$

References

1. G. Aad et al., Observation of a new particle in the search for the Standard Model Higgs boson with the ATLAS detector at the LHC. Phys. Lett. B **716**, 1–29 (2012)
2. S. Chatrchyan et al., Observation of a New Boson at a Mass of 125 GeV with the CMS Experiment at the LHC. Phys. Lett. B **716**, 30–61 (2012)
3. G.C. Branco, P.M. Ferreira, L. Lavoura, M.N. Rebelo, M. Sher, J.P. Silva, Theory and phenomenology of two-Higgs-doublet models. Phys. Rept. **516**, 1–102 (2012)
4. T.D. Lee, A Theory of Spontaneous T Violation. Phys. Rev. D **8**, 1226–1239 (1973)
5. H.E. Haber, G.L. Kane, The Search for Supersymmetry: Probing Physics Beyond the Standard Model. Phys. Rept. **117**, 75–263 (1985)
6. J.E. Kim, Light Pseudoscalars, Particle Physics and Cosmology. Phys. Rept. **150**, 1–177 (1987)
7. N. Turok, J. Zadrozny, Electroweak baryogenesis in the two doublet model. Nucl. Phys. B **358**, 471–493 (1991)
8. V. Barger, P. Langacker, M. McCaskey, M. Ramsey-Musolf, G. Shaughnessy, Complex Singlet Extension of the Standard Model. Phys. Rev. D **79**, 015018 (2009)
9. R.M. Schabinger, J.D. Wells, A Minimal spontaneously broken hidden sector and its impact on Higgs boson physics at the large hadron collider. Phys. Rev. D **72**, 093007 (2005)
10. C.-W. Chiang, M.J. Ramsey-Musolf, E. Senaha, Standard Model with a Complex Scalar Singlet: Cosmological Implications and Theoretical Considerations. Phys. Rev. D **97**(1), 015005 (2018)
11. J. McDonald, Gauge singlet scalars as cold dark matter. Phys. Rev. D **50**, 3637–3649 (1994)

12. L. Lopez Honorez, E. Nezri, J. F. Oliver, M. H. G. Tytgat, The Inert Doublet Model: An Archetype for Dark Matter. JCAP **02**, 028 (2007)
13. L. Lopez Honorez, C. E. Yaguna, The inert doublet model of dark matter revisited. JHEP **09**, 046 (2010)
14. M. Carena, H.E. Haber, I. Low, N.R. Shah, C.E.M. Wagner, Alignment limit of the NMSSM Higgs sector. Phys. Rev. D **93**(3), 035013 (2016)
15. S.L. Glashow, Partial Symmetries of Weak Interactions. Nucl. Phys. **22**, 579–588 (1961)
16. S. Weinberg, A Model of Leptons. Phys. Rev. Lett. **19**, 1264–1266 (1967)
17. A. Salam, Weak and Electromagnetic Interactions. Conf. Proc. C **680519**, 367–377 (1968)
18. R. Davis Jr., D.S. Harmer, K.C. Hoffman, Search for neutrinos from the sun. Phys. Rev. Lett. **20**, 1205–1209 (1968)
19. J. N. Bahcall, "Solving the mystery of the missing neutrinos," 6 (2004)
20. B. Pontecorvo, Inverse beta processes and nonconservation of lepton charge. Zh. Eksp. Teor. Fiz. **34**, 247 (1957)
21. L. Wolfenstein, Neutrino Oscillations in Matter. Phys. Rev. D **17**, 2369–2374 (1978)
22. S.P. Mikheyev, A.Y. Smirnov, Resonance amplification of oscillations in matter and spectroscopy of solar neutrinos. Sov. J. Nucl. Phys. **42**, 913–917 (1985)
23. F. Kaether, W. Hampel, G. Heusser, J. Kiko, T. Kirsten, Reanalysis of the GALLEX solar neutrino flux and source experiments. Phys. Lett. B **685**, 47–54 (2010)
24. B.T. Cleveland, T. Daily, R. Davis Jr., J.R. Distel, K. Lande, C.K. Lee, P.S. Wildenhain, J. Ullman, Measurement of the solar electron neutrino flux with the Homestake chlorine detector. Astrophys. J. **496**, 505–526 (1998)
25. B. Aharmim et al., Combined analysis of all three phases of solar neutrino data from the sudbury neutrino observatory. Phys. Rev. C **88**, 025501 (2013)
26. G. Bellini et al., Measurement of the solar 8B neutrino rate with a liquid scintillator target and 3 MeV energy threshold in the Borexino detector. Phys. Rev. D **82**, 033006 (2010)
27. G. Bellini, J. Benziger, D. Bick, G. Bonfini, D. Bravo, B. Caccianiga, L. Cadonati, F. Calaprice, A. Caminata, P. Cavalcante, A. Chavarria, A. Chepurnov, D. D'Angelo, S. Davini, A. Derbin, A. Empl, A. Etenko, K. Fomenko, D. Franco, F. Gabriele, C. Galbiati, S. Gazzana, C. Ghiano, M. Giammarchi, M. Göger-Neff, A. Goretti, M. Gromov, C. Hagner, E. Hungerford, A. Ianni, A. Ianni, V. Kobychev, D. Korablev, G. Korga, D. Kryn, M. Laubenstein, B. Lehnert, T. Lewke, E. Litvinovich, F. Lombardi, P. Lombardi, L. Ludhova, G. Lukyanchenko, I. Machulin, S. Manecki, W. Maneschg, S. Marcocci, Q. Meindl, E. Meroni, M. Meyer, L. Miramonti, M. Misiaszek, M. Montuschi, P. Mosteiro, V. Muratova, L. Oberauer, M. Obolensky, F. Ortica, K. Otis, M. Pallavicini, L. Papp, L. Perasso, A. Pocar, G. Ranucci, A. Razeto, A. Re, A. Romani, N. Rossi, R. Saldanha, C. Salvo, S. Schönert, H. Simgen, M. Skorokhvatov, O. Smirnov, A. Sotnikov, S. Sukhotin, Y. Suvorov, R. Tartaglia, G. Testera, D. Vignaud, R.B. Vogelaar, F. von Feilitzsch, H. Wang, J. Winter, M. Wojcik, A. Wright, M. Wurm, O. Zaimidoroga, S. Zavatarelli, K. Zuber, G. Zuzel, B. Collaboration, Neutrinos from the primary proton-proton fusion process in the sun. Nature **512**, 383–386 (2014)
28. J. Hosaka et al., Solar neutrino measurements in super-Kamiokande-I. Phys. Rev. D **73**, 112001 (2006)
29. J. Hosaka et al., Three flavor neutrino oscillation analysis of atmospheric neutrinos in Super-Kamiokande. Phys. Rev. D **74**, 032002 (2006)
30. M.G. Aartsen et al., Determining neutrino oscillation parameters from atmospheric muon neutrino disappearance with three years of IceCube DeepCore data. Phys. Rev. D **91**(7), 072004 (2015)
31. A. Gando et al., Constraints on θ_{13} from A Three-Flavor Oscillation Analysis of Reactor Antineutrinos at KamLAND. Phys. Rev. D **83**, 052002 (2011)
32. M. Apollonio et al., Limits on neutrino oscillations from the CHOOZ experiment. Phys. Lett. B **466**, 415–430 (1999)
33. A. Piepke, Final results from the Palo Verde neutrino oscillation experiment. Prog. Part. Nucl. Phys. **48**, 113–121 (2002)
34. F.P. An et al., New Measurement of Antineutrino Oscillation with the Full Detector Configuration at Daya Bay. Phys. Rev. Lett. **115**(11), 111802 (2015)
35. S.-B. Kim, Measurement of neutrino mixing angle Θ_{13} and mass difference Δm^2_{ee} from reactor antineutrino disappearance in the RENO experiment. Nucl. Phys. B **908**, 94–115 (2016)
36. J. Kopp, P.A.N. Machado, M. Maltoni, T. Schwetz, Sterile Neutrino Oscillations: The Global Picture. JHEP **05**, 050 (2013)
37. P. Adamson et al., Measurement of Neutrino and Antineutrino Oscillations Using Beam and Atmospheric Data in MINOS. Phys. Rev. Lett. **110**(25), 251801 (2013)
38. K. Abe et al., Observation of Electron Neutrino Appearance in a Muon Neutrino Beam. Phys. Rev. Lett. **112**, 061802 (2014)
39. P. Adamson et al., First measurement of electron neutrino appearance in NOvA. Phys. Rev. Lett. **116**(15), 151806 (2016)
40. J. Schechter, J.W.F. Valle, Neutrino Masses in SU(2) x U(1) Theories. Phys. Rev. D **22**, 2227 (1980)
41. E. Ma, U. Sarkar, Neutrino masses and leptogenesis with heavy Higgs triplets. Phys. Rev. Lett. **80**, 5716–5719 (1998)
42. R. Foot, H. Lew, X.G. He, G.C. Joshi, Seesaw Neutrino Masses Induced by a Triplet of Leptons. Z. Phys. C **44**, 441 (1989)
43. R.N. Mohapatra, J.W.F. Valle, Neutrino Mass and Baryon Number Nonconservation in Superstring Models. Phys. Rev. D **34**, 1642 (1986)
44. M.C. Gonzalez-Garcia, J.W.F. Valle, Fast Decaying Neutrinos and Observable Flavor Violation in a New Class of Majoron Models. Phys. Lett. B **216**, 360–366 (1989)
45. G.C. Branco, D. Emmanuel-Costa, M.N. Rebelo, P. Roy, Four Zero Neutrino Yukawa Textures in the Minimal Seesaw Framework. Phys. Rev. D **77**, 053011 (2008)
46. S. Choubey, W. Rodejohann, P. Roy, Phenomenological consequences of four zero neutrino Yukawa textures. Nucl. Phys. B **808**, 272–291 (2009). [Erratum: Nucl.Phys.B 818, 136–136 (2009)]
47. B. Adhikary, A. Ghosal, P. Roy, Neutrino Masses, Cosmological Bound and Four Zero Yukawa Textures. Mod. Phys. Lett. A **26**, 2427–2435 (2011)
48. B. Adhikary, A. Ghosal, P. Roy, Baryon asymmetry from leptogenesis with four zero neutrino Yukawa textures. JCAP **01**, 025 (2011)
49. G.C. Branco, M.N. Rebelo, J.I. Silva-Marcos, Leptogenesis, Yukawa textures and weak basis invariants. Phys. Lett. B **633**, 345–354 (2006)
50. J.-W. Mei, Running neutrino masses, leptonic mixing angles and CP-violating phases: From M(Z) to Lambda(GUT). Phys. Rev. D **71**, 073012 (2005)
51. C. Hagedorn, J. Kersten, M. Lindner, Stability of texture zeros under radiative corrections in see-saw models. Phys. Lett. B **597**, 63–72 (2004)
52. S. Antusch, J. Kersten, M. Lindner, M. Ratz, M.A. Schmidt, Running neutrino mass parameters in see-saw scenarios. JHEP **03**, 024 (2005)
53. P. O. Ludl, W. Grimus, A complete survey of texture zeros in the lepton mass matrices. JHEP **07**, 090 (2014). [Erratum: JHEP 10, 126 (2014)]
54. P.M. Ferreira, L. Lavoura, New textures for the lepton mass matrices. Nucl. Phys. B **891**, 378–400 (2015)
55. P.O. Ludl, W. Grimus, A complete survey of texture zeros in general and symmetric quark mass matrices. Phys. Lett. B **744**, 38–42 (2015)

56. W. Grimus, A.S. Joshipura, L. Lavoura, M. Tanimoto, Symmetry realization of texture zeros. Eur. Phys. J. C **36**, 227–232 (2004)
57. R.M. Fonseca, W. Grimus, Classification of lepton mixing matrices from finite residual symmetries. JHEP **09**, 033 (2014)
58. Y. Giraldo, R. Martinez, E. Rojas, J.C. Salazar, Flavored axions and the flavor problem. Eur. Phys. J. C **82**(12), 1131 (2022)
59. F. Björkeroth, L. Di Luzio, F. Mescia, E. Nardi, $U(1)$ flavour symmetries as Peccei-Quinn symmetries. JHEP **02**, 133 (2019)
60. T.P. Cheng, M. Sher, Mass Matrix Ansatz and Flavor Nonconservation in Models with Multiple Higgs Doublets. Phys. Rev. D **35**, 3484 (1987)
61. K. Matsuda, H. Nishiura, Can four-zero-texture mass matrix model reproduce the quark and lepton mixing angles and CP violating phases? Phys. Rev. D **74**, 033014 (2006)
62. A. E. Carcamo Hernandez, R. Martinez, J. A. Rodriguez, Different kind of textures of Yukawa coupling matrices in the two Higgs doublet model type III. Eur. Phys. J. C **50**, 935–948 (2007)
63. P. Langacker, M. Plumacher, Flavor changing effects in theories with a heavy Z' boson with family nonuniversal couplings. Phys. Rev. D **62**, 013006 (2000)
64. K. Leroux, D. London, Flavor changing neutral currents and leptophobic Z' gauge bosons. Phys. Lett. B **526**, 97–103 (2002)
65. S.F. King, S. Moretti, R. Nevzorov, Theory and phenomenology of an exceptional supersymmetric standard model. Phys. Rev. D **73**, 035009 (2006)
66. C. Alvarado, R. Martinez, F. Ochoa, Quark mass hierarchy in 3-3-1 models. Phys. Rev. D **86**, 025027 (2012)
67. L.E. Ibanez, G.G. Ross, Fermion masses and mixing angles from gauge symmetries. Phys. Lett. B **332**, 100–110 (1994)
68. P. Binetruy, P. Ramond, Yukawa textures and anomalies. Phys. Lett. B **350**, 49–57 (1995)
69. Y. Nir, Gauge unification, Yukawa hierarchy and the mu problem. Phys. Lett. B **354**, 107–110 (1995)
70. V. Jain, R. Shrock, Models of fermion mass matrices based on a flavor dependent and generation dependent U(1) gauge symmetry. Phys. Lett. B **352**, 83–91 (1995)
71. E. Dudas, S. Pokorski, C.A. Savoy, Yukawa matrices from a spontaneously broken Abelian symmetry. Phys. Lett. B **356**, 45–55 (1995)
72. F. Pisano, V. Pleitez, An SU(3) x U(1) model for electroweak interactions. Phys. Rev. D **46**, 410–417 (1992)
73. P.H. Frampton, Chiral dilepton model and the flavor question. Phys. Rev. Lett. **69**, 2889–2891 (1992)
74. R. Foot, H.N. Long, T.A. Tran, $SU(3)_L \otimes U(1)_N$ and $SU(4)_L \otimes U(1)_N$ gauge models with right-handed neutrinos. Phys. Rev. D **50**(1), R34–R38 (1994)
75. H.N. Long, The 331 model with right handed neutrinos. Phys. Rev. D **53**, 437–445 (1996)
76. H.N. Long, SU(3)-L x U(1)-N model for right-handed neutrino neutral currents. Phys. Rev. D **54**, 4691–4693 (1996)
77. H.N. Long, Scalar sector of the 3 3 1 model with three Higgs triplets. Mod. Phys. Lett. A **13**, 1865–1874 (1998)
78. R.A. Diaz, R. Martinez, J.A. Rodriguez, A New supersymmetric SU(3)(L) x U(1)(X) gauge model. Phys. Lett. B **552**, 287–292 (2003)
79. R.A. Diaz, R. Martinez, F. Ochoa, The Scalar sector of the SU(3)(c) x SU(3)(L) x U(1)(X) model. Phys. Rev. D **69**, 095009 (2004)
80. R.A. Diaz, R. Martinez, F. Ochoa, SU(3)(c) x SU(3)(L) x U(1)(X) models for beta arbitrary and families with mirror fermions. Phys. Rev. D **72**, 035018 (2005)
81. F. Ochoa, R. Martinez, Family dependence in SU(3)(c) x SU(3)(L) x U(1)(X) models. Phys. Rev. D **72**, 035010 (2005)
82. S.M. Barr, Light Fermion Mass Hierarchy and Grand Unification. Phys. Rev. D **21**, 1424 (1980)
83. T.R. Taylor, G. Veneziano, Quenching the Cosmological Constant. Phys. Lett. B **228**, 311–316 (1989)
84. S.M. Barr, A Simple and Predictive Model for Quark and Lepton Masses. Phys. Rev. Lett. **64**, 353 (1990)
85. S. Weinberg, Electromagnetic and weak masses. Phys. Rev. Lett. **29**, 388–392 (1972)
86. R.N. Mohapatra, Gauge Model for Chiral Symmetry Breaking and Muon electron Mass Ratio. Phys. Rev. D **9**, 3461 (1974)
87. S.M. Barr, A. Zee, A New Approach to the electron-Muon Mass Ratio. Phys. Rev. D **15**, 2652 (1977)
88. B.S. Balakrishna, Fermion Mass Hierarchy From Radiative Corrections. Phys. Rev. Lett. **60**, 1602 (1988)
89. S.M. Barr, Flavor without flavor symmetry. Phys. Rev. D **65**, 096012 (2002)
90. L. Ferretti, S.F. King, A. Romanino, Flavour from accidental symmetries. JHEP **11**, 078 (2006)
91. S.M. Barr, Doubly Lopsided Mass Matrices from Unitary Unification. Phys. Rev. D **78**, 075001 (2008)
92. P.H. Frampton, T.W. Kephart, Fermion Mixings in SU(9) Family Unification. Phys. Lett. B **681**, 343–346 (2009)
93. K.S. Babu, S.M. Barr, Large neutrino mixing angles in unified theories. Phys. Lett. B **381**, 202–208 (1996)
94. J. Sato, T. Yanagida, Large lepton mixing in a coset space family unification on E(7) / SU(5) x U(1)**3. Phys. Lett. B **430**, 127–131 (1998)
95. N. Irges, S. Lavignac, P. Ramond, Predictions from an anomalous U(1) model of Yukawa hierarchies. Phys. Rev. D **58**, 035003 (1998)
96. S.M. Barr, I. Dorsner, A General classification of three neutrino models and U(e3). Nucl. Phys. B **585**, 79–104 (2000)
97. N. Haba, H. Murayama, Anarchy and hierarchy. Phys. Rev. D **63**, 053010 (2001)
98. X.-G. He, Y.-Y. Keum, R.R. Volkas, A(4) flavor symmetry breaking scheme for understanding quark and neutrino mixing angles. JHEP **04**, 039 (2006)
99. Y.H. Ahn, S.K. Kang, C.S. Kim, Spontaneous CP Violation in A_4 Flavor Symmetry and Leptogenesis. Phys. Rev. D **87**(11), 113012 (2013)
100. R. González Felipe, H. Serôdio, J. P. Silva, Models with three Higgs doublets in the triplet representations of A_4 or S_4. Phys. Rev. D **87**(5), 055010 (2013)
101. H. Ishimori, E. Ma, New Simple A_4 Neutrino Model for Nonzero θ_{13} and Large δ_{CP}. Phys. Rev. D **86**, 045030 (2012)
102. F. Gonzalez Canales, A. Mondragon, M. Mondragon, The S_3 Flavour Symmetry: Neutrino Masses and Mixings. Fortsch. Phys. **61**, 546–570 (2013)
103. R.N. Mohapatra, C.C. Nishi, S_4 Flavored CP Symmetry for Neutrinos. Phys. Rev. D **86**, 073007 (2012)
104. G.-J. Ding, S.F. King, C. Luhn, A.J. Stuart, Spontaneous CP violation from vacuum alignment in S_4 models of leptons. JHEP **05**, 084 (2013)
105. E. Ma, Neutrino Mixing and Geometric CP Violation with Delta(27) Symmetry. Phys. Lett. B **723**, 161–163 (2013)
106. C.C. Nishi, Generalized CP symmetries in $\Delta(27)$ flavor models. Phys. Rev. D **88**(3), 033010 (2013)
107. G. Altarelli, F. Feruglio, Tri-bimaximal neutrino mixing from discrete symmetry in extra dimensions. Nucl. Phys. B **720**, 64–88 (2005)
108. H. Ishimori, Y. Shimizu, M. Tanimoto, A. Watanabe, Neutrino masses and mixing from S_4 flavor twisting. Phys. Rev. D **83**, 033004 (2011)
109. A. Kadosh, E. Pallante, An A(4) flavor model for quarks and leptons in warped geometry. JHEP **08**, 115 (2010)
110. G.-J. Ding, Y.-L. Zhou, Dirac Neutrinos with S_4 Flavor Symmetry in Warped Extra Dimensions. Nucl. Phys. B **876**, 418–452 (2013)

111. Y. Giraldo, Texture Zeros and WB Transformations in the Quark Sector of the Standard Model. Phys. Rev. D **86**, 093021 (2012)
112. G. C. Branco, D. Emmanuel-Costa, R. Gonzalez Felipe, Texture zeros and weak basis transformations. Phys. Lett. B **477**, 147–155 (2000)
113. Y. Giraldo, E. Rojas, CKM mixings from mass matrices with five texture zeros. Phys. Rev. D **104**(7), 075009 (2021)
114. P. Ramond, R.G. Roberts, G.G. Ross, Stitching the Yukawa quilt. Nucl. Phys. B **406**, 19–42 (1993)
115. H. Fritzsch, Z.-Z. Xing, Mass and flavor mixing schemes of quarks and leptons. Prog. Part. Nucl. Phys. **45**, 1–81 (2000)
116. G.C. Branco, L. Lavoura, F. Mota, Nearest Neighbor Interactions and the Physical Content of Fritzsch Mass Matrices. Phys. Rev. D **39**, 3443 (1989)
117. X.-G. He, W.-S. Hou, Relating the Long B Lifetime to a Very Heavy Top Quark. Phys. Rev. D **41**, 1517 (1990)
118. H. Fritzsch, Weak Interaction Mixing in the Six - Quark Theory. Phys. Lett. B **73**, 317–322 (1978)
119. H. Fritzsch, Calculating the Cabibbo Angle. Phys. Lett. B **70**, 436–440 (1977)
120. H. Fritzsch, Quark Masses and Flavor Mixing. Nucl. Phys. B **155**, 189–207 (1979)
121. D.-S. Du, Z.-Z. Xing, A Modified Fritzsch ansatz with additional first order perturbation. Phys. Rev. D **48**, 2349–2352 (1993)
122. H. Fritzsch, Z.-Z. Xing, Four zero texture of Hermitian quark mass matrices and current experimental tests. Phys. Lett. B **555**, 63–70 (2003)
123. R. L. Workman et al., Review of Particle Physics. PTEP **2022**, 083C01 (2022)
124. Z.-Z. Xing, H. Zhang, Complete parameter space of quark mass matrices with four texture zeros. J. Phys. G **30**, 129–136 (2004)
125. Y.-F. Zhou, Textures and hierarchies in quark mass matrices with four texture zeros 9 (2003)
126. R. H. Benavides, Y. Giraldo, L. Mu noz, W. A. Ponce, E. Rojas, Five Texture Zeros for Dirac Neutrino Mass Matrices. J. Phys. G, **47**(11), 115002 (2020)
127. Y. Giraldo, Seeking Texture Zeros in the Quark Mass Matrix Sector of the Standard Model. Nucl. Part. Phys. Proc. **267–269**, 76–78 (2015)
128. F. Wilczek, Axions and family symmetry breaking. Phys. Rev. Lett. **49**, 1549–1552 (1982)
129. L. Calibbi, F. Goertz, D. Redigolo, R. Ziegler, J. Zupan, Minimal axion model from flavor. Phys. Rev. D **95**(9), 095009 (2017)
130. C.Q. Geng, J.N. Ng, Flavor Connections and Neutrino Mass Hierarchy Invariant Invisible Axion Models Without Domain Wall Problem. Phys. Rev. D **39**, 1449 (1989)
131. Z.G. Berezhiani, M.Y. Khlopov, Cosmology of Spontaneously Broken Gauge Family Symmetry. Z. Phys. C **49**, 73–78 (1991)
132. M. Hindmarsh, P. Moulatsiotis, Constraints on variant axion models. Phys. Rev. D **56**, 8074–8081 (1997)
133. Y. Giraldo, R. Martínez, E. Rojas, J. C. Salazar, A minimal axion model for mass matrices with five texture-zeros. **4** (2023)
134. F. Björkeroth, E.J. Chun, S.F. King, Flavourful Axion Phenomenology. JHEP **08**, 117 (2018)
135. M. Reig, J.W.F. Valle, F. Wilczek, SO(3) family symmetry and axions. Phys. Rev. D **98**(9), 095008 (2018)
136. M. Linster, R. Ziegler, A Realistic $U(2)$ Model of Flavor. JHEP **08**, 058 (2018)
137. Y.H. Ahn, Compact model for Quarks and Leptons via flavored-Axions. Phys. Rev. D **98**(3), 035047 (2018)
138. F. Arias-Aragon, L. Merlo, The minimal flavour violating axion. JHEP **10**, 168 (2017). [Erratum: JHEP 11, 152 (2019)]
139. Y. Ema, K. Hamaguchi, T. Moroi, K. Nakayama, Flaxion: a minimal extension to solve puzzles in the standard model. JHEP **01**, 096 (2017)
140. T. Alanne, S. Blasi, F. Goertz, Common source for scalars: Flavored axion-Higgs unification. Phys. Rev. D **99**(1), 015028 (2019)
141. S. Bertolini, L. Di Luzio, H. Kolešová, M. Malinský, Massive neutrinos and invisible axion minimally connected. Phys. Rev. D **91**(5), 055014 (2015)
142. A. Celis, J. Fuentes-Martín, H. Serôdio, A class of invisible axion models with FCNCs at tree level. JHEP **12**, 167 (2014)
143. Y.H. Ahn, Flavored Peccei-Quinn symmetry. Phys. Rev. D **91**, 056005 (2015)
144. C. Cheung, Axion Protection from Flavor. JHEP **06**, 074 (2010)
145. M.E. Albrecht, T. Feldmann, T. Mannel, Goldstone Bosons in Effective Theories with Spontaneously Broken Flavour Symmetry. JHEP **10**, 089 (2010)
146. T. Appelquist, Y. Bai, M. Piai, SU(3) Family Gauge Symmetry and the Axion. Phys. Rev. D **75**, 073005 (2007)
147. R.D. Peccei, H.R. Quinn, CP Conservation in the Presence of Instantons. Phys. Rev. Lett. **38**, 1440–1443 (1977)
148. R.D. Peccei, H.R. Quinn, Constraints Imposed by CP Conservation in the Presence of Instantons. Phys. Rev. D **16**, 1791–1797 (1977)
149. S. Weinberg, A New Light Boson? Phys. Rev. Lett. **40**, 223–226 (1978)
150. F. Wilczek, Problem of Strong P and T Invariance in the Presence of Instantons. Phys. Rev. Lett. **40**, 279–282 (1978)
151. J.E. Kim, Weak Interaction Singlet and Strong CP Invariance. Phys. Rev. Lett. **43**, 103 (1979)
152. M.S. Turner, Windows on the Axion. Phys. Rept. **197**, 67–97 (1990)
153. G.G. Raffelt, Astrophysical methods to constrain axions and other novel particle phenomena. Phys. Rept. **198**, 1–113 (1990)
154. J. Preskill, M.B. Wise, F. Wilczek, Cosmology of the Invisible Axion. Phys. Lett. B **120**, 127–132 (1983)
155. L.F. Abbott, P. Sikivie, A Cosmological Bound on the Invisible Axion. Phys. Lett. B **120**, 133–136 (1983)
156. M. Dine, W. Fischler, The Not So Harmless Axion. Phys. Lett. B **120**, 137–141 (1983)
157. M.A. Shifman, A.I. Vainshtein, V.I. Zakharov, Can Confinement Ensure Natural CP Invariance of Strong Interactions? Nucl. Phys. B **166**, 493–506 (1980)
158. M. Dine, W. Fischler, M. Srednicki, A Simple Solution to the Strong CP Problem with a Harmless Axion. Phys. Lett. B **104**, 199–202 (1981)
159. A.R. Zhitnitsky, On Possible Suppression of the Axion Hadron Interactions. (In Russian). Sov. J. Nucl. Phys. **31**, 260 (1980)
160. L. Di Luzio, M. Giannotti, E. Nardi, L. Visinelli, The landscape of QCD axion models. Phys. Rept. **870**, 1–117 (2020)
161. N. Viaux, M. Catelan, P.B. Stetson, G. Raffelt, J. Redondo, A.A.R. Valcarce, A. Weiss, Neutrino and axion bounds from the globular cluster M5 (NGC 5904). Phys. Rev. Lett. **111**, 231301 (2013)
162. E. Arik et al., Probing eV-scale axions with CAST. JCAP **02**, 008 (2009)
163. Y. Inoue, Y. Akimoto, R. Ohta, T. Mizumoto, A. Yamamoto, M. Minowa, Search for solar axions with mass around 1 eV using coherent conversion of axions into photons. Phys. Lett. B **668**, 93–97 (2008)
164. M. M. Miller Bertolami, B. E. Melendez, L. G. Althaus, J. Isern, Revisiting the axion bounds from the Galactic white dwarf luminosity function. JCAP **10**, 069 (2014)
165. M. Giannotti, I.G. Irastorza, J. Redondo, A. Ringwald, K. Saikawa, Stellar Recipes for Axion Hunters. JCAP **10**, 010 (2017)
166. J. Isern, E. García-Berro, S. Torres, R. Cojocaru, S. Catalán, Axions and the luminosity function of white dwarfs: the thin and thick discs, and the halo. Mon. Not. R. Astron. Soc. **478**, 2569–2575 (2018)

167. O. Straniero, I. Dominguez, M. Giannotti, and A. Mirizzi, Axion-electron coupling from the RGB tip of Globular Clusters (2018). arXiv e-prints, p. arXiv:1802.10357
168. R. Verma, Exploring the predictability of symmetric texture zeros in quark mass matrices. Phys. Rev. D **96**(9), 093010 (2017)
169. Z.-Z. Xing, Flavor structures of charged fermions and massive neutrinos. Phys. Rept. **854**, 1–147 (2020)
170. B.R. Desai, A.R. Vaucher, Quark mass matrices with four and five texture zeroes, and the CKM matrix, in terms of mass eigenvalues. Phys. Rev. D **63**, 113001 (2001)
171. W.A. Ponce, J.D. Gómez, R.H. Benavides, Five texture zeros and CP violation for the standard model quark mass matrices. Phys. Rev. D **87**(5), 053016 (2013)
172. Y. Giraldo, E. Rojas, Five Non-Fritzsch Texture Zeros for Quarks Mass Matrices in the Standard Model. in 38th International Symposium on Physics in Collision, 11 (2018)
173. C. Hagedorn, W. Rodejohann, Minimal mass matrices for dirac neutrinos. JHEP **07**, 034 (2005)
174. G. Ahuja, M. Gupta, M. Randhawa, R. Verma, Texture specific mass matrices with Dirac neutrinos and their implications. Phys. Rev. D **79**, 093006 (2009)
175. X.-W. Liu, S. Zhou, Texture Zeros for Dirac Neutrinos and Current Experimental Tests. Int. J. Mod. Phys. A **28**, 1350040 (2013)
176. R. Verma, Lower bound on neutrino mass and possible CP violation in neutrino oscillations. Phys. Rev. D **88**, 111301 (2013)
177. R. Verma, Lepton textures and neutrino oscillations. Int. J. Mod. Phys. A **29**(21), 1444009 (2014)
178. P. Fakay, S. Sharma, G. Ahuja, M. Gupta, Leptonic mixing angle θ_{13} and ruling out of minimal texture for Dirac neutrinos. PTEP **2014**(2), 023B03 (2014)
179. L.M. Cebola, D. Emmanuel-Costa, R.G. Felipe, Confronting predictive texture zeros in lepton mass matrices with current data. Phys. Rev. D **92**(2), 025005 (2015)
180. R.R. Gautam, M. Singh, M. Gupta, Neutrino mass matrices with one texture zero and a vanishing neutrino mass. Phys. Rev. D **92**(1), 013006 (2015)
181. G. Ahuja, S. Sharma, P. Fakay, M. Gupta, General lepton textures and their implications. Mod. Phys. Lett. A **30**(34), 1530025 (2015)
182. M. Singh, Texture One Zero Dirac Neutrino Mass Matrix With Vanishing Determinant or Trace Condition. Nucl. Phys. B **931**, 446–468 (2018)
183. G. Ahuja, M. Gupta, Texture zero mass matrices and nature of neutrinos. Int. J. Mod. Phys. A **33**(31), 1844032 (2018)
184. J. Barranco, D. Delepine, L. Lopez-Lozano, Neutrino Mass Determination from a Four-Zero Texture Mass Matrix. Phys. Rev. D **86**, 053012 (2012)
185. Y.A. Garnica, S.F. Mantilla, R. Martinez, H. Vargas, From Peccei Quinn symmetry to mass hierarchy problem. J. Phys. G **48**(9), 095002 (2021)
186. A. Ringwald, K. Saikawa, Axion dark matter in the post-inflationary Peccei-Quinn symmetry breaking scenario. Phys. Rev. D 93(8), 085031 (2016). [Addendum: Phys.Rev.D 94, 049908 (2016)]
187. I. Brivio, M.B. Gavela, L. Merlo, K. Mimasu, J.M. No, R. del Rey, V. Sanz, ALPs Effective Field Theory and Collider Signatures. Eur. Phys. J. C **77**(8), 572 (2017)
188. R. H. Benavides, D. V. Forero, L. Mu noz, J. M. Mu noz, A. Rico, A. Tapia, Five texture zeros in the lepton sector and neutrino oscillations at DUNE. Phys. Rev. D **107**(3), 036008 (2023)
189. H. Georgi, D.B. Kaplan, L. Randall, Manifesting the Invisible Axion at Low-energies. Phys. Lett. B **169**, 73–78 (1986)
190. M.B. Gavela, R. Houtz, P. Quilez, R. Del Rey, O. Sumensari, Flavor constraints on electroweak ALP couplings. Eur. Phys. J. C **79**(5), 369 (2019)
191. M. Bauer, M. Neubert, A. Thamm, Collider Probes of Axion-Like Particles. JHEP **12**, 044 (2017)
192. A. Salvio, A. Strumia, W. Xue, Thermal axion production. JCAP **01**, 011 (2014)
193. E. Cortina Gil et al. Measurement of the very rare $K^+ \to \pi^+ \nu\bar{\nu}$ decay. JHEP **06**, 093 (2021)
194. R.D. Bolton et al., Search for rare Muon decays with the crystal box detector. Phys. Rev. D **38**, 2077 (1988)
195. A. Jodidio, B. Balke, J. Carr, G. Gidal, K.A. Shinsky, H.M. Steiner, D.P. Stoker, M. Strovink, R.D. Tripp, B. Gobbi, C.J. Oram, Erratum: Search for right-handed currents in muon decay [phys. rev. d 34, 1967 (1986)]. Phys. Rev. D **37**, 237–238 (1988)
196. R. Bayes et al., Search for two body muon decay signals. Phys. Rev. D **91**(5), 052020 (2015)
197. H. Albrecht et al., A Search for lepton flavor violating decays tau –> e alpha, tau –> mu alpha. Z. Phys. C **68**, 25–28 (1995)
198. H. Georgi, D.V. Nanopoulos, Suppression of Flavor Changing Effects From Neutral Spinless Meson Exchange in Gauge Theories. Phys. Lett. B **82**, 95–96 (1979)
199. C. O'Hare, cajohare/axionlimits: Axionlimits. https://cajohare.github.io/AxionLimits/ (2020)
200. S. Chaudhuri, P.W. Graham, K. Irwin, J. Mardon, S. Rajendran, Y. Zhao, Radio for hidden-photon dark matter detection. Phys. Rev. D **92**(7), 075012 (2015)
201. D. Alesini, D. Babusci, D. Di Gioacchino, C. Gatti, G. Lamanna, C. Ligi, The KLASH proposal. **7** (2017)
202. C. Gatti et al. The Klash Proposal: Status and Perspectives. in 14th Patras Workshop on Axions, WIMPs and WISPs, 11 (2018)
203. I. Stern, ADMX Status. PoS ICHEP2016, 198 (2016)
204. M. Lawson, A.J. Millar, M. Pancaldi, E. Vitagliano, F. Wilczek, Tunable axion plasma haloscopes. Phys. Rev. Lett. **123**(14), 141802 (2019)
205. S. Beurthey et al., "MADMAX Status Report," 3 (2020)
206. E. Armengaud et al., Conceptual Design of the International Axion Observatory (IAXO). JINST **9**, T05002 (2014)
207. I. Shilon, A. Dudarev, H. Silva, U. Wagner, H.H.J. ten Kate, New Superconducting Toroidal Magnet System for IAXO, the International AXion Observatory. AIP Conf. Proc. **1573**(1), 1559–1566 (2015)
208. J.L. Ouellet et al., First Results from ABRACADABRA-10 cm: A Search for Sub-μeV Axion Dark Matter. Phys. Rev. Lett. **122**(12), 121802 (2019)
209. C. Bartram et al. Search for Invisible Axion Dark Matter in the 3.3–4.2 μeV Mass Range. Phys. Rev. Lett. 127(26), 261803 (2021)
210. T. Braine et al., Extended Search for the Invisible Axion with the Axion Dark Matter Experiment. Phys. Rev. Lett. **124**(10), 101303 (2020)
211. C. Bartram et al., Axion dark matter experiment: Run 1B analysis details. Phys. Rev. D **103**(3), 032002 (2021)
212. V. Anastassopoulos et al., New CAST Limit on the Axion-Photon Interaction. Nature Phys. **13**, 584–590 (2017)
213. S. Andriamonje et al., An Improved limit on the axion-photon coupling from the CAST experiment. JCAP **04**, 010 (2007)
214. S. Lee, S. Ahn, J. Choi, B. R. Ko, Y. K. Semertzidis, Axion Dark Matter Search around 6.7 μeV. Phys. Rev. Lett. **124**(10), 101802 (2020)
215. J. Jeong, S. Youn, S. Bae, J. Kim, T. Seong, J.E. Kim, Y.K. Semertzidis, Search for Invisible Axion Dark Matter with a Multiple-Cell Haloscope. Phys. Rev. Lett. **125**(22), 221302 (2020)
216. O. Kwon et al., First Results from an Axion Haloscope at CAPP around 10.7 μeV. Phys. Rev. Lett. **126**(19), 191802 (2021)
217. K.M. Backes et al., A quantum-enhanced search for dark matter axions. Nature **590**(7845), 238–242 (2021)
218. L. Zhong et al., Results from phase 1 of the HAYSTAC microwave cavity axion experiment. Phys. Rev. D **97**(9), 092001 (2018)
219. P. Gondolo, G.G. Raffelt, Solar neutrino limit on axions and keV-mass bosons. Phys. Rev. D **79**, 107301 (2009)

220. A. Ayala, I. Domínguez, M. Giannotti, A. Mirizzi, O. Straniero, Revisiting the bound on axion-photon coupling from Globular Clusters. Phys. Rev. Lett. **113**(19), 191302 (2014)
221. M. Regis, M. Taoso, D. Vaz, J. Brinchmann, S.L. Zoutendijk, N.F. Bouché, M. Steinmetz, Searching for light in the darkness: Bounds on ALP dark matter with the optical MUSE-faint survey. Phys. Lett. B **814**, 136075 (2021)
222. D. Grin, G. Covone, J.-P. Kneib, M. Kamionkowski, A. Blain, E. Jullo, A Telescope Search for Decaying Relic Axions. Phys. Rev. D **75**, 105018 (2007)
223. V. Prasolov, *Problems and theorems in linear algebra* (American Mathematical Society, USA, 1944)
224. S. Hassani, *Mathematical Physics: A Modern Introduction to Its Foundations* (Springer International Publishing, USA, 2013)
225. Z.-Z. Xing, Z.-H. Zhao, On the four-zero texture of quark mass matrices and its stability. Nucl. Phys. B **897**, 302–325 (2015)
226. M. Gupta, G. Ahuja, Flavor mixings and textures of the fermion mass matrices. Int. J. Mod. Phys. A **27**, 1230033 (2012)
227. H. Fusaoka, Y. Koide, Updated estimate of running quark masses. Phys. Rev. D **57**, 3986–4001 (1998)
228. J. Cardozo, J. H. Mu noz, N. Quintero, E. Rojas, Analysing the charged scalar boson contribution to the charged-current *B* meson anomalies. J. Phys. G **48**(3), 035001 (2021)
229. I. Esteban, M.C. Gonzalez-Garcia, A. Hernandez-Cabezudo, M. Maltoni, T. Schwetz, Global analysis of three-flavour neutrino oscillations: synergies and tensions in the determination of θ_{23}, δ_{CP}, and the mass ordering. JHEP **01**, 106 (2019)
230. G. Alonso-Álvarez, M.B. Gavela, P. Quilez, Axion couplings to electroweak gauge bosons. Eur. Phys. J. C **79**(3), 223 (2019)
231. G. Grilli di Cortona, E. Hardy, J. Pardo Vega, G. Villadoro, The QCD axion, precisely. JHEP **01**, 034 (2016)

IOP Publishing Journal of Physics G: Nuclear and Particle Physics
J. Phys. G: Nucl. Part. Phys. **51** (2024) 035004 (16pp) https://doi.org/10.1088/1361-6471/ad1e21

Alternative 3-3-1 models with exotic electric charges

Eduard Suarez[1,*], Richard H Benavides[2,*], Yithsbey Giraldo[1,*], William A Ponce[3,*] and Eduardo Rojas[1,*]

[1] Departamento de Física, Universidad de Nariño, Calle 18 Carrera 50, A.A. 1175, San Juan de Pasto, Colombia
[2] Facultad de Ciencias Exactas y Aplicadas, Instituto Tecnológico Metropolitano, Calle 73 No 76 A—354, Vía el Volador, Medellín, Colombia
[3] Instituto de Física, Universidad de Antioquia, Calle 70 No. 52-21, Apartado Aéreo 1226, Medellín, Colombia

E-mail: esuarezar@gmail.com, yithsbey@gmail.com, eduro4000@gmail.com, richardbenavides@itm.edu.co and william.ponce@udea.edu.co

Received 3 August 2023, revised 30 November 2023
Accepted for publication 12 January 2024
Published 1 February 2024

Abstract

We report the most general classification of 3-3-1 models with $\beta = \sqrt{3}$. We found several solutions where anomaly cancellation occurs among fermions of different families. These solutions are particularly interesting as they generate non-universal heavy neutral vector bosons. Non-universality in the standard model fermion charges under an additional gauge group generates charged lepton flavor violation and flavor changing neutral currents; we discuss under what conditions the new models can evade constraints coming from these processes. In addition, we also report the *Large Hadron Collider*~(LHC) constraints.

Keywords: 3-3-1 models, 3-3-1 models with exotic electric charges, 3-3-1 models with $\beta = \sqrt{3}$, non-universal models, Pleitez and Frampton non-universal 3-3-1 model, universal one-family models, non-universal heavy neutral vector bosons

1. Introduction

Models with exotic fermions based on the gauge group symmetry $SU(3) \otimes SU(3) \otimes U(1)$ (hereafter 3-3-1 models for short) have been proposed since the early 1970s [1–11]; however,

* Authors to whom any correspondence should be addressed

many of these models lacked important properties of what is known nowadays as 3-3-1 models. For a model to be interesting from a modern perspective [12], it must be chiral, the triangle anomalies must be canceled out only with a number of generations multiple of 3, and most importantly, it must contain the standard model (SM).

In the 1990s, non-universal models without exotic leptons gained popularity as they were very convenient in addressing flavor problems [13, 14]. These models have also been helpful in explaining neutrino masses [15–24], dark matter [25–35], charge quantization [36], strong CP violation [37, 38], muon anomalous magnetic moment (g-2 muon anomaly) [39–41] and flavor anomalies [42–45].

Pleitez and Frampton proposed the non-universal 3-3-1 models [13, 14] as examples of electroweak extensions with lepton number violation, where the number of families is determined by anomaly cancellation. In the literature, there are many examples of models without exotic electric charges, these models have been appropriately classified, and their phenomenology is well known [46–48]. The original model of Pleitez and Framton has exotic electric charges in the quark sector and corresponds to what is known in the literature as $\beta = \sqrt{3}$ [12]. As far as we know, an exhaustive classification of models with this β does not exist in the literature, and therefore a work in this line is necessary. It is important to notice that there are solutions for arbitrary β [49]; however, this solution does not account for all the possible models for a given β. As we will see, the parameter β cannot be arbitrarily large, from the matching conditions $|\beta| \lessapprox \cot\theta_W \sim 1.8$. This condition constitutes a very important restriction regarding the possible realizations of the 3-3-1 symmetry at low energies as it limits the number of possible non-trivial cases to a countable set.

In section 2, we review the basics of the 3-3-1 models. In section 3, we propose sets of fermions corresponding to families of quarks and leptons with the left-handed triplets, anti-triplets, and singlets of $SU(3)_L$. In section 4, we show the anomaly-free sets (AFSs) that constitute the basis for model building. This section lists all possible 3-3-1 models with $\beta = \sqrt{3}$ modulo lepton vector arrays. Finally, in section 5, we show the collider constraints and the conditions the models must satisfy to avoid flavor changing neutral currents and charged lepton flavor violation (CLFV) restrictions.

2. 3-3-1 models

In the subsequent discussion, we work the electroweak gauge group $SU(3)_c \otimes SU(3)_L \otimes U(1)_X$, expanding the electroweak sector of the SM, $SU(2)_L \otimes U(1)_Y$, to $SU(3)_L \otimes U(1)_X$. Furthermore, we assume that, similar to the SM, the color group $SU(3)_c$ is vector-like (i.e. anomaly-free). Left-handed quarks (color triplets) and left-handed leptons (color singlets) transform under the two fundamental representations of $SU(3)_L$ (i.e. 3 and 3^*).

Two categories of models will emerge: universal single-family models, where anomalies cancel within each family similar to the SM, and family models, where anomalies are canceled through interactions among multiple families.

In the context of 3-3-1 models, the most complete electric charge operator for this electroweak sector is

$$Q = \alpha\, T_{L3} + \beta T_{L8} + X\mathbb{1}, \tag{1}$$

here, $T_{La} = \lambda_a/2$, where λ_a, ; $a = 1, 2, ..., 8$ represents the Gell-Mann matrices for $SU(3)_L$ normalized as Tr $(\lambda_a\lambda_b) = 2\delta_{ab}$, and $\mathbb{1} = \text{Diag}(1, 1, 1)$ is the diagonal 3×3 unit matrix. Assuming $\alpha = 1$, the $SU(2)_L$ isospin group of the SM is fully covered in $SU(3)_L$. The parameter $\beta = \frac{2b}{\sqrt{3}}$ is a free parameter that defines the model (β is proportional to b present in

Table 1. Z' chiral charges for the SM leptons and the right-handed neutrino when embedded in S_{L1}. Here, θ_W is the electroweak mixing angle.

$\ell = (\nu_L,\, e_L)^T \subset 3,\ e_R \subset 1$ (as in S_{L1})		
Fields	$g_{Z'}\epsilon_L^{Z'}$	$g_{Z'}\epsilon_R^{Z'}$
ν_e	$\frac{g_L}{\cos\theta_W}\frac{2\cos^2\theta_W - 3}{\sqrt{3(1-4\sin^2\theta_W)}}$	0
e	$\frac{g_L}{\cos\theta_W}\frac{2\cos^2\theta_W - 3}{\sqrt{3(1-4\sin^2\theta_W)}}$	$\frac{g_L}{\cos\theta_W}\frac{\sqrt{3}\,\sin^2\theta_W}{\sqrt{1-4\sin^2\theta_W}}$

the electric charge of the exotic vector boson K_μ). The X values are determined through anomaly cancellation. The 8 gauge fields A_μ^a of $SU(3)_L$ can be expressed as [46, 47]

$$\sum_a \lambda_a A_\mu^a = \sqrt{2}\begin{pmatrix} D_{1\mu}^0 & W_\mu^+ & K_\mu^{(b+1/2)} \\ W_\mu^- & D_{2\mu}^0 & K_\mu^{(b-1/2)} \\ K_\mu^{-(b+1/2)} & K_\mu^{-(b-1/2)} & D_{3\mu}^0 \end{pmatrix}, \tag{2}$$

here, $D_{1\mu}^0 = A_\mu^3/\sqrt{2} + A_\mu^8/\sqrt{6}$, $D_{2\mu}^0 = -A_\mu^3/\sqrt{2} + A_\mu^8/\sqrt{6}$, and $D_{3\mu}^0 = -2A_\mu^8/\sqrt{6}$. The superscripts on the gauge bosons in equation (2) indicate the electric charge of the particles, some of which are functions of the parameter b.

2.1. The minimal model

In references [14, 50], it was demonstrated that, for $b = 3/2$ (i.e. $\beta = \sqrt{3}$), the following fermion structure is free of all gauge anomalies: $\psi_{lL}^T = (l^-,\, \nu_l^0,\, l^+)_L \sim (1,\, 3^*,0)$, $Q_{iL}^T = (u_i,\, d_i,\, X_i)_L \sim (3,\, 3,\, -1/3)$, and $Q_{3L}^T(d_3,\, u_3,\, Y) \sim (3,\, 3^*,2/3)$, where $l = e,\ \mu,\ \tau$ represents the lepton family index, $i = 1,\, 2$ for the first two quark families, and the quantum numbers after the tilde ($\sim$) denote the 3-3-1 representation. The right-handed fields are $u_{aL}^c \sim (3^*,1,\, -2/3)$, $d_{aL}^c \sim (3^*,1,\, 1/3)$, $X_{iL}^c \sim (3^*,1,\, 4/3)$, and $Y_L^c \sim (3^*,1,\, -5/3)$, where $a = 1,\, 2,\, 3$ is the quark family index, and there are three exotic quarks with electric charges: $-4/3$ and $5/3$. This version is referred to as *minimal* in the literature because it avoids the use of exotic leptons, including possible right-handed neutrinos.

3. Lepton and quark generations

In what follows, we will propose sets of leptons S_{Li} and quarks S_{Qi} containing triplets (anti-triplets) and singlets of $SU(3)$. These sets must contain at least one SM generation of SM fermions. From equation (1), for $\beta = \sqrt{3}$, the electric charges of the 3 and 3^* triplets are: $Q_{\rm QED}(3) = {\rm Diag}(1+X,\ X,\ -1+X)$ and $Q_{\rm QED}(3^\star) = {\rm Diag}(-1+X,\ X,\ 1+X)$, respectively. The general expressions for the Z' charges, with the $Z - Z'$ mixing angle equals to zero, are shown in appendix A. For the SM fields embedded in the sets: S_{L1}, S_{L2},S_{L3}, S_{Q1} and S_{Q2}, the Z' charges are shown in tables 1–5, respectively.

- Lepton generation $S_{L1} = [(\nu_e^0,\, e^-,\, E_2^{--}) \oplus e^+ \oplus E_2^{++}]_L$ with quantum numbers (1, 3, -1); (1, 1, 1) and (1, 1, 2) respectively. The Z' charges for the SM fields are shown in table 1:
- Set $S_{L2} = [(e^-,\, \nu_e^0,\, E_1^+) \oplus e^+ \oplus E_1^-]_L$ with quantum numbers (1, 3^*, 0); (1, 1, 1) and (1, 1, -1), respectively. The Z' charges for the SM fields are shown in table 2:

Table 2. Z' chiral charges for the SM leptons and the right-handed neutrino when embedded in S_{L2}. Here, θ_W is the electroweak mixing angle.

$\ell = (\nu_L, e_L)^T \subset 3^*$, $e_R \subset 1$ (as in S_{L2})		
Fields	$g_{Z'}\epsilon_L^{Z'}$	$g_{Z'}\epsilon_R^{Z'}$
ν_e	$\frac{g_L}{\cos\theta_W}\frac{\sqrt{1-4\sin^2\theta_W}}{2\sqrt{3}}$	0
e	$\frac{g_L}{\cos\theta_W}\frac{\sqrt{1-4\sin^2\theta_W}}{2\sqrt{3}}$	$\frac{g_L}{\cos\theta_W}\frac{\sqrt{3}\sin^2\theta_W}{\sqrt{1-4\sin^2\theta_W}}$

Table 3. Z' chiral charges for the SM leptons and the right-handed neutrino when embedded in S_{L3}. Here, θ_W is the electroweak mixing angle.

$\ell = (\nu_L, e_L)^T$, $e_R \subset 3^*$ (as in S_{L3})		
Fields	$g_{Z'}\epsilon_L^{Z'}$	$g_{Z'}\epsilon_R^{Z'}$
ν_e	$\frac{g_L}{\cos\theta_W}\frac{\sqrt{1-4\sin^2\theta_W}}{2\sqrt{3}}$	0
e	$\frac{g_L}{\cos\theta_W}\frac{\sqrt{1-4\sin^2\theta_W}}{2\sqrt{3}}$	$\frac{g_L}{\cos\theta_W}\frac{\sqrt{1-4\sin^2\theta_W}}{\sqrt{3}}$

Table 4. Z' chiral charges for the SM quarks when they are embedded in S_{Q1}. Here, θ_W is the electroweak mixing angle.

$q = (u_L, d_L)^T \subset 3^*$, $u_R, d_R \subset 1$ (as in S_{Q1})		
Fields	$g_{Z'}\epsilon_L^{Z'}$	$g_{Z'}\epsilon_R^{Z'}$
u	$\frac{g_L}{\cos\theta_W}\frac{1}{2\sqrt{3(1-4\sin^2\theta)}}$	$-\frac{g_L}{\cos\theta_W}\frac{2\sin^2\theta_W}{\sqrt{3(1-4\sin^2\theta)}}$
d	$\frac{g_L}{\cos\theta_W}\frac{1}{2\sqrt{3(1-4\sin^2\theta)}}$	$\frac{g_L}{\cos\theta_W}\frac{\sin^2\theta_W}{\sqrt{3(1-4\sin^2\theta)}}$

Table 5. Z' chiral charges for the SM quarks when they are embedded in S_{Q2}. Here, θ_W is the electroweak mixing angle.

$q = (u_L, d_L)^T \subset 3$, $u_R, d_R \subset 1$ (as in S_{Q2})		
Fields	$g_{Z'}\epsilon_L^{Z'}$	$g_{Z'}\epsilon_R^{Z'}$
u	$\frac{g_L}{\cos\theta_W}\frac{1-2\sin^2\theta_W}{2\sqrt{3(1-4\sin^2\theta)}}$	$-\frac{g_L}{\cos\theta_W}\frac{2\sin^2\theta_W}{\sqrt{3(1-4\sin^2\theta)}}$
d	$\frac{g_L}{\cos\theta_W}\frac{1-2\sin^2\theta_W}{2\sqrt{3(1-4\sin^2\theta)}}$	$\frac{g_L}{\cos\theta_W}\frac{\sin^2\theta_W}{\sqrt{3(1-4\sin^2\theta)}}$

- Set $S_{L3} = [(e^-, \nu_e^0, e^+)]_L$ with quantum numbers $(1, 3^*, 0)$. The Z' charges for the SM fields are shown in table 3:
- Set $S_{Q1} = [(d, u, Q_1^{5/3}) \oplus u^c \oplus d^c \oplus Q_1^c]_L$ with quantum numbers $(3, 3^*, 2/3)$; $(3^*, 1, -2/3)$; $(3^*, 1, 1/3)$ and $(3^*, 1, -5/3)$, respectively. The Z' for the SM fields are shown in table 4:
- Set $S_{Q2} = [(u, d, Q_2^{-4/3}) \oplus u^c \oplus d^c \oplus Q_2^c]_L$ with quantum numbers $(3, 3, -1/3)$; $(3^*, 1, -2/3)$; $(3^*, 1, 1/3)$ and $(3^*, 1, 4/3)$, respectively. The Z' charges for the SM fields are shown in table 5:

Table 6. Contribution to the anomalies for each family of quarks S_{Q_i}, leptons S_{L_i} and exotics S_{E_i}, for 3-3-1 models with $\beta = \sqrt{3}$.

Anomalías	S_{L1}	S_{L2}	S_{L3}	S_{Q1}	S_{Q2}	S_{E1}	S_{E2}
$[SU(3)_C]^2U(1)_X$	0	0	0	0	0	0	0
$[SU(3)_L]^2U(1)_X$	-1	0	0	2	-1	1	0
$[\text{Grav}]^2U(1)_X$	0	0	0	0	0	0	0
$[U(1)_X]^3$	6	0	0	-12	6	-6	0
$[SU(3)_L]^3$	1	-1	-1	-3	3	-1	1

Table 7. AFSs for $\beta = \sqrt{3}$. We have classified the AFS according to the content of quark families, i.e. Q_i^{I}, Q_i^{II}, and Q_i^{III}. Combinations of these sets with three SM quark and three SM lepton families can be considered as 3-3-1 models.

i	Vector-like lepton set (L_i)	One quark set (Q_i^{I})	Two quarks set (Q_i^{II})	Three quarks set (Q_i^{III})
1	$S_{E2}+S_{L2}$	$S_{E2}+2S_{L1}+S_{Q1}$	$S_{L1}+S_{L2}+S_{Q1}+S_{Q2}$	$3S_{L1}+2S_{Q1}+S_{Q2}$
2	$S_{E1}+S_{L1}$	$S_{E1}+2S_{L2}+S_{Q2}$	$S_{L1}+S_{L3}+S_{Q1}+S_{Q2}$	$3S_{L2}+S_{Q1}+2S_{Q2}$
3	$S_{E2}+S_{L3}$	$S_{E1}+S_{L2}+S_{L3}+S_{Q2}$		$3S_{L3}+S_{Q1}+2S_{Q2}$
4		$S_{E1}+2S_{L3}+S_{Q2}$		$2S_{L2}+S_{L3}+S_{Q1}+2S_{Q2}$
5				$S_{L2}+2S_{L3}+S_{Q1}+2S_{Q2}$

- To cancel anomalies, it is advantageous introducing triplets and anti-triplets of exotic leptons; for example, $S_{E1} = [(N_1^0, E_4^+, E_3^{++}) \oplus E_4^- \oplus E_3^{--}]_L$ with quantum numbers (1, 3^*, 1); (1, 1, -1) and (1, 1, -2), respectively. We do not report the Z' charges of exotic fermion fields because we assume they have a very high mass.
- Additional exotic lepton sets. $S_{E2} = [(E_5^+, N_2^0, E_6^-) \oplus E_5^- \oplus E_6^+]_L$ with quantum numbers (1, 3, 0); (1, 1, -1) and (1, 1, 1), respectively. A more economical set is $S_{E3} = [(E_5^+, N_2^0, E_5^-)]$ which has identical contributions to the anomalies as S_{E2} but different Z' charges. However, these details are irrelevant for the low energy phenomenology, so we do not include S_{E3} in table 6.

4. Irreducible anomaly free sets and models

Table 6 shows the contribution of each set to the anomalies. From table 6, it is possible to obtain the irreducible AFSs [48], shown in table 7. The irreducible AFSs Q_i^{I}, Q_i^{II} and Q_i^{III} in table 7 correspond to fermion sets with one quark family, two quark families, or three quark families, respectively. These sets can be combined to build three family models as shown in table 8. There are 33 different models (without considering all the possible embeddings). These models can also be extended by adding vector-like lepton sets, L_i, indicated in the second column of table 7. To exemplify the possible embeddings we show some cases in table 10. The choice of models in table 10 show how the phenomenology depends on the SM fermion embedding in the model. For example, in the case of M10, the embedding determines whether it is strongly coupled. M17 was chosen because it had several embeddings. M3 is the minimal model. M4 is similar to the minimal model but is not universal in the lepton sector.

In general, we obtain three classes of models as we can see below:

Table 8. Three-family models built from the irreducible anomaly-free sets (table 7). It is possible to obtain (trivially) new models by adding vector-like lepton sets; we are not considering these possibilities in our counting unless they are necessary to complete the lepton families.

	Models	
M1	$Q_1^{\rm III}$	$3S_{L1}+2S_{Q1}+S_{Q2}$
M2	$Q_2^{\rm III}$	$3S_{L2}+S_{Q1}+2S_{Q2}$
M3	$Q_3^{\rm III}$	$3S_{L3}+S_{Q1}+2S_{Q2}$
M4	$Q_4^{\rm III}$	$2S_{L2}+S_{L3}+S_{Q1}+2S_{Q2}$
M5	$Q_5^{\rm III}$	$S_{L2}+2S_{L3}+S_{Q1}+2S_{Q2}$
M6	$Q_1^{\rm II}+Q_1^{\rm I}$	$3S_{L1}+S_{L2}+S_{E2}+2S_{Q1}+S_{Q2}$
M7	$Q_1^{\rm II}+Q_2^{\rm I}$	$S_{L1}+3S_{L2}+S_{E1}+S_{Q1}+2S_{Q2}$
M8	$Q_1^{\rm II}+Q_3^{\rm I}$	$S_{L1}+2S_{L2}+S_{L3}+S_{E1}+S_{Q1}+2S_{Q2}$
M9	$Q_1^{\rm II}+Q_4^{\rm I}$	$S_{L1}+S_{L2}+2S_{L3}+S_{E1}+S_{Q1}+2S_{Q2}$
M10	$Q_2^{\rm II}+Q_1^{\rm I}$	$3S_{L1}+S_{L3}+S_{E2}+2S_{Q1}+S_{Q2}$
M11	$Q_2^{\rm II}+Q_2^{\rm I}$	$S_{L1}+2S_{L2}+S_{L3}+S_{E1}+S_{Q1}+2S_{Q2}$
M12	$Q_2^{\rm II}+Q_3^{\rm I}$	$S_{L1}+S_{L2}+2S_{L3}+S_{E1}+S_{Q1}+2S_{Q2}$
M13	$Q_2^{\rm II}+Q_4^{\rm I}$	$S_{L1}+3S_{L3}+S_{E1}+S_{Q1}+2S_{Q2}$
M14	$Q_1^{\rm I}+Q_2^{\rm I}+Q_3^{\rm I}$	$2S_{L1}+3S_{L2}+S_{L3}+2S_{E1}+S_{E2}+S_{Q1}+2S_{Q2}$
M15	$Q_1^{\rm I}+Q_2^{\rm I}+Q_4^{\rm I}$	$2S_{L1}+2S_{L2}+2S_{L3}+2S_{E1}+S_{E2}+S_{Q1}+2S_{Q2}$
M16	$Q_1^{\rm I}+Q_3^{\rm I}+Q_4^{\rm I}$	$2S_{L1}+S_{L2}+3S_{L3}+2S_{E1}+S_{E2}+S_{Q1}+2S_{Q2}$
M17	$Q_2^{\rm I}+Q_3^{\rm I}+Q_4^{\rm I}$	$3S_{L2}+3S_{L3}+3S_{E1}+3S_{Q2}$
M18	$3Q_1^{\rm I}$	$6S_{L1}+3S_{E2}+3S_{Q1}$
M19	$2Q_1^{\rm I}+Q_2^{\rm I}$	$4S_{L1}+2S_{L2}+2S_{E2}+S_{E1}+2S_{Q1}+S_{Q2}$
M20	$2Q_1^{\rm I}+Q_3^{\rm I}$	$4S_{L1}+S_{L2}+S_{L3}+S_{E1}+2S_{E2}+2S_{Q1}+S_{Q2}$
M21	$2Q_1^{\rm I}+Q_4^{\rm I}$	$4S_{L1}+2S_{L3}+S_{E1}+2S_{E2}+2S_{Q1}+S_{Q2}$
M22	$3Q_2^{\rm I}$	$6S_{L2}+3S_{E1}+3S_{Q2}$
M23	$2Q_2^{\rm I}+Q_1^{\rm I}$	$2S_{L1}+4S_{L2}+2S_{E1}+S_{E2}+S_{Q1}+2S_{Q2}$
M24	$2Q_2^{\rm I}+Q_3^{\rm I}$	$5S_{L2}+S_{L3}+3S_{E1}+3S_{Q2}$
M25	$2Q_2^{\rm I}+Q_4^{\rm I}$	$4S_{L2}+2S_{L3}+3S_{E1}+3S_{Q2}$
M26	$3Q_3^{\rm I}$	$3S_{L2}+3S_{L3}+3S_{E1}+3S_{Q2}$
M27	$2Q_3^{\rm I}+Q_1^{\rm I}$	$2S_{L1}+2S_{L2}+2S_{L3}+2S_{E1}+S_{E2}+S_{Q1}+2S_{Q2}$
M28	$2Q_3^{\rm I}+Q_2^{\rm I}$	$4S_{L2}+2S_{L3}+3S_{E1}+3S_{Q2}$
M29	$2Q_3^{\rm I}+Q_4^{\rm I}$	$2S_{L2}+4S_{L3}+3S_{E1}+3S_{Q2}$
M30	$3Q_4^{\rm I}$	$6S_{L3}+3S_{E1}+3S_{Q2}$
M31	$2Q_4^{\rm I}+Q_1^{\rm I}$	$2S_{L1}+4S_{L3}+2S_{E1}+S_{E2}+S_{Q1}+2S_{Q2}$
M32	$2Q_4^{\rm I}+Q_2^{\rm I}$	$2S_{L2}+4S_{L3}+3S_{E1}+3S_{Q2}$
M33	$2Q_4^{\rm I}+Q_3^{\rm I}$	$S_{L2}+5S_{L3}+3S_{E1}+3S_{Q2}$

- Completely non-universal models: this happens if we embed each of the SM families in different sets; for example, one of the possible embeddings for the M12 model in table 8 is to put the first lepton family in S_{L3} and the remaining lepton families in S_{L1} and S_{L2}. This class of models usually has very strong restrictions from FCNC and CLFV.
- Universal Models: in several AFSs, there are embeddings with the three families of SM leptons in sets with the same quantum numbers; the same applies for the three families of the SM quarks. For example, in the M26 model in table 8, it is possible to embed all the three SM families in the sets $3S_{L3}+3S_{Q2}$. The remaining fields are considered exotic fermions and are necessary to cancel anomalies.

Table 9. The lepton families S_{L_1} and S_{L_2} are strongly coupled (For S_{L_1} and S_{L_2} the left-handed lepton doublet $\ell$and the right-handed charged lepton singlet e_R have couplings greater than 1, respectively). Therefore only S_{L_3} is phenomenologically viable for the first family. Depending on the quark content, i.e. S_{Q_1} or S_{Q_2}, we have two different constraints.

Particle content first generation	LHC-lower limit in TeV
$S_{L3} + S_{Q1}$	7.3
$S_{L3} + S_{Q2}$	6.4

- The $2 + 1$ models: most AFSs have embeddings where two families are in sets with the same quantum numbers, and the third family is a different set. To avoid the strongest FCNC restrictions, it is necessary that the left-handed doublets of the first two SM quark families have identical quantum numbers. This condition is also desirable for Lepton families, although some models could avoid the FCNC constraints without satisfying this condition. A typical example of these models is the Pisano–Pleitez–Frampton minimal model [13, 14]. $3S_{L3} + S_{Q1} + 2S_{Q2}$ (the M3 model in table 8). This model is universal in the lepton sector and non-universal in the quark sector.

5. LHC and low energy constraints

We consider the ATLAS search for high-mass dilepton resonances in the mass range of 250 GeV to 6 TeV in proton–proton collisions at a center-of-mass energy of $\sqrt{s} = 13$ TeV during Run 2 of the LHC with an integrated luminosity of 139 fb^{-1} [51]. This data was collected from searches of Z' bosons decaying dileptons. We obtain the lower limit on the Z' mass from the intersection of the theoretical predictions for the cross-section with the corresponding upper limit reported by ATLAS at a 95% confidence level. We use the expressions given in [52–54] to calculate the theoretical cross-section. We assume that the $Z - Z'$ mixing angle θ (see appendix D) equals zero for these bounds. In table 9, the LHC constraints for some models are presented. It is important to stress that the leptons of the first family, i.e. the electron and its neutrino, should be embedded in S_{L3} since it is the only scenario where the right-handed electron has Z' couplings less than 1. In table 9, this is the best option for models with the first two lepton generations embedded in S_{L3}, as it happens for the minimal model (M3), since having identical quantum numbers for the first and second lepton families avoids possible issues with CLFV and FCNC. To avoid the strongest FCNC constraints in the quark sector, the charges of the left-handed quarks of the first two families should be identical [55]; this feature is assumed to calculate the lower mass limits in table 9. It is important to stress the non-universal Z' couplings modify processes such as [56]: coherent $\mu - e$ conversion in a muon atom, $K^0 - \bar{K}^0$ and $B - \bar{B}$ mixing, ϵ, and ϵ'/ϵ, lepton, and semileptonic decays (e.g. $\mu \to e\gamma$) which, if observed in the future, the Non-universal Models will be favored over the universal ones. For models with a Z' boson coupling in a different way to the third family, there are different predictions for the branching rations $B(t \to Hu)$ and $B(t \to Hc)$. These predictions are strongly constrained by colliders [57]. In table 10, SC stands for strongly coupled, indicating that in the sets S_{L1} and S_{L2}, the coupling of the right-handed electron is greater than one, and therefore, the collider constraints are very strong. Even though Z' with couplings greater than one to the SM fields of the first generation are quite

Table 10. Alternative embeddings of the SM fields for some of the models in table 8. The lepton sets in square brackets contain the SM fields. The superscripts correspond to the particle content of the SM, where ℓ ($\bar{\ell}$) stands for a left-handed lepton doublet embedded in a $SU(3)_L$ triplet (anti-triplet), and e'^{+} (e^{+}) is the right-handed charged lepton embedded in a $SU(3)_L$ triplet (singlet). The check mark ✓means that at least two (2+1) or three (universal) families have the same charges under the gauge symmetry. The cross×stands for the opposite. LHC constraints are obtained from table 9 for embeddings in which we can choose the same Z' charges for the first two families, otherwise, we leave the space blank. To avoid a strongly coupled model in the Lepton sector, it is necessary to embed the first Lepton family (electron and electron neutrino) in S_{L3}. This feature will be helpful to distinguish between the different embeddings. The embedding also defines the content of exotic particles in each case.

Model	j	SM Lepton embeddings	Universal	$2+1$	Quark configuration	LHC-lower limit
$M3 = Q_3^{\mathrm{III}}$(Minimal)	—	$[3S_{L3}^{\bar{\ell}+e'^{+}}]$	✓	×	$2S_{Q2}+S_{Q1}$	6.4 TeV
$M4 = Q_4^{\mathrm{III}}$	—	$[2S_{L2}^{\bar{\ell}+e^{+}}+S_{L3}^{\bar{\ell}+e'^{+}}]$	×	✓	$2S_{Q2}+S_{Q1}$	6.4 TeV
$M6 = (Q_1^{\mathrm{I}}+Q_1^{\mathrm{II}})^j$	1	$[3S_{L1}^{\ell+e^{+}}]+S_{L2}+S_{E2}$	✓	×	$2S_{Q1}+S_{Q2}$	SC
	2	$[2S_{L1}^{\ell+e^{+}}+S_{L2}^{\bar{\ell}+e^{+}}]+S_{L1}+S_{E2}$	×	✓	$2S_{Q1}+S_{Q2}$	SC
$M17 = (Q_2^{\mathrm{I}}+Q_3^{\mathrm{I}}+Q_4^{\mathrm{I}})^j$	1	$[3S_{L2}^{\bar{\ell}+e^{+}}]+3S_{L3}+3S_{E1}$	✓	×	$3S_{Q2}$	SC
	2	$[3S_{L3}^{\bar{\ell}+e'^{+}}]+3S_{L2}+3S_{E1}$	✓	×	$3S_{Q2}$	6.4 TeV
	3	$[2S_{L2}^{\bar{\ell}+e^{+}}+S_{L3}^{\bar{\ell}+e'^{+}}]+S_{L2}+2S_{L3}+3S_{E1}$	×	✓	$3S_{Q2}$	6.4 TeV
	4	$[S_{L2}^{\ell+e^{+}}+2S_{L3}^{\bar{\ell}+e'^{+}}]+2S_{L2}+S_{L3}+3S_{E1}$	×	✓	$3S_{Q2}$	6.4 TeV
$M10 = (Q_1^{\mathrm{I}}+Q_2^{\mathrm{II}})^j$	1	$[3S_{L1}^{\ell+e^{+}}]+S_{L3}+S_{E2}$	✓	×	$2S_{Q1}+S_{Q2}$	SC
	2	$[2S_{L1}^{\ell+e^{+}}+S_{L3}^{\bar{\ell}+e'^{+}}]+S_{L1}+S_{E2}$	×	✓	$2S_{Q1}+S_{Q2}$	7.3 TeV

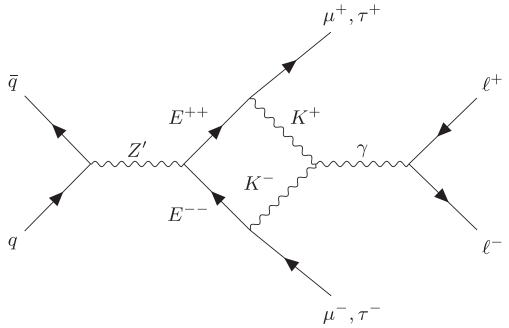

Figure 1. Doubly charged exotic lepton contribution to the process $q\bar{q} \to Z' \to E^{++}E^{--} \to \ell^+\ell^-\gamma \to \ell^+\ell^-\mu^+\mu^-(\tau^+\tau^-)$.

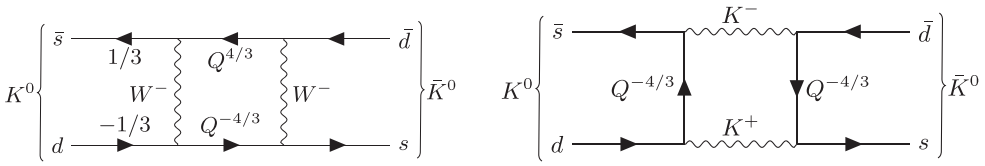

Figure 2. Exotic quark contribution to the $K^0 - \bar{K}^0$ mixing.

disfavored by colliders [52], strongly coupled models are also attractive in several phenomenological approaches [55, 58]; for this reason, it is important to realize the existence of these models, which naturally appear in 3-3-1 models with large β values. Regarding constraints on exotic particles, the restrictions on the mass of a sequential heavy lepton are above 100 GeV [59]. For exotic quarks t' and b', the allowed mass ranges are above 1370 GeV and 1570 GeV, respectively [59]. The restrictions on fields with exotic electric charges are weaker because the identification algorithms assume the charges are proportional to the charge of the electron [60]. The presence of doubly charged exotic leptons can generate new decay channels in proton–proton collisions at very high energies. In figure 1, the Feynman diagram for the process $q\bar{q} \to Z' \to E^{++}E^{--} \to \ell^+\ell^-\gamma \to \ell^+\ell^-\mu^+\mu^-(\tau^+\tau^-)$, generating four boosted leptons in the final state (the doubly charged exotic lepton appears in S_{L1}, which strongly couples the Z'; for this reason, to avoid collider constraints, we restrict to leptons of the second or third family). On the other hand, exotic quarks modify the $K^0 - \bar{K}^0$ mixing, as shown in figure 2. Fermions with exotic electric charges can contribute to several processes; however, an exhaustive study of these processes is beyond the purpose of this work.

6. Conclusions

Since that for 3-3-1 models, the absolute value of the parameter β must be less than $\beta \lessapprox \cot\theta_W = 1.8$ (for $\sin^2\theta_W = 0.231$ in the $\overline{\text{MS}}$ renormalization scheme at the Z-pole energy scale), and the values of β are further limited by the Requirement that the vector boson charges be integers, the possible values of this parameter are reduced to a few cases. For a realistic model, the maximum possible value corresponds to $\beta = \sqrt{3} \sim 1.73$. This case is important since it contains the Pleitez-Frampton minimal model. We have constructed three sets of lepton families, S_{Li}, two quark families, S_{Qi}, and two exotic lepton families S_{Ei}, and we

calculated their contribution to anomalies. In our analysis, we obtained 14 irreducible AFSs, from which we built 33 non-trivial 3-3-1 models (without considering the different embeddings) with at least three quark and three lepton families for each case. Each of these embeddings constitutes a phenomenologically distinguishable model; however, we limited our analysis of the possible embeddings to a few cases. In the same way, from our analysis of the 3-3-1 models with $\beta = \sqrt{3}$ we report the couplings of the SM fields to the Z' boson for all the possible quark and lepton families and the corresponding lower limits on the Z' mass. We also discuss the conditions under which the reported models avoid FCNC and CLFV. We also observed that strongly coupled models appear naturally and require a high value for the Z' mass. They can be helpful in specific phenomenological approaches based on models with strong dynamics. In the future, a detailed analysis of each model will be necessary; however, this is beyond the scope of the present work.

Acknowledgments

This research was partly supported by the 'Vicerrectoría de Investigaciones e Interacción Social VIIS de la Universidad de Nariño', project numbers 2686, 1928, 2172, 2693, and 2679. ER, RHB and YG acknowledge additional financial support from Minciencias CD 82315 CT ICETEX 2021-1080.

Data availability statement

All data that support the findings of this study are included within the article (and any supplementary files).

Appendix A. Z' charges for a general 3-3-1 model

At low energy, the 3-3-1 models, i.e. the gauge symmetry $SU(3)_C \otimes SU(3)_L \otimes U(1)_X$ reduces to the low energy effective theory $SU(3)_C \otimes SU(2)_L \otimes U(1)_{8L} \otimes U(1)_X \to SU(3)_C \otimes SU(2)_L \otimes U(1)_Y$. From the covariant derivatives, for the neutral currents, we obtain the interaction Lagrangian

$$-\mathcal{L} \supset g_L J^{\mu}_{3L} A_{3L\mu} + g_L J^{\mu}_{8L} A_{8L\mu} + g_X J^{\mu}_{X} A_{X\mu}, \tag{A1}$$

which can be written as

$$\begin{aligned} -\mathcal{L}_{NC} &= g_i J_{i\mu} A_i^{\mu} = g_j J_{j\mu} O_{jk} O^T_{kl} A_l^{\mu}, \\ &= \tilde{g}_k \tilde{J}_{k\mu} \tilde{A}_k^{\mu}, \end{aligned} \tag{A2}$$

where $\tilde{A}_k^{\mu} = O^T_{kl} A_l^{\mu}$, then $(A_1^{\mu}, A_2^{\mu}) = (A_{8L}^{\mu}, A_X^{\mu})$, $(\tilde{A}_1^{\mu}, \tilde{A}_2^{\mu}) = (B^{\mu}, Z'^{\mu})$, $(g_1 J_1^{\mu}, g_2 J_2^{\mu}) = (g_L A_{8L}^{\mu}, g_X A_X^{\mu})$ and $(\tilde{g}_1 \tilde{A}_1^{\mu}, \tilde{g}_2 \tilde{A}_2^{\mu}) = (g_Y J_Y^{\mu}, g_{Z'} J_{Z'}^{\mu})$. At high energies, the symmetry is broken following the breaking chain $SU(3)_C \otimes SU(3)_L \otimes U_X(1) \to SU(3)_C \otimes SU(2)_L \otimes U_{8L}(1) \otimes U_X(1) = SU(3)_C \otimes SU(2)_L \otimes U_Y(1) \otimes U'(1)$, i.e.

$$\begin{pmatrix} A_{3L} \\ B^{\mu} \\ Z'^{\mu} \end{pmatrix} = \begin{pmatrix} 1 & 0_{1\times 2} \\ 0_{2\times 1} & O^T_{2\times 2} \end{pmatrix} \begin{pmatrix} A_{3L} \\ A^{\mu}_{8L} \\ A^{\mu}_{X} \end{pmatrix}. \tag{A3}$$

Next step $SU(3)_C \otimes SU(2)_L \otimes U_Y(1) \otimes U'(1) \to SU(3)_C \otimes U_{\rm QED}(1)$, i.e.

$$\begin{pmatrix} A^\mu \\ Z^\mu \\ Z'^\mu \end{pmatrix} = \begin{pmatrix} \sin\theta_W & \cos\theta_W & 0 \\ \cos\theta_W & -\sin\theta_W & 0 \\ 0 & 0 & 1 \end{pmatrix} \begin{pmatrix} A_{3L} \\ B^\mu \\ Z'^\mu \end{pmatrix} \tag{A4}$$

where the fields correspond to the SM photon A^μ and the Z^μ boson, and a heavy vector-boson Z'. Proceeding similarly for the currents, and limiting ourselves to the fields on which the orthogonal submatrix $Q_{2\times 2}$ acts, from equation (A2) we obtain $\tilde{g}_k \tilde{J}^\mu_k = g_j J^\mu_j O_{jk}$, i.e.

$$\begin{aligned} \tilde{g}_k \tilde{J}_{k\mu} &= \left(g_Y J^\mu_Y, \quad g_{Z'} J^\mu_{Z'}\right) = \left(g_L J^\mu_{L8}, \quad g_X J^\mu_X\right) \begin{pmatrix} O_{11} & O_{12} \\ O_{21} & O_{22} \end{pmatrix}, \\ &= \left(g_L J^\mu_{L8} O_{11} + g_X J^\mu_X O_{21}, \quad g_L J^\mu_{L8} O_{12} + g_X J^\mu_X O_{22}\right). \end{aligned} \tag{A5}$$

Without further assumption

$$\begin{pmatrix} O_{11} & O_{12} \\ O_{21} & O_{22} \end{pmatrix} = \begin{pmatrix} \cos\omega & -\sin\omega \\ \sin\omega & \cos\omega \end{pmatrix}, \tag{A6}$$

so that

$$\begin{aligned} g_Y J^\mu_Y &= \quad g_L J^\mu_{L8} \cos\omega + g_X J^\mu_X \sin\omega, \\ g_{Z'} J^\mu_{Z'} &= -g_L J^\mu_{L8} \sin\omega + g_X J^\mu_X \cos\omega. \end{aligned} \tag{A7}$$

The charge operator in a three-dimensional representation is given by

$$Q_{\rm QED} = T_{L3} + \beta T_{L8} + X\mathbb{1}, \tag{A8}$$

hence

$$Y = \beta T_{L8} + X. \tag{A9}$$

From this expression, it is possible to obtain a relation between the currents (the currents are proportional to the charges)

$$J^\mu_Y = \beta J^\mu_{L8} + J^\mu_X. \tag{A10}$$

Comparing this result with (A7)

$$\beta = \frac{g_L \cos\omega}{g_Y}, \qquad 1 = \frac{g_X \sin\omega}{g_Y}. \tag{A11}$$

From $\cos^2\omega + \sin^2\omega = 1$, we obtain

$$\left(\frac{\beta}{g_L}\right)^2 + \left(\frac{1}{g_X}\right)^2 = \frac{1}{g_Y^2}. \tag{A12}$$

In the SM, $g_L \approx 0.652$ and $g_Y = g_L \tan\theta_W$,

$$g_X = \frac{g_L \tan\theta_W}{\sqrt{1 - \beta^2 \tan^2\theta_W}}. \tag{A13}$$

This expression shows that the parameter β cannot be arbitrarily large from the matching conditions $\beta \lessapprox \cot\theta_W$; some care must be taken on this approximation since this is a renormalization-scheme dependent inequality. From these expressions, we obtain

$$\cos\omega = \frac{\beta}{g_L} g_Y = \beta \tan\theta_W, \quad \sin\omega = \sqrt{1 - \beta^2 \tan^2\theta_W}\,. \tag{A14}$$

From equation (A7), $g_{Z'}\epsilon_{Z'} = -g_L T_{8L}\sin\omega + g_X X_X \cos\omega$, we obtain

$$\begin{aligned} g_{Z'}\epsilon_{Z'} &= -g_L T_{L8}\sqrt{1 - \beta^2\tan^2\theta_W} + \beta\frac{g_L \tan^2\theta_W X}{\sqrt{1 - \beta^2\tan^2\theta_W}}, \\ &= g_L\left(-T_{L8}\tilde{\alpha} + \beta\frac{\tan^2\theta_W}{\tilde{\alpha}}X\right), \end{aligned} \tag{A15}$$

where $\tilde{\alpha} = \sqrt{1 - \beta^2\tan^2\theta_W} = \frac{1}{\cos\theta_W}\sqrt{1 - 4\sin^2\theta_W}$ for $\beta = \sqrt{3}$.

Appendix B. Chiral charges for the 3 representation

In what follows, we propose sets of fermions representing the particle content of a generation of leptons or quarks, for left-handed triplets 3, and for right-handed fermions in an $SU(3)_L$ singlet, in general we have

$$g_{Z'}\epsilon_L^{Z'}(3) = g_L\begin{pmatrix} -\frac{1}{2\sqrt{3}}\tilde{\alpha} + \beta\frac{\tan^2\theta_W}{\tilde{\alpha}}X & 0 & 0 \\ 0 & -\frac{1}{2\sqrt{3}}\tilde{\alpha} + \beta\frac{\tan^2\theta_W}{\tilde{\alpha}}X & 0 \\ 0 & 0 & \frac{1}{\sqrt{3}}\tilde{\alpha} + \beta\frac{\tan^2\theta_W}{\tilde{\alpha}}X \end{pmatrix}, \quad \epsilon_R^{Z'} = g_L\beta\frac{\tan^2\theta_W}{\tilde{\alpha}}X_R. \tag{B1}$$

Here we add the subindex R to the X-charge of the right-handed singlet to emphasize that it differs from the quantum number of the left-handed triplet, i.e. X. If the charge conjugate of the right-handed fermion is identified with the third component of a triplet, then $\epsilon_R^{Z'} = -g_L\left(\frac{1}{\sqrt{3}}\tilde{\alpha} + \beta\frac{\tan^2\theta_W}{\tilde{\alpha}}X\right)$.

Appendix C. The conjugate representation $3^\star$

To cancel the anomalies of $SU(3)_L$, triplets must be put in the conjugate representation. In general, for any set of generators T^a of an $SU(N)$ symmetry with $N \leqslant 3$ there exists another set of generators $-T^{a^*}$, which satisfy the same algebra. This set of generators spawns the so-called conjugate representation of $SU(N)$. With these generators, we can build charge operators and multiplets containing the SM particles. To compare with the conjugate representation, we use the projectors

$$p_{12} = \begin{pmatrix} 1 & 0 & 0 \\ 0 & 1 & 0 \\ 0 & 0 & 0 \end{pmatrix}, \quad \tilde{p}_{12} = \begin{pmatrix} 0 & 1 & 0 \\ 1 & 0 & 0 \\ 0 & 0 & 0 \end{pmatrix}. \tag{C1}$$

They should not be confused with permutation operators, as the purpose of these operators is to compare only the first two rows of the charge operators. $\tilde{p}_{12}$ also permutes the first two eigenvalues to make a proper comparison with the conjugate operator. We can obtain the X^C, i.e. the charge of the triplet $3^\star$ in the conjugate representation, from the equation

$$\tilde{p}_{12}(T_{L3} + \beta T_{L8} + X\mathbb{1})\tilde{p}_{12}^{T} = p_{12}(-T_{L3} - \beta T_{L8} + X^{C}\mathbb{1})p_{12}^{T}, \tag{C2}$$

only the signs of the $SU(3)$ generators were changed. This matrix equation is equivalent to a couple of linear equations. These equations have the solution $X^C = \left(\frac{\beta}{\sqrt{3}} + X\right) = (1 + X)$. An equivalent treatment is to obtain the conjugate representation from $T_{3L} - \beta T_{8L} + X^c$, which generates the exact electric charges but in a different order. We verify that both approaches contribute identically to the anomalies, developing the same particle content and models. For left-handed triplets in the conjugate representation $3^\star$, and right-handed fermions in an $SU(3)_L$ singlet, we have, in general,

$$g_{Z'}\epsilon_L^{Z'}(3^\star) = g_L\begin{pmatrix} +\frac{1}{2\sqrt{3}}\tilde{\alpha} + \beta\frac{\tan^2\theta_W}{\tilde{\alpha}}X^C & 0 & 0 \\ 0 & +\frac{1}{2\sqrt{3}}\tilde{\alpha} + \beta\frac{\tan^2\theta_W}{\tilde{\alpha}}X^C & 0 \\ 0 & 0 & -\frac{1}{\sqrt{3}}\tilde{\alpha} + \beta\frac{\tan^2\theta_W}{\tilde{\alpha}}X^C \end{pmatrix}, \quad \epsilon_R^{Z'} = g_L\beta\frac{\tan^2\theta_W}{\tilde{\alpha}}X^C. \tag{C3}$$

If the charge conjugate of the right-handed fermion is identified with the third component of a triplet, then $\epsilon_R^{Z'} = -g_L\left(-\frac{1}{\sqrt{3}}\tilde{\alpha} + \beta\frac{\tan^2\theta_W}{\tilde{\alpha}}X^C\right)$.

Appendix D. *Z-Z′* mixing

Mixing angle θ between Z and Z' is tightly constrained [61], i.e. $\theta < 10^{-3}$; however, in several phenomenological analyzes, it is still useful delivering expressions for the mass eigenstates.

$$\begin{aligned} Z_1^\mu &= Z^\mu\cos\theta + Z'^\mu\sin\theta, \\ Z_2^\mu &= -Z^\mu\sin\theta + Z'^\mu\cos\theta. \end{aligned} \tag{D1}$$

At low energies, Z_1 is identified with the SM Z boson. In order to keep the Lagrangian invariant, this field rotation must be compensated by the corresponding rotation of the currents

$$\begin{aligned} g_1 J_1^\mu &= g_Z J_Z^\mu\cos\theta + g_{Z'}J_{Z'}^\mu\sin\theta, \\ g_2 J_2^\mu &= -g_Z J_Z^\mu\sin\theta + g_{Z'}J_{Z'}^\mu\cos\theta. \end{aligned} \tag{D2}$$

From which we get

$$\begin{aligned} g_1 Q_1 &= g_Z Q_Z\cos\theta + g_{Z'}Q_{Z'}\sin\theta, \\ g_2 Q_2 &= -g_Z Q_Z\sin\theta + g_{Z'}Q_{Z'}\cos\theta. \end{aligned} \tag{D3}$$

ORCID iDs

Yithsbey Giraldo https://orcid.org/0000-0002-5348-8033
Eduardo Rojas https://orcid.org/0000-0002-7412-1345

References

[1] Schechter J and Ueda Y 1973 Unified weak-electromagnetic gauge schemes based on the three-dimensional unitary group *Phys. Rev.* D **8** 484
[2] Albright C H, Jarlskog C and Tjia M O 1975 Implications of gauge theories for heavy leptons *Nucl. Phys.* B **86** 535
[3] Fayet P 1974 A gauge theory of weak and electromagnetic interactions with spontaneous parity breaking *Nucl. Phys.* B **78** 14
[4] Fritzsch H and Minkowski P 1976 SU(3) as gauge group of the vector-like weak and electromagnetic interactions *Phys. Lett.* B **63** 99
[5] Segre G, Weyers J and Vector-Like A 1976 Theory with a parity violating neutral current and natural symmetry *Phys. Lett.* B **65** 243
[6] Mohapatra R N and Pati J C 1976 Essential restriction on the symmetry of a unified theory for the case of massive gluons *Phys. Lett.* B **63** 204
[7] Lee B W and Weinberg S 1977 SU(3) $\times$ U(1) gauge theory of the weak and electromagnetic interactions *Phys. Rev. Lett.* **38** 1237
[8] Lee B W and Shrock R E 1978 An su(3) $\times$ U(1) theory of weak and electromagnetic interactions *Phys. Rev.* D **17** 2410
[9] Langacker P, Segre G and Golshani M 1978 Gauge theory of weak and electromagnetic interactions with an SU(3) $\times$ U(1) symmetry *Phys. Rev.* D **17** 1402
[10] Georgi H and Pais A 1979 Generalization of gim: horizontal and vertical flavor mixing *Phys. Rev.* D **19** 2746
[11] Singer M, Valle J W F and Schechter J 1980 Canonical neutral current predictions from the weak electromagnetic gauge group su(3) X u(1) *Phys. Rev.* D **22** 738
[12] Pleitez V 2021 Challenges for the 3-3-1 models *5th Colombian Meeting on High Energy Physics* arXiv:2112.10888
[13] Pisano F and Pleitez V 1992 An SU(3) $\times$ U(1) model for electroweak interactions *Phys. Rev.* D **46** 410
[14] Frampton P H 1992 Chiral dilepton model and the flavor question *Phys. Rev. Lett.* **69** 2889
[15] Queiroz F, C A de, Pires S and da Silva P S R 2010 A minimal 3-3-1 model with naturally sub-eV neutrinos *Phys. Rev.* D **82** 065018
[16] Caetano W, Cogollo D, Pires C A de S and Rodrigues da Silva P S 2012 Combining type I and type II seesaw mechanisms in the minimal 3-3-1 model *Phys. Rev.* D **86** 055021
[17] Ferreira J G Jr, Pinheiro P R D, Pires C A d S and da Silva P S R 2011 The minimal 3-3-1 model with only two higgs triplets *Phys. Rev.* D **84** 095019
[18] Mohapatra R N and Senjanovic G 1980 Neutrino mass and spontaneous parity nonconservation *Phys. Rev. Lett.* **44** 912
[19] Dias A G, Pires C A de S and Rodrigues da Silva P S 2005 Naturally light right-handed neutrinos in a 3-3-1 model *Phys. Lett.* B **628** 85
[20] Dias A G, Pires C A de S and Rodrigues da Silva P S 2010 The left-right SU(3)(l) $\times$ SU(3)(r) $\times$ U(1)(x) model with light, kev and heavy neutrinos *Phys. Rev.* D **82** 035013
[21] Cogollo D, Diniz H and Pires C A de S 2009 Kev right-handed neutrinos from type ii seesaw mechanism in a 3-3-1 model *Phys. Lett.* B **677** 338
[22] Ky N A and Van N T H 2005 Scalar sextet in the 331 model with right-handed neutrinos *Phys. Rev.* D **72** 115017
[23] Palcu A 2006 Implementing canonical seesaw mechanism in the exact solution aa 3-3-1 gauge model without exotic electric charges *Mod. Phys. Lett.* A **21** 2591
[24] Dias A G, Pires C A de S and da Silva P S R 2011 How the inverse see-saw mechanism can reveal itself natural, canonical and independent of the right-handed neutrino mass *Phys. Rev.* D **84** 053011
[25] Fregolente D and Tonasse M D 2003 Selfinteracting dark matter from an SU(3)(l) $\times$ U(1)(N) electroweak model *Phys. Lett.* B **555** 7
[26] Long H N and Lan N Q 2003 Selfinteracting dark matter and higgs bosons in the SU(3)(C) $\times$ SU(3)(L) $\times$ U(1)(N) model with right-handed neutrinos *EPL* **64** 571
[27] Filippi S, Ponce W A and Sanchez L A 2006 Dark matter from the scalar sector of 3-3-1 models without exotic electric charges *Europhys. Lett.* **73** 142
[28] Mizukoshi J K, Pires C A de S, Queiroz F S and Rodrigues da Silva P S 2011 Wimps in a 3-3-1 model with heavy sterile neutrinos *Phys. Rev.* D **83** 065024

[29] Profumo S and Queiroz F S 2014 Constraining the Z' mass in 331 models using direct dark matter detection *Eur. Phys. J.* C **74** 2960
[30] Kelso C, Pires C A de S, Profumo S, Queiroz F S and Rodrigues da Silva P S 2014a A 331 wimpy dark radiation model *Eur. Phys. J.* C **74** 2797
[31] Rodrigues da Silva P S and Brief A 2016 Review on wimps in 331 electroweak gauge models *Phys. Int.* **7** 15
[32] Queiroz F S 2015 Non-thermal wimps as dark radiation *AIP Conf. Proc* vol 1604 p 83 arXiv:1310.3026
[33] Cogollo D, Gonzalez-Morales A X, Queiroz F S and Teles P R 2014 Excluding the light dark matter window of a 331 model using lhc and direct dark matter detection data *J. Cosmol. Astropart. Phys.* JCAP11(2014)002
[34] Kelso C, Long H N, Martinez R and Queiroz F S 2014b Connection of $g-2_{\mu}$, electroweak, dark matter, and collider constraints on 331 models *Phys. Rev.* D **90** 113011
[35] Dong P V, Ngan N T K and Soa D V 2014 Simple 3-3-1 model and implication for dark matter *Phys. Rev.* D **90** 075019
[36] de Sousa Pires C A and Ravinez O P 1998 Charge quantization in a chiral bilepton gauge model *Phys. Rev.* D **58** 035008
[37] Pal P B 1995 The strong cp question in SU(3)(C) $\times$ SU(3)(L) $\times$ U(1)(N) models *Phys. Rev.* D **52** 1659
[38] Dias A G, Pires C A de S and Rodrigues da Silva P S 2003 Discrete symmetries, invisible axion and lepton number symmetry in an economic 3-3-1 model *Phys. Rev.* D **68** 115009
[39] de Jesus A S, Kovalenko S, Queiroz F S, Pires C A de S and Villamizar Y S 2020 Dead or alive? Implications of the muon anomalous magnetic moment for 3-3-1 models *Phys. Lett.* B **809** 135689
[40] Hue L T, Thanh P N and Tham T D 2020 Anomalous magnetic dipole moment $(g-2)\mu$ in 3-3-1 model with inverse seesaw neutrinos *Commun. Phys.* **30** 221
[41] Hue L T, Phan K H, Nguyen T P, Long H N and Hung H T 2022 An explanation of experimental data of $(g-2)_{e,\mu}$ in 3-3-1 models with inverse seesaw neutrinos *Eur. Phys. J.* C **82** 722
[42] Buras A J, De Fazio F, Girrbach J and Carlucci M V 2013 The anatomy of quark flavour observables in 331 models in the flavour precision era *J. High Energy Phys.* JHEP02(2013)023
[43] Addazi A, Ricciardi G, Scarlatella S, Srivastava R and Valle J W F 2022 Interpreting B anomalies within an extended 331 gauge theory *Phys. Rev.* D **106** 035030
[44] Descotes-Genon S, Moscati M and Ricciardi G 2018 Nonminimal 331 model for lepton flavor universality violation in $b \to s\ell\ell$ decays *Phys. Rev.* D **98** 115030
[45] Wei M and Chong-Xing Y 2017 Charged higgs bosons from the 3-3-1 models and the $\mathcal{R}(D^{(*)})$ anomalies *Phys. Rev.* D **95** 035040
[46] Ponce W A, Florez J B and Sanchez L A 2002 Analysis of SU(3)(c) $\times$ SU(3)(L) $\times$ U(1)(X) local gauge theory *Int. J. Mod. Phys.* A **17** 643
[47] Ponce W A, Giraldo Y and Sanchez L A 2003 Minimal scalar sector of 3-3-1 models without exotic electric charges *Phys. Rev.* D **67** 075001
[48] Benavides R H, Giraldo Y, Muñoz L, Ponce W A and Rojas E 2022 Systematic study of the $SU(3)_c \otimes SU(3)_L \otimes U(1)_X$ local gauge symmetry *J. Phys.* G **49** 105007
[49] Diaz R A, Martinez R and Ochoa F 2005 SU(3)(c) $\times$ SU(3)(L) $\times$ U(1)(X) models for beta arbitrary and families with mirror fermions *Phys. Rev.* D **72** 035018
[50] Valle J W F and Singer M 1983 Lepton number violation with quasi Dirac neutrinos *Phys. Rev.* D **28** 540
[51] Aad G(ATLAS) *et al* 2019 Search for high-mass dilepton resonances using 139 fb $^{-1}$ of pp collision data collected at $\sqrt{s} = 13$ TeV with the ATLAS detector *Phys. Lett.* B **796** 68
[52] Erler J, Langacker P, Munir S and Rojas E 2011 Z' Bosons at colliders: a Bayesian viewpoint *J. High Energy Phys.* JHEP11(2011)076
[53] Salazar C, Benavides R H, Ponce W A and Rojas E 2015 LHC constraints on 3-3-1 models *J. High Energy Phys.* JHEP07(2015)096
[54] Benavides R H, Muñoz L, Ponce W A, Rodríguez O and Rojas E 2018 Electroweak couplings and LHC constraints on alternative Z' models in E_6 *Int. J. Mod. Phys.* A **33** 1850206
[55] Langacker P 2009 The physics of heavy Z' Gauge Bosons *Rev. Mod. Phys.* **81** 1199
[56] Langacker P and Plumacher M 2000 Flavor changing effects in theories with a heavy Z' boson with family nonuniversal couplings *Phys. Rev.* D **62** 013006

[57] Tumasyan A(CMS) *et al* 2022 Search for flavor-changing neutral current interactions of the top quark and the Higgs boson decaying to a bottom quark-antiquark pair at $\sqrt{s} = 13$ TeV *J. High Energy Phys.* JHEP02(2022)169
[58] Hill C T and Simmons E H 2003 Strong dynamics and electroweak symmetry breaking *Phys. Rep.* **381** 235
Hill C T and Simmons E H 2004 *Phys. Rep.* **390** 553–554
[59] Workman R L *et al* (Particle Data Group) 2022 Review of particle physics *PTEP* **2022** 083C01
[60] Romero Abad D, Portales J R and Ramirez Barreto E 2020 Electric charge quantisation in 331 models with exotic charges *Pramana* **94** 84
[61] Erler J, Langacker P, Munir S and Rojas E 2009 Improved constraints on z-prime bosons from electroweak precision data *J. High Energy Phys.* JHEP08(2009)017

IOP Publishing Journal of Physics G: Nuclear and Particle Physics
J. Phys. G: Nucl. Part. Phys. **52** (2025) 055002 (27pp) https://doi.org/10.1088/1361-6471/add281

The standard model of particle physics as an effective theory from two non-universal $U(1)$'s

Richard H Benavides[1], Yithsbey Giraldo[2], William A Ponce[3], Oscar Rodríguez[3,4] and Eduardo Rojas[2]

[1] Instituto Tecnológico Metropolitano, Facultad de Ciencias Exactas y Aplicadas, Calle 73 N° 76-354 vía el volador, Medellín, Colombia
[2] Departamento de Física, Universidad de Nariño, Calle 18 Carrera 50, A.A. 1175, San Juan de Pasto, Colombia
[3] Instituto de Física, Universidad de Antioquia, A.A. 1226, Medellín, Colombia
[4] Facultad de Ingenierías, Universidad de San Buenaventura, Carrera 56C N° 51-110, Medellín, Colombia

E-mail: richardbenavides@itm.edu.co, yithsbey@gmail.com, william.ponce@udea.edu.co, oscara.rodriguez@udea.edu.co and eduro4000@gmail.com

Received 17 January 2025, revised 7 April 2025
Accepted for publication 30 April 2025
Published 20 May 2025

Abstract

We study the possibility of obtaining the Standard Model (SM) of particle physics as an effective theory of a more fundamental one, whose electroweak sector includes two non-universal local $U(1)$ gauge groups, with the chiral anomaly cancellation taking place through an interplay among families. As a result of the spontaneous symmetry breaking, a massive gauge boson Z' arises, which couples differently to the third family of fermions (by assumption, we restrict ourselves to the scenario in which the Z' couples in the same way to the first two families). Two Higgs doublets and one scalar singlet are necessary to generate the SM fermion masses and break the gauge symmetries. We show that in our model, the flavor-changing neutral currents (FCNC) of the Higgs sector are identically zero if each right-handed SM fermion is only coupled with a single Higgs doublet. This result represents a FCNC cancellation mechanism different from the usual procedure in Two-Higgs Doublet Models. The non-universal nature of our solutions Requires the presence of three right-handed neutrino fields, one for each family. Our model generates all elements of the Dirac mass matrix for quarks and leptons, which is quite non-trivial for non-universal models. Thus, we can fit all the masses and mixing angles with two scalar doublets. Finally, we show the distribution of solutions for the scalar boson masses in our model by scanning well-motivated intervals for the

model parameters. We consider two possibilities for the scalar potential and compare these results with the Higgs-like resonant signals recently reported by the ATLAS and CMS experiments at the LHC. Finally, we also report collider, electroweak, and flavor constraints on the model parameters.

Keywords: non-universality, right-handed neutrinos, flavor physics

1. Introduction

The Standard Model of particle physics (SM) based on the local gauge group $SU(3)_C \otimes SU(2)_L \otimes U(1)_Y$ [1] has been very successful so far, in the sense that its predictions are in good agreement with the present experimental results, including the latest discovery of the Higgs boson [2–4], a fundamental ingredient of the model that contributes to our understanding of the origin of mass for the subatomic particles. However, the SM fails short in explaining things as: hierarchical charged fermion masses, fermion mixing angles, charge quantization, strong CP violation, replication of families, neutrino masses and oscillations, and the matter-antimatter asymmetry of the Universe. Besides, gravity is excluded from the context of the model and good candidates for dark matter and dark energy present in the Universe are not provided [5–12].

Replication of families, also known as the 'family problem', refers to the fact that the SM is not able to predict the number N of fermion families existing in nature, something related with the universality of the model, which means that the gauge anomalies, in particular those associated with the $U(1)_Y$ hypercharge, cancel out exactly for each family; the only restriction, $N \leqslant 8$, comes from the asymptotic freedom of $SU(3)_C$ also known as quantum chromodynamics or QCD [13]. Experimental results at the CERN-LEP facilities early in the 1990s implied the existence of at least three families, each one having a neutral lepton with a mass less than half the mass of the neutral Z gauge boson [14]; this result was initially interpreted as an exact value for the total number of families in nature, which is not quite correct. As a matter of fact, the LEP data does not exclude the existence of additional families having heavy neutrinos.

Therefore, it is widely believed that the SM is not truly fundamental, with the prevailing view that the model is just a low-energy effective description of a more complete theory. There are several good candidates for this, all of them grouped in what is now known as 'the physics beyond the Standard Model' (BSM) [15–17]. Thus, there are numerous works with gauge extensions of the $U(1)$ type, either to explain neutrino masses or dark matter, etc. see references:[18–23] as to show some of them. However, our goal is to introduce two non-universal $U(1)$ symmetry gauge to SM to obtain it as an effective model. The consideration of Z' bosons with non-universal couplings is justified for theoretical and experimental reasons. From a theoretical perspective, these models arise naturally in several scenarios, for example in string models [24–27] and 3-3-1 models [28–32]. However, from a phenomenological point of view, they are convenient for studying experimental anomalies at low energies, for example: anomalous decays of B-mesons [33–37], Cabibbo angle anomaly [38], muon anomalous magnetic moment (or muon g-2) [39–41] and rare charm decays [42]. Recently CMS reported for the first time searches for neutral vector bosons with non-universal couplings [43] due to the multiple applications of this class of models. Thus, searching for signals associated with these models remains a relevant task in exploring physics BSM [44].

Table 1. Here, i runs over the number of families ($i = 1, 2, 3$), and $a = 1, 2$.

	$\ell_i \equiv (\nu_{iL}, e_{iL})^T$	ν_{iR}	e_{iR}	$q_i \equiv (u_{iL}, d_{iL})^T$	u_{iR}	d_{iR}	$\Phi_a = (\phi_a^+, \phi_a^0)^T$	σ
$\hat{T}_3$	$\left(\frac{1}{2}, -\frac{1}{2}\right)^T$	0	0	$\left(\frac{1}{2}, -\frac{1}{2}\right)^T$	0	0	$\left(\frac{1}{2}, -\frac{1}{2}\right)^T$	0
$\hat{Y}$	-1	0	-2	$\frac{1}{3}$	$\frac{4}{3}$	$-\frac{2}{3}$	1	0
$\hat{Q}$	$(0, -1)^T$	0	-1	$\left(\frac{2}{3}, -\frac{1}{3}\right)^T$	$\frac{2}{3}$	$-\frac{1}{3}$	$(1, 0)^T$	0
$\hat{\alpha}$	α_{li}	α_{ν_i}	α_{ei}	α_{qi}	α_{ui}	α_{di}	α_a	α_σ
$\hat{\beta}$	β_{li}	$\beta_{\nu i}$	β_{ei}	β_{qi}	β_{ui}	β_{di}	β_a	β_σ

In what follows, and in order to shed some light on the shortcomings of the SM, we propose an extension of it; that is, a new model for three families based on the local gauge group $SU(3)_C \otimes SU(2)_L \otimes U(1)_\alpha \otimes U(1)_\beta$, where the charges associated with the two Abelian factors are non-universal, in the sense that they are not the same for the three assumed families. The fermion content of our model is the same as that of the SM, extended with three right-handed neutrinos ν_{iR} ($i = 1, 2, 3$), one for each family.

2. The model

In this section, we elaborate on the mathematical aspects of the new model in consideration, which is a minimal extension of the SM, both in its gauge sector and in its fermion sector. As a consequence, the scalar sector must also be enlarged, something we are going to do in the most economical possible way.

As mentioned above, the model to be considered here is based on the local gauge symmetry $SU(3)_C \otimes SU(2)_L \otimes U(1)_\alpha \otimes U(1)_\beta$, where $SU(3)_C$ and $SU(2)_L$ are the same as in the SM, and the two Abelian factors are non-universal, capable of projecting the SM $U(1)_Y$ hypercharge to a lower energy scale. So, as a result of the spontaneous symmetry breaking, a new gauge boson associated with a non-universal neutral weak current appears.

The fermion fields in our model are the same as in the SM, together with three neutral Weyl states associated with the three right-handed neutrino components, one for each family. This popular fermion extension of the SM has been used to explain neutrino masses and oscillations, the baryon asymmetry of the Universe, dark matter and dark radiation, and in our approach, it has the peculiarity that, unlike what happens in the SM, the three new fields have non-vanishing charges under both $U(1)$ factors.

As for the scalar sector, we first introduce a SM singlet field σ able to spontaneously break the $U(1)_\alpha \otimes U(1)_\beta$ symmetry down to $U(1)_Y$. To break the remaining symmetry and at the same time implement the Higgs mechanism, at least one $SU(2)_L$ scalar doublet Φ_2 (developing a vacuum expectation value (VEV) at an energy scale v_2) must be introduced, in such a way that the remaining symmetry $SU(3)_C \otimes U(1)_Q$ survives down to laboratory energies. We choose the quantum numbers of this doublet such that it only provides tree-level masses to the third fermion family. To generate (at tree level) the other fermion masses and the mixing matrices, at least one more $SU(2)_L$ scalar doublet Φ_1 must be included. This doublet develops a VEV at an energy scale $v_1 < v_2$. Table 1 shows the fermion and scalar content of our model, along with the notation used for the different Abelian charges, as well as the weak-isospin T_3,

hypercharge Y, and electric charge Q of the particles. In our analysis, we will assume that $\chi_{f_1} = \chi_{f_2} \neq \chi_{f_3}$, where χ_{f_i} stands for the Abelian α, β charges, $f = q, u, d, l, \nu, e$ and $i = 1, 2, 3$, that is, we consider a model with universal couplings for the first two fermion families, but not for the third one, a convenient condition in the implementation of models with minimal flavor violation, that in turn provides a way to distinguish the third family from the first two ones. In this way, our model is characterized by 24 parameters associated with the fermion sector and 6 more with the scalar one, for a total of 30 free parameters which can be fixed by demanding a renormalizable model, reproducting the SM hypercharges, and appropriate Yukawa couplings to provide fermion masses.

2.1. Cancellation of chiral anomalies

Regarding the renormalizability of the theory, we must ensure an anomaly-free scenario, which is achieved by imposing the following relations among the $U(1)$ fermion charges:

$$\begin{aligned}
[SU(3)_C]^2 \otimes U(1)_\alpha &: \sum_i (2\alpha_{qi} - \alpha_{ui} - \alpha_{di}) = 0, \\
[SU(2)_L]^2 \otimes U(1)_\alpha &: \sum_i (3\alpha_{qi} + \alpha_{li}) = 0, \\
[\mathrm{grav}]^2 \otimes U(1)_\alpha &: \sum_i (6\alpha_{qi} - 3\alpha_{ui} - 3\alpha_{di} + 2\alpha_{li} - \alpha_{\nu i} - \alpha_{ei}) = 0, \\
[U(1)_\alpha]^2 U(1)_\beta &: \sum_i (6\alpha_{qi}^2\beta_{qi} - 3\alpha_{ui}^2\beta_{ui} - 3\alpha_{di}^2\beta_{di} + 2\alpha_{li}^2\beta_{li} - \alpha_{\nu i}^2\beta_{\nu i} - \alpha_{ei}^2\beta_{ei}) = 0, \\
[U(1)_\alpha]^3 &: \sum_i (6\alpha_{qi}^3 - 3\alpha_{ui}^3 - 3\alpha_{di}^3 + 2\alpha_{li}^3 - \alpha_{\nu i}^3 - \alpha_{ei}^3) = 0,
\end{aligned} \tag{1}$$

together with the five corresponding equations for the $U(1)_\beta$ group. These are obtained from the previous ones via the $\alpha \leftrightarrow \beta$ exchanging for a total of 10 equations. Given that the number of involved unknowns is greater (24 assuming universality in the first two fermion families), the number of possible solutions is infinite, so, just like in the SM, chiral anomaly cancellation is not sufficient to explain the charge quantization [13].

2.2. The Lagrangian of the Model

In our model, the covariant derivative D_μ for the electroweak (EW) sector is given by

$$D^\mu = \partial^\mu + i g_L A_j^\mu \hat{T}_j + i\frac{g_\alpha}{2} B_\alpha^\mu \hat{\alpha} + i\frac{g_\beta}{2} B_\beta^\mu \hat{\beta}, \tag{2}$$

where $\hat{T}_j$, A_j^μ (with $j = 1, 2, 3$) and g_L denote, respectively, the generators, the gauge fields, and the coupling constant associated with the weak isospin gauge group $SU(2)_L$, while $\hat{\chi}$, B_χ^μ and g_χ, with $\chi = \alpha, \beta$, are the corresponding quantities related with the two Abelian $U(1)$ factors. The terms in the Lagrangian describing the relevant interactions in our analysis are then:

$$
\begin{aligned}
\mathcal{L} \supset & -V(\Phi_1, \Phi_2, \sigma) \\
& +|D^\mu \Phi_1|^2 + |D^\mu \Phi_2|^2 + |D^\mu \sigma|^2 \\
& +i\bar{q}_j \not{D} q_j + i\bar{u}_{jR} \not{D} u_{jR} + i\bar{d}_{jR} \not{D} d_{jR} + i\bar{l}_j \not{D} l_j + i\bar{\nu}_{jR} \not{D} \nu_{jR} + i\bar{e}_{jR} \not{D} e_{jR} \\
& -Y^e_{jk} \bar{\ell}_j \Phi_1 e_{kR} - Y^\nu_{jk} \bar{\ell}_j \tilde{\Phi}_1 \nu_{kR} - Y^d_{jk} \bar{q}_j \Phi_1 d_{kR} - Y^u_{jk} \bar{q}_j \tilde{\Phi}_1 u_{kR} \\
& -Y^e_{j3} \bar{\ell}_j \Phi_2 e_{3R} - Y^\nu_{j3} \bar{\ell}_j \tilde{\Phi}_2 \nu_{3R} - Y^d_{j3} \bar{q}_j \Phi_2 d_{3R} - Y^u_{j3} \bar{q}_j \tilde{\Phi}_2 u_{3R} + \text{h.c.}\,,
\end{aligned} \tag{3}
$$

where sum over repeated indices is implied, with j and k taking the values $\{1, 2, 3\}$ and $\{1, 2\}$, respectively. The term in the first line denotes the scalar potential. Due to the non-universal character of our model, a single scalar doublet Φ_1 is not enough to provide masses to all fermion particles and, simultaneously, to generate realistic mixing matrices. To this end, at least another Higgs doublet Φ_2 developing a VEV is required. Additionally, a scalar singlet must be introduced to break the abelian symmetries. The symmetry group $SU(2) \otimes U(1) \otimes U(1)$ has five generators, four of which are broken, such that at low energies only the electromagnetic gauge group $U(1)_{\text{QED}}$ survives. For a model with just two Higgs doublets, by applying the Higgs mechanism we obtain, in addition to the SM fields, two exotic fields: a CP even neutral scalar field and a charged one, the remaining ones are absorbed as goldstone bosons by the vector fields. To accommodate the experimental anomalies it is necessary to include a scalar singlet to break the $U(1) \otimes U(1)$ at high energies such that, in addition to the SM fields we get two CP even scalar fields and a pseudoscalar. This is also convenient if we want the Z' scale to be larger than the electroweak scale since the quadratic sum of the VEVs of the doublets must equal $v_{\text{SM}} = 246.24\,\text{GeV}$. The scalar potential is analyzed in appendix A. The terms in the second line correspond to the scalar-gauge interactions responsible for the masses and mixings in the gauge sector (see appendix B). Terms in the third line give rise to fermion-gauge interactions, as discussed in section 3, and the Yukawa couplings present in the model are shown in the fourth and fifth lines. The invariance of the Yukawa interaction terms under the $U(1)_\alpha \otimes U(1)_\beta$ gauge symmetry implies the following relations between the $\chi(=\alpha, \beta)$ charges:

$$
\begin{aligned}
\chi_{lj} - \chi_1 - \chi_{ea} &= 0, \\
\chi_{lj} - \chi_2 - \chi_{e3} &= 0, \\
\chi_{lj} + \chi_1 - \chi_{\nu a} &= 0, \\
\chi_{lj} + \chi_2 - \chi_{\nu 3} &= 0, \\
\chi_{qj} - \chi_1 - \chi_{da} &= 0, \\
\chi_{qj} - \chi_2 - \chi_{d3} &= 0, \\
\chi_{qj} + \chi_1 - \chi_{ua} &= 0, \\
\chi_{qj} + \chi_2 - \chi_{u3} &= 0.
\end{aligned} \tag{4}
$$

2.3. Spontaneous symmetry breaking

Our aim is to break the gauge symmetry of the model in two steps, namely,

$$
SU(2)_L \otimes U(1)_\alpha \otimes U(1)_\beta \xrightarrow{\langle\sigma\rangle} SU(2)_L \otimes U(1)_Y \xrightarrow{\langle\Phi_a\rangle} U(1)_Q \tag{5}
$$

where $a = 1, 2$. To achieve this, we allow the SM scalar singlet σ (charged under both $U(1)$'s factors) to acquire a VEV at a high energy scale, inducing a mixing between the B_χ fields that give rise to both: the SM gauge boson B associated with the $U(1)_Y$ hypercharge symmetry and a new massive gauge boson Z' with non-universal couplings to fermions. If θ is the angle

parameterizing this mixing, then

$$\begin{pmatrix} B_\alpha^\mu \\ B_\beta^\mu \end{pmatrix} = \begin{pmatrix} \cos\theta & -\sin\theta \\ \sin\theta & \cos\theta \end{pmatrix} \begin{pmatrix} B^\mu \\ Z'^\mu \end{pmatrix}. \tag{6}$$

Finally, at a lower energy scale (the EW one), the neutral components of the scalar doublets Φ_1 and Φ_2 develop VEVs inducing the last breaking. Consequently, the B and A_3 fields mix, giving rise to the massless photon A^μ and the massive SM neutral gauge boson Z. The corresponding mixing angle is the well-known Weinberg angle θ_W:

$$\begin{pmatrix} A_3^\mu \\ B^\mu \end{pmatrix} = \begin{pmatrix} \sin\theta_W & \cos\theta_W \\ \cos\theta_W & -\sin\theta_W \end{pmatrix} \begin{pmatrix} A^\mu \\ Z^\mu \end{pmatrix}. \tag{7}$$

The unbroken electric charge generator $\hat{Q}$ can be expressed as a linear combination of the three diagonal (broken) generators of the gauge group after the spontaneous symmetry breaking, that is

$$\hat{Q} = \hat{T}_{3L} + \frac{1}{2}(a_Y \hat{\alpha} + b_Y \hat{\beta}), \tag{8}$$

from which it follows that the SM hypercharge $\hat{Y}$ can be identified as

$$\hat{Y} = a_Y\, \hat{\alpha} + b_Y \hat{\beta}, \tag{9}$$

where a_Y and b_Y are two non-vanishing free parameters. However, these parameters turn be useless for our purposes, so they will be set to 1 for simplicity[5] In accordance with equation (9), the $U(1)$ charges displayed in table 1 must satisfy the following relations:

$$\begin{aligned} \alpha_{li} + \beta_{li} &= -1, \\ \alpha_{\nu i} + \beta_{\nu i} &= 0, \\ \alpha_{ei} + \beta_{ei} &= -2, \\ \alpha_{qi} + \beta_{qi} &= 1/3, \\ \alpha_{ui} + \beta_{ui} &= 4/3, \\ \alpha_{di} + \beta_{di} &= -2/3, \\ \alpha_a + \beta_a &= 1, \\ \alpha_\sigma + \beta_\sigma &= 0, \end{aligned} \tag{10}$$

for $i = 1, 2, 3$ and $a = 1, 2$. Thus, the breaking induced by the singlet σ at an energy scale v_σ allows to reproduce the SM hypercharges correctly.

2.4. Mass and mixing matrices for fermions

Let's now consider the generation of fermion mass, which takes place when Φ_2 induces the breaking that gives rise to the local gauge $SU(3)_C \otimes U(1)_Q$ symmetry conserved at low energies. As mentioned, for non-universal models, at least two scalar doublets are needed to provide masses to all the fermion particles and generate the mixing matrices. As usual, the VEV of the scalar doublets are given by

$$\langle \Phi_a \rangle = \begin{pmatrix} 0 \\ \frac{v_a}{\sqrt{2}} \end{pmatrix}, \ (a = 1, 2). \tag{11}$$

[5] From equation (10), one of them can be absorbed in a redefinition of the scalar singlet hypercharges ($a_Y = -b_Y \beta_\sigma \alpha_\sigma$).

Table 2. Here $i = 1, 2, 3$ and $a = 1, 2$. The corresponding $U(1)_\beta$ charges can be easily obtained by replacing β instead of α.

Field	$U(1)_\alpha$	Field	$U(1)_\alpha$	Field	$U(1)_\alpha$
u_{iL}	α_{q1}	u_{aR}	$\alpha_{\nu 1} + 4\alpha_{q1}$	Φ_1	$\alpha_{\nu 1} + 3\alpha_{q1}$
		u_{3R}	$\alpha_{\nu 3} + 4\alpha_{q1}$		
d_{iL}		d_{aR}	$-\alpha_{\nu 1} - 2\alpha_{q1}$		
		d_{3R}	$-\alpha_{\nu 3} - 2\alpha_{q1}$	Φ_2	$\alpha_{\nu 3} + 3\alpha_{q1}$
ν_{iL}	$-3\alpha_{q1}$	ν_{aR}	$\alpha_{\nu 1}$		
		ν_{3R}	$\alpha_{\nu 3}$		
e_{iL}		e_{aR}	$-\alpha_{\nu 1} - 6\alpha_{q1}$	σ	α_σ
		e_{3R}	$-\alpha_{\nu 3} - 6\alpha_{q1}$		

In this model, it is possible to generate Dirac masses for all the SM fermions including the SM neutrinos. In this case, the smallness of the neutrino masses relies on the Yukawa couplings as it does happen in the SM. The tree-level Dirac masses come from the Lagrangian equation (3). The resulting mass matrices take the form

$$M^f = \frac{1}{\sqrt{2}} \begin{pmatrix} v_1 Y^f_{11} & v_1 Y^f_{12} & v_2 Y^f_{13} \\ v_1 Y^f_{21} & v_1 Y^f_{22} & v_2 Y^f_{23} \\ v_1 Y^f_{31} & v_1 Y^f_{32} & v_2 Y^f_{33} \end{pmatrix}, \tag{12}$$

for $f = u, d, \nu, e$. From here, we see that despite the non-universality of the model, it is possible to have saturated mass matrices for leptons and quarks, i.e. with all the matrix elements different from zero, which is a fairly non-trivial result. As a consequence, the CKM and PMNS mixing matrices can be easily generated, with the mixing between the first two fermion families induced by Φ_1, while both Φ_1 and Φ_2 contribute to all the mixing elements involving the third family.

Our model is capable of reproducing all the elements of the Dirac mass matrix (therefore, it has no texture zeros) so that it is always possible to reproduce the values of the masses and mixing angles, for both quarks and leptons [45–50].

It is important to emphasize that all elements of the mass matrix are generated for each type of SM fermion, such that for each flavor there are 9 complex parameters, which is equivalent to $2 \times 18 = 36$ real parameters for both the up-type and the down-type quark mass matrices. Since the CKM matrix and the quark masses amount to 9 parameters and a phase, the number of free parameters exceeds the number of physical parameters to be fitted [45]. In the lepton sector, the neutrino masses are not known, and just two square mass differences are experimentally available [51]; that is: $\delta m_{21} = m_2^2 - m_1^2$, $\delta m_{31} = m_3^2 - m_1^2$ (where $\{m_i\}_{i=1,2,3}$ are the neutrino masses), in this case there are only eight real parameters and a phase, but again the number of free parameters in the Yukawa couplings are enough to fit masses and mixing [50]. This freedom allows for the fitting of the quark and lepton masses and the CKM and PMNS mixing matrices with the most recent data from the literature [51].

2.5. Non-universal U(1) charges

By solving the system of equations formed by equations (1), (4) and (10), we obtain a unique solution for the $U(1)$ fermion and scalar charges. The resulting expressions, shown in table 2, are given in terms of just three parameters, namely: α_{q1}, $\alpha_{\nu 1}$ and $\alpha_{\nu 3}$[6]. From this it follows

[6] The α charge of the singlet σ, α_σ, remains as a free parameter, but it does not affect the fermion charges, as can be seen in table 2.

that the non-universality of the solution depends exclusively on the right-handed neutrino charges; so, in what follows, we will assume that $\alpha_{\nu 1} \neq \alpha_{\nu 3}$. Under this condition, the cancellation of chiral anomalies takes place among different families, and not family by family as it does in the SM.

As is well known from the literature on FCNCs, the strongest constraints on tree-level flavor couplings come usually from $F^0 - \bar{F}^0$ mixing processes ($F = K, B_d, D$) [52], to avoid this problem with neutral scalar currents, in most models with two Higgs doublets, discrete symmetries are proposed to cancel the scalar currents with flavor changes. Four 2HDMs are known in the literature, Type-I, Type-II, Type-X, and Type-Y [53], in these models each doublet is charged differently under the discrete symmetry such that one type of particle receives its mass from only one doublet. For example, type-up quarks receive the mass from the same scalar doublet. This is impossible for non-universal models since the charges $U(1)$ of the same type of quarks are different because the model is not universal. In our model, the up-type quarks of the first two families couple with one Higgs doublet while the up-type quark of the third family must couple with the other doublet. This result is guaranteed since the charges of the Higgs doublets are not equal. This is a different mechanism compared to the one in the models mentioned above; however, it can be considered as a particular case of condition III of the general theorem proved in reference [54].

3. EW currents and $Z^{'}$ couplings

Ignoring the kinetic terms, the part of the Lagrangian equation (3) describing the interactions between fermions and gauge bosons can be written as

$$-\mathcal{L} \supset \frac{g_L}{\sqrt{2}}(J^{\mu}_{W^+}W^+_{\mu} + \text{h.c.}) + \frac{g_L}{2}J^{\mu}_3 A_{3,\mu} + \frac{g_\alpha}{2}J^{\mu}_\alpha B_{\alpha,\mu} + \frac{g_\beta}{2}J^{\mu}_\beta B_{\beta,\mu}, \tag{13}$$

where the W^+_μ field has been defined as $W^{+\mu} = (A^\mu_1 - iA^\mu_2)/\sqrt{2}$ and the currents are given by

$$\begin{aligned}
J^{\mu}_W &= \bar{\nu}_{iL}\gamma^\mu e_{iL} + \bar{u}_{iL}\gamma^\mu d_{iL},\\
J^{\mu}_3 &= \bar{u}_{iL}\gamma^\mu u_{iL} + \bar{\nu}_{iL}\gamma^\mu \nu_{iL} - \bar{d}_{iL}\gamma^\mu d_{iL} - \bar{e}_{iL}\gamma^\mu e_{iL},\\
J^{\mu}_\chi &= \chi_{qi}(\bar{u}_{iL}\gamma^\mu u_{iL} + \bar{d}_{iL}\gamma^\mu d_{iL}) + \chi_{li}(\bar{\nu}_{iL}\gamma^\mu \nu_{iL} + \bar{e}_{iL}\gamma^\mu e_{iL})\\
&\quad + \chi_{ui}\,\bar{u}_{iR}\gamma^\mu u_{iR} + \chi_{di}\,\bar{d}_{iR}\gamma^\mu d_{iR} + \chi_{\nu i}\,\bar{\nu}_{iR}\gamma^\mu \nu_{iR} + \chi_{ei}\,\bar{e}_{iR}\gamma^\mu e_{iR},
\end{aligned} \tag{14}$$

with a sum over the i index is implied and $\chi = \alpha, \beta$. In the basis defined by equation (6), the Lagrangian in equation (13) can be expressed as

$$-\mathcal{L} \supset \frac{g_L}{\sqrt{2}}(J^{\mu}_{W^+}W^+_{\mu} + \text{h.c.}) + \frac{g_L}{2}J^{\mu}_3 W_{3\mu} + \frac{g_Y}{2}J^{\mu}_Y B_\mu + g_{Z'}J^{\mu}_{Z'}Z'_\mu, \tag{15}$$

where the interactions of fermions with the Z' boson are given by

$$\begin{aligned}
g_{Z'}J^{\mu}_{Z'} &= g_\beta J^{\mu}_\beta \cos\theta - g_\alpha J^{\mu}_\alpha \sin\theta,\\
&= g_{Z'}\sum_f \bar{f}_i\gamma^\mu(\tilde{\epsilon}^L_{fi}P_L + \tilde{\epsilon}^R_{fi}P_R)f_i,\\
&= g_{Z'}\sum_f \bar{f}_i\gamma^\mu(\tilde{g}^V_{fi} - \tilde{g}^A_{fi}\gamma^5)f_i.
\end{aligned} \tag{16}$$

Here, f runs over $\{u, d, \nu, e\}$, $i = 1, 2, 3$ (corresponding with the SM family), $P_{L,R} = (1 \mp \gamma^5)/2$ are the chirality projectors and

$$g_{Z'}\tilde{\epsilon}_{fi}^{L,R} = \frac{1}{2}[g_\beta\hat{\beta}(f_{iL,R})\cos\theta - g_\alpha\hat{\alpha}(f_{iL,R})\sin\theta], \tag{17}$$

$$\tilde{g}_{fi}^{V,A} = \frac{1}{2}(\tilde{\epsilon}_{fi}^{L} \pm \tilde{\epsilon}_{fi}^{R}). \tag{18}$$

In equation (17), $\tilde{\epsilon}_{fi}^{L(R)}$ denotes the left(right)-handed chiral coupling of the f_i fermion to the Z' boson, while in equation (18), $\tilde{g}_{fi}^{V(A)}$ represents the corresponding vector (axial-vector) coupling. As for the couplings to the B field, we have that

$$\begin{aligned} g_Y J_Y^\mu &= g_\alpha J_\alpha^\mu \cos\theta + g_\beta J_\beta^\mu \sin\theta, \\ &= g_Y \sum_f \bar{f}_{iL}\gamma^\mu \hat{Y}(f_{iL}) f_{iL} + \bar{f}_{iR}\gamma^\mu \hat{Y}(f_{iR}) f_{iR}, \end{aligned} \tag{19}$$

with

$$g_Y \hat{Y}(f_{iL,R}) = g_\alpha\hat{\alpha}(f_{iL,R})\cos\theta + g_\beta\hat{\beta}(f_{iL,R})\sin\theta. \tag{20}$$

By comparing equations (9) and (20), taking into account our choice $a_Y = b_Y = 1$, we get the following relations among the coupling constants g_α, g_β, g_Y and the mixing angle θ:

$$g_\alpha \cos\theta = g_\beta \sin\theta = \frac{g_Y}{\sqrt{2}}, \tag{21}$$

from which it follows that

$$\tan\theta = \frac{g_\alpha}{g_\beta} \qquad \text{and} \qquad \frac{1}{g_\alpha^2} + \frac{1}{g_\beta^2} = \frac{2}{g_Y^2}. \tag{22}$$

By changing to the basis defined by equation (7), the Lagrangian in equation (15) can be rewritten as

$$-\mathcal{L} \supset eJ_\gamma^\mu A_\mu + g_Z J_Z^\mu Z_\mu + g_{Z'} J_{Z'}^\mu Z'_\mu + g_W J_{W^+}^\mu W_\mu^+ + \text{h.c.}, \tag{23}$$

where

$$\begin{aligned} g_W &= \frac{g_L}{\sqrt{2}}, \\ eJ_\gamma^\mu &= e\sum_f \bar{f}_i\gamma^\mu \hat{Q}(f_i) f_i, \\ g_Z J_Z^\mu &= \frac{g_L}{2\cos\theta_W}\sum_f \bar{f}_i\gamma^\mu(\epsilon_{fi}^L P_L + \epsilon_{fi}^R P_R) f_i, \end{aligned} \tag{24}$$

with the chiral couplings to the Z boson defined as

$$\epsilon_{fi}^{L,R} = 2\left\{\hat{T}_3(f_{iL,R}) - \sin^2\theta_W\left[\hat{T}_3(f_{iL,R}) + \frac{1}{2}\hat{Y}(f_{iL,R})\right]\right\}. \tag{25}$$

To obtain these expressions, the identification $e = g_L \sin\theta_W = g_Y \cos\theta_W$ was made, which implies the well-known relation

$$g_Y = g_L \tan\theta_W. \tag{26}$$

Taking into account the relations in equations (21) and (26), as well as the charges reported in table 2, and the parameters x, y, z and w defined as

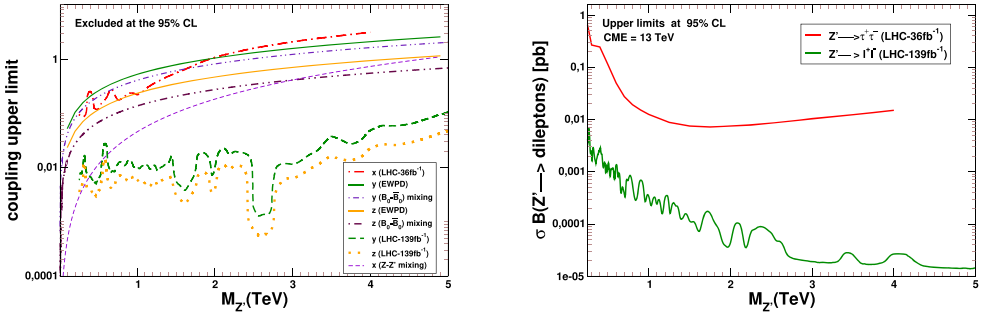

Figure 1. Left: Upper limit on the model parameters x, y, z. Right: 95% CL upper limits on the fiducial Z' production cross-section times the $Z' \to \ell^+\ell^-$ branching [59] (green continuous line) and the corresponding upper limits on the Z' decaying to $\tau\overline{\tau}$ pairs [60] (red continuous line).

Table 3. Chiral couplings between the fermion sector and the Z' gauge boson.

f	$\nu_{1,2}$	ν_3	$e_{1,2}$	e_3	$u_{1,2}$	u_3	$d_{1,2}$	d_3
$g_{Z'}\tilde{\epsilon}_f^L$	$-z$	$-z$	$-z$	$-z$	$\frac{1}{3}z$	$\frac{1}{3}z$	$\frac{1}{3}z$	$\frac{1}{3}z$
$g_{Z'}\tilde{\epsilon}_f^R$	$-y$	$-x$	$y-2z$	$x-2z$	$-y+\frac{4}{3}z$	$-x+\frac{4}{3}z$	$y-\frac{2}{3}z$	$x-\frac{2}{3}z$

$$
\begin{aligned}
x &\equiv \frac{g_L \tan\theta_W}{2\sqrt{2}}(\cot\theta + \tan\theta)\alpha_{\nu 3},\\
y &\equiv \frac{g_L \tan\theta_W}{2\sqrt{2}}(\cot\theta + \tan\theta)\alpha_{\nu 1},\\
z &\equiv \frac{g_L \tan\theta_W}{2\sqrt{2}}[\cot\theta - 3(\cot\theta + \tan\theta)\alpha_{q1}],\\
w &\equiv \frac{g_L \tan\theta_W}{2\sqrt{2}}(\cot\theta + \tan\theta)\alpha_{\sigma},
\end{aligned}
\tag{27}
$$

the Z' chiral couplings given by equation (17) can be expressed as indicated in table 3[7]. These charges are best suited for a phenomenological analysis of the new neutral vector boson, as it will be explained in the next section. Regarding the scalar fields Φ_1 and Φ_2, their Z' couplings are given by $z - y$ and $z - x$, respectively.

4. Low energy and collider constraints

For the process $\bar{q}q \longrightarrow Z' \longrightarrow \ell^+\ell^-$, ATLAS reports upper limits on the fiducial cross-section times the $Z' \to \ell^+\ell^-$ branching from searches of high-mass dilepton resonances (dielectron and dimuon) during Run 2 of the Large Hadron Collider (LHC) at a center-of-mass energy of $\sqrt{s} = 13\,\text{TeV}$ and an integrated luminosity of $139\,\text{fb}^{-1}$. From these constraints, we obtain upper limits on the y and z couplings corresponding to the green dashed and orange dotted

[7] From here, we see that there are two families with identical charges and a different third one. However, universal models are still possible, for example, setting $z = x = y = 1$ yields the well-known expressions for the $B - L$ charges.

lines in the left-handed plot in figure 1. These limits are obtained from the intersection of the theoretical cross-section (for further details see our previous publications [55–58]) with the 95% CL upper limit on the cross-section reported by the ATLAS collaboration [59] (the green continuous line in the right plot figure 1). For the upper limits on the x parameter (red dot-dashed line in the left plot Figure 1), we use the ATLAS 95% upper limits on the production cross-section times branching fraction for a Z' boson decaying to a $\tau\overline{\tau}$ pair (the green continuous line in the right plot figure 1). This data was collected by ATLAS in searches of Z' bosons using a data sample corresponding to an integrated luminosity of 36.1 fb^{-1} from proton–proton collisions at a center of mass energy of 13 TeV [60].

Constraints on a parameter are obtained by marginalizing the other parameters. In the case of the parameter x, which represents the coupling strength between Z' and the fermions of the third family, the Z' is produced from an annihilation $b\overline{b} - > Z'$. Due to the strong collider constraints on the first two families, only Z' couplings with the third family are possible at low energies. In our model, this implies that $y, z \ll x$, as we can see from table 3. This implies that at low energies, the unique generator with unsuppressed coupling strengths is $T_{3R}(3)$. This symmetry is a well-known EW extension of the SM. The argument '3′ refers to the third family, and the subscript $3R$ refers to the generator $\sigma_3/2$, whose representation in the third family of the SM is $(b_R,\, t_R)^T$. If we allow right-handed neutrinos, as is, in fact, the case in our model, a lepton representation $(\tau_R,\, \nu_{\tau R})^T$ is also possible.

From reference [61], the $Z - Z'$ mixing angle Θ is restricted to be less than 10^{-3}, which holds true for most models. Based on this result, we can assume Θ identically zero, which is a typical assumption in collider constraints [62].

We also report Electroweak Precision data constraints on the y and z parameters (green and orange continuous lines in the left panel of figure 1), obtained using the GAPP package [61, 63], which includes low-energy weak neutral current experiments (this includes weak charges of the cesium atom and electron, as well as the constraints coming from cross-section ratios of neutrinos and antineutrino deep inelastic scattering. Measurements of the top and W masses are also in this set of observables) and Z-pole observables.

As our model is non-universal, it has two possible sources of FCNC: the non-universal couplings of the Z' and the couplings of the SM fermions to two scalar doublets. Since the charges of the first two families are equal, we can ignore constraints from observables with flavor changes between quarks and leptons of the first two families, such as: K^0–-mixing, μ–e conversion, etc. In our case, one of the strongest constraints on the parameters comes from B^0–$\bar{B}^0$-mixing. figure 1 shows the upper limits on the y and z parameters at a 95% confidence level. An extended Higgs sector generates a mixture of Z and Z' that is proportional to the couplings of the Higgs to Z' and to the expectation values of the neutral components of the scalar doublets. As shown in appendix D, the $Z - Z'$ constraints are relevant for the x parameter because z and y are strongly constrained for colliders. As can be seen from the purple dashed line in figure 1, this is the most restrictive constraint on the x parameter.

In two Higgs doublet models, FCNC can be avoided if the mass matrix for SM fermions with the same electric charge and isospin is generated from a single Higgs doublet. As we show in the appendix C, if the right-handed SM fermion is a singlet under the gauge group and if each right-handed SM singlet fermion couples to only one Higgs doublet (there is no problem if the scalar doublet has non-zero couplings to several right-handed fermions.), then there are no FCNC for the scalar sector; this is the case in our model.

5. Analysis of Higgs-like resonant signals

Recently, several anomalies have been reported in searches of high-mass scalar resonances in proton–proton collisions at the LHC. The 2HDMs are the most straightforward extensions of the SM that can explain these observations. Additionally, our model includes a scalar singlet σ that gives mass to the Z'. The Higgs mechanism requires at least two CP-odd bosons to provide mass to the Z and the Z' and one charged scalar boson to give mass to the SM W boson, which leaves us with three CP even scalar bosons, one CP-odd scalar boson and one charged scalar. Our analysis aims to determine the typical masses for these bosons in the best-motivated parameter space and compare them with the experimental anomalies reported in the literature. As explained in detail in the appendix A, of the three neutral scalar fields in the interaction space, h_1, h_2, and ξ, we can obtain using a unitary transformation, the neutral states in the mass space, H_1, H_2, H_3. Great interest has generated an anomaly that can be explained by a light neutral scalar Higgs with a mass $M_{H1} \approx 95$ GeV [64] and a charged Higgs around $M_{C^{\pm}} \approx 130$ GeV [65]. For the charged Higgs, in [66] a detailed analysis of the phenomenological implications of a new resonance with a three sigma significance was studied. On a mass basis, we will denote as M_A the only CP-odd field that is not absorbed as a Goldstone boson. An excess of events was also found in channels involving the productions of SM gauge bosons, $\gamma\gamma$ and $Z\gamma$ (for further analysis, look in [67] and references therein). This analysis provides a good indication of new scalar resonances decaying into two photons with invariant masses of 95 [68] and 152 GeV [67]. Other excesses over the expected value in the SM for dibosons are reported at 680 GeV [69], which are compatible with the excess in $\gamma\gamma$ and $b\bar{b}$ reported by the CMS collaboration [70]. A more complete review of these anomalies and additional references can be found at [71]. In this reference, they also mention an excess reported by the ATLAS collaboration that can be interpreted as a pseudoscalar with a mass of 650 GeV produced in association with a scalar with a mass of 450 GeV.

Recently, a deviation from the background-only expectation occurred for high scalar resonances with masses (575 200) GeV and a local (global) significance of 3.5 (2.0) standard deviations, as reported by the ATLAS collaboration [72]. It is important to stress that this analysis shows good agreement with the background-only hypothesis for the masses (65 090) GeV, where CMS reported an excess with a local (global) significance of 3.8 (2.8) standard deviations [70].

To account for these experimental anomalies from the scalar potential of our model (see equation 32), we consider two possible assignments for the charges of the scalar singlet σ. One of them leads to a cubic coupling among the scalar fields, while the other to quartic term (the remaining terms in the scalar potential 32 are always present regardless of the σ charge). If the Z' coupling of σ is $x - y$, that is, $\alpha_\sigma = \alpha_{\nu 3} - \alpha_{\nu 1}$, then the following term is allowed:

$$\mu[(\Phi_1^{\dagger}\Phi_2)\sigma + \text{ h.c.}].$$

In this case, the coupling constant μ has dimensions of mass, and in order to have a consistent mass spectrum, its values must be in the range $-77.3\ \text{GeV} \leqslant \mu < 0$. Similarly, if the coupling of σ to the Z' boson is $\frac{1}{2}(x - y)$, or equivalently $\alpha_\sigma = (\alpha_{\nu 3} - \alpha_{\nu 1})/2$, it is possible to form the term

$$\lambda[(\Phi_1^{\dagger}\Phi_2)\sigma^2 + \text{ h.c.})], \tag{28}$$

where the constant λ is dimensionless, and restricted to the range $(-0.44, 0)$. According to our scalar sector (whose scalar potential we show in appendix A), to reproduce part of the spectrum of anomalies in the scalar sector (determined by the VEVs and coupling constants) we must identify the middle-mass neutral scalar boson as the SM Higgs boson to which we

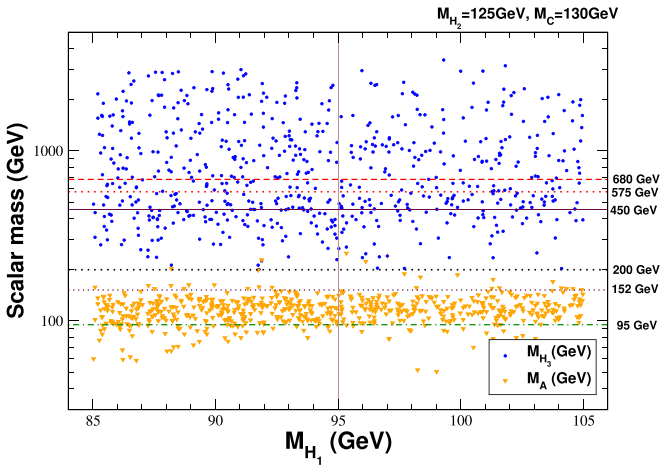

Figure 2. Distribution of the scalar mass M_{H_3} (the blue round points) and the pseudoscalar M_A (orange triangle points) for a scalar potential including the cubic term $\mu\Phi_1^{\dagger}\Phi_2\,\sigma$+h.c. In this term, μ has mass dimensions and takes values in the range (−77.3,0) GeV. We vary the other dimensionless parameters of the scalar potential in the range [−1.5, 1.5], and take the VEV of the scalar singlet v_σ as a free parameter ranging from 250 to 2000 GeV. The VEV's v_1 and v_2 vary subject to the conditions $\sqrt{v_1^2+v_2^2}=v=246.24$ GeV and $v_2 \gg v_1$. The masses of the scalars and pseudoscalars: M_{H_1}, M_{H_3} and M_A are determined by the tadpole equations (33). See the text for further details (see appendix A).

assign its well-known mass of $M_{H_2}=125$ GeV. In our model, we ensure that only the massive charged scalar field coincides with the anomaly $M_{C^{\pm}}=130$ GeV. This happens while the SM vector boson W absorbs the other massless-charged field through the Higgs mechanism. Similarly, the Higgs mechanism requires a pseudoscalar field from one of the scalar doublets to give mass to the Z boson, and the pseudoscalar field of the scalar singlet to give mass to the Z'. The mass of the remaining scalar fields (M_{H_1}, M_{H_3} and M_A) are free parameters. For the other dimensionless parameters of the potential pot, their values are assumed to be in the range [−1.5, 1.5]. Regarding the VEVs of the Φ_1 and Φ_2, they are chosen such that $v_1^2+v_2^2=(246.24\ \mathrm{GeV})^2$ with $v_2 \gg v_1$. This hierarchy between VEVs is necessary to align the Higgs doublet Φ_2 with that of the SM. We take the VEV of the scalar singlet $\langle\sigma\rangle=v_\sigma/\sqrt{2}$ as a free parameter varying between 250 and 2000 GeV. Finally, in order to satisfy the collider constraints, we require z, $y \ll x$, and take $x \gtrsim 1$ for Z' masses above 2 TeV, as explained in section appendix B.

To illustrate the density of solutions, figures 2 and 3 display a total of 640 solutions spread across the M_{H_1} versus M_{H_3} and M_{H_1} versus M_A axes. It is important to emphasize our identification of the lightest CP-even Higgs scalar H_1 with the anomaly at 95 GeV. Therefore, we have considered exploring the mass interval 95 ± 10 GeV. In these figures, we can see that many of the experimental anomalies coincide with the regions with the highest density of solutions. This coincidence is important since we have made the free parameters of the theory vary in intervals that we consider natural. It is very important that in our analysis we imposed the hierarchy $m_{H_1}<m_{H_2}<m_{H_3}$. The results are identical if we choose $m_{H_2}<m_{H_1}$, and identify the Higgs with M_{H_1}. From the density plot, we see that the highest density of solutions for the pseudo-scalar mass is between 100 and 200 GeV. This result holds for both cubic and

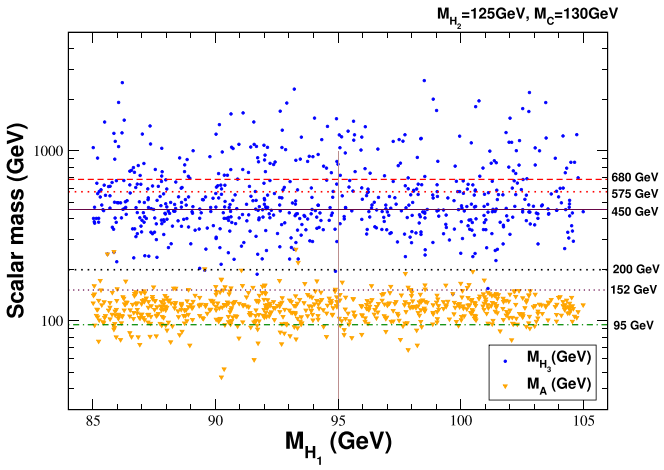

Figure 3. Distribution of the scalar mass M_{H_3} (the blue round points) and the pseudoscalar M_A (orange triangle points) for a scalar potential including the quartic term $\lambda\Phi_1^{\dagger}\Phi_2\,\sigma^2$+h.c. In this term, λ is dimensionless and takes values in the interval $(-0.44,\ 0)$. We vary the other dimensionless parameters of the scalar potential in the range $[-1.5,\ 1.5]$, and take the VEV of the scalar singlet v_σ as a free parameter ranging from 250 to 2000 GeV. The VEV's v_1 and v_2 vary subject to the conditions $\sqrt{v_1^2+v_2^2}=v=246.24$ GeV and $v_2 \gg v_1$. The masses of the scalars and pseudoscalars: M_{H_1}, M_{H_3} and M_A are determined by the tadpole equations (33). See the text for further details.

quartic potentials. In this range, we have three experimental anomalies (the one at 95 GeV, the one at 152 GeV, and the one at 200 GeV). If any of these anomalies accumulate statistics, this strongly suggests that a pseudoscalar particle could explain the resonance.

For the quartic potential (see Figure 3), the highest density of solutions is found below 1000 GeV, while for the cubic potential (see figure 2), there is a high density of solutions up to 3000 GeV. Below 1000 GeV we have three experimental anomalies with masses: 450 GeV, 575 GeV, and 680. From the density plots we see that for a quartic potential, it is more probable to have solutions in this range when compared to the cubic potential.

6. Conclusions

In this work, we assume that the SM is a low-energy effective theory of a more fundamental theory characterized by a gauge symmetry of the form $SU(3)_{\mathrm{C}} \otimes SU(2)_L \otimes U(1)_\alpha \otimes U(1)_\beta$, and whose particle content is that of the SM extended with three right-handed neutrinos, a second Higgs doublet and a scalar singlet. Additionally, we impose that both $U(1)$ charges are non-universal and contribute non-trivially to the SM hypercharge, i.e. they are not inert charges. Under these assumptions, we showed that the most general expression for the Z' chiral couplings is as those shown in table tab3. In this model, it is possible to generate all the mass matrix elements of with only two Higgs doublets. From this, it is possible to adjust the model to reproduce the CKM and PMNS mixing matrices. This feature is highly non-trivial for non-universal scenarios and represents a great advantage of this model. It is important to mention that to maintain the non-universality condition, it was preferable to avoid Majorana mass terms (if we want to reproduce the electric charges of the SM particles (which are

universal) from non-universal $U(1)$ charges, in most of the cases studied, we must avoid introducing neutrino Majorana masses).

From the assumptions of our work, as well as the collider, electroweak and flavor constraints, we also conclude that for a model with two non-inert Abelian symmetries at low energies ($M_{Z'} < 5$ TeV), only the residual symmetry $T_{3R}(3)$, in addition to the SM gauge symmetry, has an unsuppressed coupling strength. The argument]3^ says that only couplings to the third family are possible. Models with couplings to the first and second families are strongly constrained, so that only Z' couplings below 0.1 are possible, i.e. $g_{Z'}\tilde{\epsilon}_{L,R} < 0.1$. For a Z' coupling to the third family, it is possible to have Z' charges such that $g_{Z'}\tilde{\epsilon}_{L,R} \sim 1$ for Z' masses above 2 TeV.

Our work analyzes some Higgs-like anomalies recently reported by the ATLAS and CMS collaborations [67]. To this end, we show the distribution of 400 solutions in the M_{H_1}, M_{H_3} and M_{H_1}, M_A planes. These results are shown in figures 2 and 3. This analysis concludes that explaining some of the observed anomalies within the model is possible.

We show that the scalar sector FCNC cancel if each right-handed fermion couples only to a single Higgs doublet (although the scalar doublet can have non-zero couplings with several right-handed fermions). This will be the case as long as the right-handed fermions are singlets of the gauge group.

Acknowledgments

R.H.B., E.R., Y.G. and L.M. acknowledge additional financial support from Minciencias CD82315 CT ICETEX 2021-1080. This research was partly supported by the]Vicerrectoría de Investigaciones e Interacción Social (VIIS) de la Universidad de Nariño^, project numbers 2686, 2679, 2693, 3130.

Data availability statement

All data that support the findings of this study are included within the article (and any supplementary files).

Appendix A. Scalar potential

Our model contains two scalar doublets, Φ_1 and Φ_2, and a scalar singlet σ. In general, these fields can be expressed as

$$\Phi_1 = \begin{pmatrix} \phi_1^+ \\ \dfrac{v_1 + h_1 + i\,\eta_1}{\sqrt{2}} \end{pmatrix}, \Phi_2 = \begin{pmatrix} \phi_2^+ \\ \dfrac{v_2 + h_2 + i\,\eta_2}{\sqrt{2}} \end{pmatrix}, \ \sigma = \frac{v_\sigma + \xi + i\,\zeta}{\sqrt{2}}, \tag{29}$$

where $\langle\Phi_1\rangle = (0,\, v_1/\sqrt{2})^T, \langle\Phi_2\rangle = (0,\, v_2/\sqrt{2})^T$ and $v_\sigma = \sqrt{2}\,\langle\sigma\rangle$. For the doublet Φ_2 (which is close to H_1 in the Georgi basis) to be aligned with the Higgs of the SM we impose the hierarchy

$$v_\sigma > v_2 \gg v_1. \tag{30}$$

Since the Higgs doublet is a linear combination of the two scalar doublets, then

$$\sqrt{v_1^2 + v_2^2} = v = 246.24 \text{ GeV}, \tag{31}$$

The most general scalar potential consistent with the gauge symmetry $SU(2)_L \otimes U(1)_\alpha \otimes U(1)_\beta$ is [68]:

$$\begin{aligned} V(\Phi_1, \Phi_2, \sigma) = {} & \mu_1^2 |\Phi_1|^2 + \mu_2^2 |\Phi_2|^2 + \mu_\sigma^2 |\sigma|^2 + \lambda_1 |\Phi_1|^4 + \lambda_2 |\Phi_2|^4 + \lambda_\sigma |\sigma|^4 \\ & + \lambda_3 |\Phi_1|^2 |\Phi_2|^2 + \lambda_4 |\Phi_1^\dagger \Phi_2|^2 + \lambda_{1\sigma} |\Phi_1|^2 |\sigma|^2 + \lambda_{2\sigma} |\Phi_2|^2 |\sigma|^2 \\ & + \text{linear term in } \sigma \text{ (or quadratic term in } \sigma), \end{aligned} \tag{32}$$

where a linear interaction term in σ (which we will denote as the cubic term) of the form

$$\mu[(\Phi_1^\dagger \Phi_2)\sigma + \text{ h.c.}]$$

is possible if α_σ in table 2 is taken to be $\alpha_{\nu 3} - \alpha_{\nu 1}$. Here μ is a coupling with mass dimensions. On the other hand, if α_σ is equal to $\frac{1}{2}(\alpha_{\nu 3} - \alpha_{\nu 1})$, then the quadratic term in σ (which we will denote as the quartic term),

$$\lambda[(\Phi_1^\dagger \Phi_2)\sigma^2 + \text{ h.c.})],$$

is the one that is present. In this case, the coupling λ is dimensionless. By minimizing the potential in equation pot, we then obtain that

$$\begin{aligned} \mu_1^2 &= -\frac{\sqrt{2}}{2}\frac{\mu v_2 v_\sigma}{v_1} - \lambda_1 v_1^2 - \frac{\lambda_3 + \lambda_4}{2} v_2^2 - \frac{\lambda_{1\sigma}}{2} v_\sigma^2, \\ \mu_2^2 &= -\frac{\sqrt{2}}{2}\frac{\mu v_1 v_\sigma}{v_2} - \lambda_2 v_2^2 - \frac{\lambda_3 + \lambda_4}{2} v_1^2 - \frac{\lambda_{2\sigma}}{2} v_\sigma^2, \\ \mu_\sigma^2 &= -\frac{\sqrt{2}}{2}\frac{\mu v_1 v_2}{v_\sigma} - \lambda_\sigma v_\sigma^2 - \frac{\lambda_{1\sigma}}{2} v_1^2 - \frac{\lambda_{2\sigma}}{2} v_2^2. \end{aligned} \tag{33}$$

in the cubic case, while in the quartic one, the corresponding expressions can be obtained from the previous ones by making the substitution $\sqrt{2}\mu \to \lambda v_\sigma$.

A.1. Mass spectrum of the neutral scalar sector

From the potential equation (32) and the previous minimization conditions, we can build the mass matrices from the fields defined in equation (29). For the CP-even scalar field basis (h_1, h_2, ξ), the mass matrix is given in the cubic case [73] by:

$$\begin{pmatrix} 2\lambda_1 v_1^2 - \frac{\mu v_2 v_\sigma}{\sqrt{2} v_1} & \frac{\mu v_\sigma}{\sqrt{2}} + v_1 v_2(\lambda_3 + \lambda_4) & \frac{\mu v_2}{\sqrt{2}} + \lambda_{1\sigma} v_1 v_\sigma \\ \frac{\mu v_\sigma}{\sqrt{2}} + v_1 v_2(\lambda_3 + \lambda_4) & 2\lambda_2 v_2^2 - \frac{\mu v_1 v_\sigma}{\sqrt{2} v_2} & \frac{\mu v_1}{\sqrt{2}} + \lambda_{2\sigma} v_2 v_\sigma \\ \frac{\mu v_2}{\sqrt{2}} + \lambda_{1\sigma} v_1 v_\sigma & \frac{\mu v_1}{\sqrt{2}} + \lambda_{2\sigma} v_2 v_\sigma & 2\lambda_\sigma v_\sigma^2 - \frac{\mu v_1 v_2}{\sqrt{2} v_\sigma} \end{pmatrix}, \tag{34}$$

while in the quartic case, it corresponds to:

$$\begin{pmatrix} 2\lambda_1 v_1^2 - \frac{\lambda v_2 v_\sigma^2}{2 v_1} & \frac{\lambda v_\sigma^2}{2} + v_1 v_2(\lambda_3 + \lambda_4) & v_\sigma(\lambda v_2 + \lambda_{1\sigma} v_1) \\ \frac{\lambda v_\sigma^2}{2} + v_1 v_2(\lambda_3 + \lambda_4) & 2\lambda_2 v_2^2 - \frac{\lambda v_1 v_\sigma^2}{2 v_2} & v_\sigma(\lambda v_1 + \lambda_{2\sigma} v_2) \\ v_\sigma(\lambda v_2 + \lambda_{1\sigma} v_1) & v_\sigma(\lambda v_1 + \lambda_{2\sigma} v_2) & 2\lambda_\sigma v_\sigma^2 \end{pmatrix}. \tag{35}$$

These are square mass matrices of rank three with mass eigenvalues M_{H_1}, M_{H_2} and M_{H_3}, corresponding to the mass eigenstates H_1, H_2 and H_3, respectively. We will identify the states according to the mass hierarchy:

$$M_{H_1} < M_{H_2} < M_{H_3}.$$

The intermediate-mass scalar state, H_2, can be identified as the SM Higgs, while the light mass scalar state H_1 and the heavy mass scalar state H_3 are new scalar fields that, in principle, can be observed in the LHC experiments. The hierarchy equation (30) causes the scalar H_2 to align with h_2.

A.1.1. Mass spectrum of the neutral pseudoscalar sector. In the (η_1, η_2, ζ) basis, the pseudoscalar squared mass matrix takes the following form for the cubic case:

$$\frac{\mu}{\sqrt{2}}\begin{pmatrix} -\dfrac{v_2 v_\sigma}{v_1} & v_\sigma & v_2 \\ v_\sigma & -\dfrac{v_1 v_\sigma}{v_2} & -v_1 \\ v_2 & -v_1 & -\dfrac{v_1 v_2}{v_\sigma} \end{pmatrix}. \tag{36}$$

The corresponding mass matrix for the quartic case is

$$\frac{\lambda v_\sigma}{2}\begin{pmatrix} -\dfrac{v_2 v_\sigma}{v_1} & v_\sigma & 2v_2 \\ v_\sigma & -\dfrac{v_1 v_\sigma}{v_2} & -2v_1 \\ 2v_2 & -2v_1 & -4\dfrac{v_1 v_2}{v_\sigma} \end{pmatrix}. \tag{37}$$

In both cases, these mass matrices have rank 1. The two zero eigenvalues correspond to the two Goldstone bosons that give mass to the Z and Z' bosons after the spontaneous symmetry breaking. The non-zero eigenvalue corresponds to a measurable pseudoscalar with mass equal to:

$$M_A^2 = \begin{cases} -\dfrac{\mu(v_1^2 v_2^2 + v^2 v_\sigma^2)}{\sqrt{2}\, v_1 v_2 v_\sigma} & \text{(cubic case)}, \\ -\dfrac{\lambda(4v_1^2 v_2^2 + v^2 v_\sigma^2)}{2 v_1 v_2} & \text{(quartic case)}, \end{cases} \tag{38}$$

whose mixing comes mainly from η_1.

A.1.2. Mass spectrum of the charged scalar sector. In the ($\phi_1^\pm$, $\phi_2^\pm$) basis, the squared mass matrix for charged scalar particles is

$$\frac{1}{2}\begin{pmatrix} -\sqrt{2}\dfrac{\mu v_2 v_\sigma}{v_1} - \lambda_4 v_2^2 & \sqrt{2}\mu v_\sigma + \lambda_4 v_1 v_2 \\ \sqrt{2}\mu v_\sigma + \lambda_4 v_1 v_2 & -\sqrt{2}\dfrac{\mu v_1 v_\sigma}{v_2} - \lambda_4 v_1^2 \end{pmatrix}, \tag{39}$$

for the cubic case, and

$$\frac{1}{2}\begin{pmatrix} -\dfrac{\lambda v_2 v_\sigma^2}{v_1} - \lambda_4 v_2 & \lambda v_\sigma^2 + \lambda_4 v_1 v_2 \\ \lambda v_\sigma^2 + \lambda_4 v_1 v_2 & -\dfrac{\lambda v_1 v_\sigma^2}{v_2} - \lambda_4 v_1 \end{pmatrix}, \tag{40}$$

for the quartic case. As before, these mass matrices have rank 1, with the only zero eigenvalue corresponding to the Goldstone boson giving mass to the charged W boson. The remaining charged scalar acquires a mass equal to

$$M_{C^\pm}^2 = \begin{cases} -\dfrac{v^2}{2}\left(\sqrt{2}\,\dfrac{\mu v_\sigma}{v_1 v_2} + \lambda_4\right), & \text{(cubic case)}; \\ -\dfrac{v^2}{2}\left(\dfrac{\lambda v_\sigma^2}{v_1 v_2} + \lambda_4\right), & \text{(quartic case)}. \end{cases} \tag{41}$$

Appendix B. The gauge boson masses

Let us now determine the mass of the neutral gauge bosons. These are obtained from the scalar-gauge couplings introduced by the covariant derivatives of the scalar fields in the Lagrangian terms

$$\mathcal{L} \supset |D_\mu \Phi_1|^2 + |D_\mu \Phi_2|^2 + |D_\mu \sigma|^2, \tag{42}$$

where

$$D^\mu = \partial^\mu + \frac{i}{2} g_L A_j^\mu \hat{T}_j + \frac{i}{2} g_\alpha B_\alpha^\mu \hat{\alpha} + \frac{i}{2} g_\beta B_\beta^\mu \hat{\beta}, \tag{43}$$

with $\hat{T}_j$, A_j^μ ($j = 1, 2, 3$) and g_L denoting, respectively, the generators, the gauge fields and the coupling constant associated with the weak isospin gauge group $SU(2)_L$[8], while $\hat{\chi}$, B_χ^μ and g_χ, with $\chi = \alpha, \beta$, are the corresponding quantities related with the two Abelian $U(1)$ factors. For the Higgs doublets Φ_a ($a = 1, 2$) and the singlet σ, we have

$$\begin{aligned} D^\mu \Phi_a &= \left[\partial^\mu + \frac{i}{2} g_L \begin{pmatrix} A_3^\mu & \sqrt{2}\,W^\mu \\ \sqrt{2}\,W^{\mu\dagger} & -A_3^\mu \end{pmatrix} + \frac{i}{2} g_\alpha \alpha_a B_\alpha^\mu + \frac{i}{2} g_\beta \beta_a B_\beta^\mu\right]\Phi_a, \\ D^\mu \sigma &= \left(\partial^\mu + \frac{i}{2} g_\alpha \alpha_\sigma B_\alpha^\mu + \frac{i}{2} g_\beta \beta_\sigma B_\beta^\mu\right)\sigma, \end{aligned} \tag{44}$$

Here α_a (β_a) and α_σ (β_σ) denote, respectively, the $U(1)_{\alpha(\beta)}$ charges for Φ_a and σ given in table 2. Additionally, the W field has been defined as

$$W^\mu = \frac{A_1^\mu - i A_2^\mu}{\sqrt{2}}. \tag{45}$$

Taking into account the definition of Φ_a and σ given in equation (29), as well as the basis changes defined in equations (6) and (7), which imply

[8] The $SU(2)_L$ generators are defined in terms of the Pauli matrices according to $T_i = \frac{1}{2}\sigma_i$.

$$B_\chi^\mu = a_\chi A^\mu + b_\chi Z^\mu + c_\chi Z'^\mu, \qquad (\chi = \alpha, \beta);$$
$$A_3^\mu = \sin\theta_W A^\mu + \cos\theta_W Z^\mu, \tag{46}$$

with

$$a_\alpha = \cos\theta\cos\theta_W, \qquad b_\alpha = -\cos\theta\sin\theta_W, \qquad c_\alpha = -\sin\theta,$$
$$a_\beta = \sin\theta\cos\theta_W, \qquad b_\beta = -\sin\theta\sin\theta_W, \qquad c_\beta = \cos\theta, \tag{47}$$

it can be shown that the mass terms for the Z^μ, Z'^μ and W^μ gauge bosons are

$$\mathcal{L} \supset \frac{1}{2}(g_Z^2 v^2) Z_\mu Z^\mu + \frac{1}{2}[g_{Z'}^2(\gamma_1'^2 v_1^2 + \gamma_2'^2 v_2^2 + \gamma_\sigma'^2 v_\sigma^2)] Z'_\mu Z'^\mu$$
$$-\frac{1}{2}[2 g_Z g_{Z'}(\gamma_1' v_1^2 + \gamma_2' v_2^2)] Z_\mu Z'^\mu + g_W^2 v^2 W_\mu^\dagger W^\mu, \tag{48}$$

the coupling constants g_Z and g_W are defined as in the SM, i.e.

$$g_Z = \frac{g_L}{2\cos\theta_W}, \qquad g_W = \frac{g_L}{2}, \tag{49}$$

while $g_{Z'}$ is defined through the following relations:

$$g_{Z'}\gamma_a' = -\frac{1}{2}(g_\alpha \alpha_a \sin\theta - g_\beta \beta_a \cos\theta), \qquad (a = 1, 2.);$$
$$g_{Z'}\gamma_\sigma' = -\frac{1}{2}(g_\alpha \alpha_\sigma \sin\theta - g_\beta \beta_\sigma \cos\theta). \tag{50}$$

In terms of the x, y, z and w parameters defined in equation (27), these couplings can be expressed as

$$g_{Z'}\gamma_1' = z - y, \qquad g_{Z'}\gamma_2' = z - x, \qquad g_{Z'}\gamma_\sigma' = -w. \tag{51}$$

Writing the $Z - Z'$ mixing matrix as

$$M_{Z-Z'}^2 = \begin{bmatrix} g_Z^2 v^2 & -g_Z g_{Z'}\gamma_a' v_a^2 \\ -g_Z g_{Z'}\gamma_a' v_a^2 & g_{Z'}^2(\gamma_a'^2 v_a^2 + \gamma_\sigma'^2 v_\sigma^2) \end{bmatrix} \equiv \begin{pmatrix} \mathcal{A} & -\mathcal{C} \\ -\mathcal{C} & \mathcal{B} \end{pmatrix}, \tag{52}$$

with a sum over the a index implied, then the square masses of the physical neutral gauge bosons Z_1 and Z_2 are given by

$$m_{Z_{1,2}}^2 = \frac{1}{2}[\mathcal{A} + \mathcal{B} \mp \sqrt{(\mathcal{A} - \mathcal{B})^2 + 4\mathcal{C}^2}]. \tag{53}$$

If $\mathcal{O}$ is the diagonalizing orthogonal matrix defining the mass basis, i.e.

$$\begin{pmatrix} Z^\mu \\ Z'^\mu \end{pmatrix} = \mathcal{O}\begin{pmatrix} Z_1^\mu \\ Z_2^\mu \end{pmatrix} = \begin{pmatrix} \cos\Theta & -\sin\Theta \\ \sin\Theta & \cos\Theta \end{pmatrix}\begin{pmatrix} Z_1^\mu \\ Z_2^\mu \end{pmatrix}, \tag{54}$$

then the mixing angle Θ can be determined from

$$\tan 2\Theta = \frac{2\mathcal{C}}{\mathcal{B} - \mathcal{A}}. \tag{55}$$

From this expression, it is possible to obtain

$$\Theta = \frac{1}{2}\arctan\left\{\frac{g_L}{2\cos\theta_W}\frac{[(z-y)v_1^2+(z-x)v_2^2]}{[(z-y)^2v_1^2+(z-x)^2v_2^2+w^2v_\sigma^2]-\frac{g_L^2v^2}{4\cos^2\theta_W}}\right\}. \tag{56}$$

To satisfy the current constraint on the mixing angle [61] it is necessary to keep this angle below 10^{-3}, which is possible in two scenarios: (1) a light Z' mass, i.e. $M_{Z'} \ll M_Z$ or a heavy Z' mass, i.e. $M_{Z'} \gg M_Z$, which requires $x \gtrsim 1$, $z \sim y \ll 1$ and $v < v_\sigma$. As usual in calculating collider constraints [62] we assume $\theta_{Z-Z'} = 0$. In analyzing the scalar anomalies $w = x - y$ in the cubic case, or $w = \frac{x-y}{2}$ for a potential with quartic coupling term (as explained in Appendix A). For that analysis, assuming a heavy Z' mass is more convenient.

Appendix C. Analysis of scalar FCNCs

The Yukawa interactions are described by the general Lagrangian

$$-\mathcal{L}_Y = \bar{q}'_{iL}y_{ij}^{ad}\Phi_a d'_{jR} + \bar{q}'_{iL}y_{ij}^{au}\tilde{\Phi}_a u'_{jR} + \bar{l}'_{iL}y_{ij}^{ae}\Phi_a e'_{jR} + \bar{l}'_{iL}y_{ij}^{a\nu}\tilde{\Phi}_a \nu'_{jR} + \text{ h.c.}, \tag{57}$$

with $i, j = 1, 2, 3$, and $a = 1, 2$. Here

$$\Phi_a = \begin{pmatrix} \phi_a^+ \\ \dfrac{v_a + h_a + i\eta_a}{\sqrt{2}} \end{pmatrix}, \qquad \tilde{\Phi}_a = i\sigma_2\Phi_a^*. \tag{58}$$

According to the non-universal $U(1)$ charges, the Yukawa couplings present in our model are

$$\begin{aligned} -\mathcal{L}_Y = {} & \bar{q}'_{iL}y_{ia}^{1d}\Phi_1 d'_{aR} + \bar{q}'_{iL}y_{ia}^{1u}\tilde{\Phi}_1 u'_{aR} + \bar{l}'_{iL}y_{ia}^{1e}\Phi_1 e'_{aR} + \bar{l}'_{iL}y_{ia}^{1\nu}\tilde{\Phi}_1\nu'_{aR} \\ & + \bar{q}'_{iL}y_{i3}^{2d}\Phi_2 d'_{3R} + \bar{q}'_{iL}y_{i3}^{2u}\tilde{\Phi}_2 u'_{3R} + \bar{l}'_{iL}y_{i3}^{2e}\Phi_2 e'_{3R} + \bar{l}'_{iL}y_{i3}^{2\nu}\tilde{\Phi}_2\nu'_{3R} + \text{h.c.} \end{aligned} \tag{59}$$

So, the Yukawa matrices have the following structure

$$Y^{1f} = \begin{pmatrix} y_{11}^{1f} & y_{12}^{1f} & 0 \\ y_{21}^{1f} & y_{22}^{1f} & 0 \\ y_{31}^{1f} & y_{32}^{1f} & 0 \end{pmatrix}, \qquad Y^{2f} = \begin{pmatrix} 0 & 0 & y_{13}^{2f} \\ 0 & 0 & y_{23}^{2f} \\ 0 & 0 & y_{33}^{2f} \end{pmatrix}. \tag{60}$$

To analyze the FCNC, it is convenient to rotate the scalar doublets to the Giorgi basis where only one of the CP neutral even components of the doublets acquires VEV while the remaining ones are zero. Explicitly this corresponds to

$$\begin{pmatrix} \mathcal{H}_1 \\ \mathcal{H}_2 \end{pmatrix} = \begin{pmatrix} \cos\beta & \sin\beta \\ -\sin\beta & \cos\beta \end{pmatrix}\begin{pmatrix} \Phi_1 \\ \Phi_2 \end{pmatrix} \rightarrow \mathcal{H}_\alpha = R_{\alpha\beta}\Phi_\beta. \tag{61}$$

In the unitary gauge

$$\mathcal{H}_1 = \begin{pmatrix} 0 \\ \dfrac{v+h}{\sqrt{2}} \end{pmatrix}, \qquad \mathcal{H}_2 = \begin{pmatrix} \mathcal{H}^+ \\ \dfrac{\mathcal{H}^0 + i\mathcal{A}^0}{\sqrt{2}} \end{pmatrix}. \tag{62}$$

The Georgi basis should not be confused with the mass states of the scalar bosons. As discussed in [74], in this basis, the $\mathcal{H}_1$ boson gives mass to the SM fermions (the scalar singlet does not couple to SM fermions) and does not generate FCNC. Therefore, it is not convenient

to use the mass eigenstates, a mixture of the scalar singlet and the doublets, when studying the interactions between the scalar sector and the SM fermions. In most observables, the scalar boson is a virtual particle, and the boson that interacts with the SM fermions is the projection onto the subspace formed by the two doublets. In 2HDM, this feature is very useful since FCNC in the scalar sector can only be generated by $\mathcal{H}_2$. Therefore, in this work, we focus on the CP-even neutral component of this doublet.

In terms of the new basis,

$$\begin{aligned} y_{ij}^{\alpha f}\,\Phi_\alpha &= x_{ij}^{\alpha f}\,\mathcal{H}_\alpha, \\ y_{ij}^{\alpha f}\,\tilde{\Phi}_\alpha &= x_{ij}^{\alpha f}\,\tilde{\mathcal{H}}_\alpha, \end{aligned} \tag{63}$$

the rotated yukawa couplings are

$$\begin{aligned} x_{ij}^{1f} &= \cos\beta \quad y_{ij}^{1f} + \sin\beta \quad y_{ij}^{2f}, \\ x_{ij}^{2f} &= -\sin\beta \quad y_{ij}^{1f} + \cos\beta \quad y_{ij}^{2f}. \end{aligned} \tag{64}$$

Thus

$$\begin{aligned} \mathcal{L}_Y &= -\bar{q}'_{iL}x_{ij}^{\alpha d}\mathcal{H}_\alpha d'_{jR} - \bar{q}'_{iL}x_{ij}^{\alpha u}\tilde{\mathcal{H}}_\alpha u'_{jR} - \bar{l}'_{iL}x_{ij}^{\alpha e}\mathcal{H}_\alpha e'_{jR} - \bar{l}'_{iL}x_{ij}^{\alpha \nu}\tilde{\mathcal{H}}_\alpha \nu'_{jR} + h.c., \\ &= -\bar{q}'_{iL}x_{ij}^{1d}\mathcal{H}_1 d'_{jR} - \bar{q}'_{iL}x_{ij}^{2d}\mathcal{H}_2 d'_{jR} - \bar{q}'_{iL}x_{ij}^{1u}\tilde{\mathcal{H}}_1 u'_{jR} - \bar{q}'_{iL}x_{ij}^{2u}\tilde{\mathcal{H}}_2 u'_{jR} \\ &\quad - \bar{l}'_{iL}x_{ij}^{1e}\mathcal{H}_1 e'_{jR} - \bar{l}'_{iL}x_{ij}^{2e}\mathcal{H}_2 e'_{jR} - \bar{l}'_{iL}x_{ij}^{1\nu}\tilde{\mathcal{H}}_1 \nu'_{jR} - \bar{l}'_{iL}x_{ij}^{2\nu}\tilde{\mathcal{H}}_2 \nu'_{jR} + h.c., \\ &= -\frac{1}{\sqrt{2}}(v+h)(\bar{d}'_{iL}x_{ij}^{1d}d'_{jR} + \bar{u}'_{iL}x_{ij}^{1u}u'_{jR} + \bar{e}'_{iL}x_{ij}^{1e}e'_{jR} + \bar{\nu}'_{iL}x_{ij}^{1\nu}\nu'_{jR}) \\ &\quad - \frac{1}{\sqrt{2}}(\mathcal{H}^0 + i\mathcal{A}^0)(\bar{d}'_{iL}x_{ij}^{2d}d'_{jR} + \bar{e}'_{iL}x_{ij}^{2e}e'_{jR}) - \frac{1}{\sqrt{2}}(\mathcal{H}^0 - i\mathcal{A}^0)(\bar{u}'_{iL}x_{ij}^{2u}u'_{jR} + \bar{\nu}'_{iL}x_{ij}^{2\nu}\nu'_{jR}) \\ &\quad - \mathcal{H}^+(\bar{u}'_{iL}x_{ij}^{2d}d'_{jR} + \bar{\nu}'_{iL}x_{ij}^{2e}e'_{jR}) + \mathcal{H}^-(\bar{d}'_{iL}x_{ij}^{2u}u'_{jR} + \bar{e}'_{iL}x_{ij}^{2\nu}\nu'_{jR}) + h.c., \end{aligned}$$

where we have taken into account that $\tilde{\mathcal{H}}_2 = \left(\frac{\mathcal{H}^0 - i\mathcal{A}^0}{\sqrt{2}}, -\mathcal{H}^-\right)^T$. Next, we define the fermion mass eigenstates as:

$$f_L \equiv V_L^{f\dagger} f'_L, \qquad f_R \equiv V_R^{f\dagger} f'_R, \tag{65}$$

with $V_{L(R)}^f$ are appropriated unitary matrices. In terms of the non-prime fields, we get

$$\begin{aligned} \mathcal{L}_Y &= -\frac{1}{\sqrt{2}}(v+h)(\bar{d}_{iL}z_{ij}^{1d}d_{jR} + \bar{e}_{iL}z_{ij}^{1e}e_{jR} + \bar{u}_{iL}z_{ij}^{1u}u_{jR} + \bar{\nu}_{iL}z_{ij}^{1\nu}\nu_{jR}) \\ &\quad - \frac{1}{\sqrt{2}}(\mathcal{H}^0 + i\mathcal{A}^0)(\bar{d}_{iL}z_{ij}^{2d}d_{jR} + \bar{e}_{iL}z_{ij}^{2e}e_{jR}) - \frac{1}{\sqrt{2}}(\mathcal{H}^0 - i\mathcal{A}^0)(\bar{u}_{iL}z_{ij}^{2u}u_{jR} + \bar{\nu}_{iL}z_{ij}^{2\nu}\nu_{jR}) \\ &\quad - \mathcal{H}^+(\bar{u}_{iL}z_{ij}^{2ud}d_{jR} + \bar{\nu}_{iL}z_{ij}^{2\nu e}e_{jR}) + \mathcal{H}^-(\bar{d}_{iL}z_{ij}^{2du}u_{jR} + \bar{e}_{iL}z_{ij}^{2e\nu}\nu_{jR}) + h.c., \end{aligned} \tag{66}$$

where

$$z^{\alpha f} \equiv V_L^{f\dagger}x^{\alpha f}V_R^f, \qquad z^{2gf} \equiv V_L^{g\dagger}x^{2f}V_R^f. \tag{67}$$

In this way, from equation (64), we get

$$z^{1f} = \cos\beta(V_L^{f\dagger}y^{1f}V_R^f) + \sin\beta(V_L^{f\dagger}y^{2f}V_R^f), \tag{68}$$

$$z^{2f} = -\sin\beta(V_L^{f\dagger}y^{1f}V_R^f) + \cos\beta(V_L^{f\dagger}y^{2f}V_R^f), \tag{69}$$

$$z^{2gf} = -\sin\beta(V_L^{g\dagger} y^{1f} V_R^f) + \cos\beta(V_L^{g\dagger} y^{2f} V_R^f). \tag{70}$$

In the Georgi basis, only the CP-odd component of $\mathcal{H}_1$ acquires VEV, and therefore, the interaction of the SM fermions with this doublet generates the masses of quarks and leptons; consequently, in the mass eigenstates the matrix z^{1f} must be diagonal, i.e.

$$z^{1f} = \begin{pmatrix} \frac{\sqrt{2}m_1^f}{v} & 0 & 0 \\ 0 & \frac{\sqrt{2}m_2^f}{v} & 0 \\ 0 & 0 & \frac{\sqrt{2}m_3^f}{v} \end{pmatrix}, \tag{71}$$

where m_i^f corresponds to the mass of the fermion f_i. Because in our model, the right-handed quarks and leptons are singlets under the gauge group we can define the right-handed fermions as: $f_j'' = (V_R^f)_{ij} f_j$ for all f, such that V_R^f completely disappears from the Lagrangian. This transformation leaves all the terms invariant under the gauge group since the gauge singlets are of the form $\bar{f}_{Ri} f_i$ or $\bar{f}_{Ri}\partial_\mu f_i$ and V_R^f is a global transformation. We are not modifying the Yukawa interaction terms since we are only redefining them. In this way, the coupling of fermions to scalar bosons is

$$z^{\alpha f} \equiv V_L^{f\dagger} x^{\alpha f} V_R^f \to V_L^{f\dagger} x^{\alpha f}.$$

A consequence of this result is that if the Yukawa coupling of a scalar boson to one of the right-handed fermions is zero in the interaction space, i.e. $y_{ij}^{\alpha f} = 0$ for all j, then in mass eigenstates, the corresponding Yukawa coupling is also identically zero, i.e. $V_{ik}^f y_{kj}^{\alpha f} = 0$ for all j. That is, if the diagonalization matrix V_L^f of the left-handed fermions f is given by

$$V_L^f = \begin{pmatrix} v_{11}^f & v_{12}^f & v_{13}^f \\ v_{21}^f & v_{22}^f & v_{23}^f \\ v_{31}^f & v_{32}^f & v_{33}^f \end{pmatrix}, \tag{72}$$

the equation (60) implies that

$$V_L^{f\dagger} y^{1f} = \begin{pmatrix} v_{11}^* y_{11}^{1f} + v_{21}^* y_{21}^{1f} + v_{31}^* y_{31}^{1f} & v_{11}^* y_{12}^{1f} + v_{21}^* y_{22}^{1f} + v_{31}^* y_{32}^{1f} & 0 \\ v_{12}^* y_{11}^{1f} + v_{22}^* y_{21}^{1f} + v_{32}^* y_{31}^{1f} & v_{12}^* y_{12}^{1f} + v_{22}^* y_{22}^{1f} + v_{32}^* y_{32}^{1f} & 0 \\ v_{13}^* y_{11}^{1f} + v_{23}^* y_{21}^{1f} + v_{33}^* y_{31}^{1f} & v_{13}^* y_{12}^{1f} + v_{23}^* y_{22}^{1f} + v_{33}^* y_{32}^{1f} & 0 \end{pmatrix},$$
$$V_L^{f\dagger} y^{2f} = \begin{pmatrix} 0 & 0 & v_{11}^* y_{13}^{2f} + v_{21}^* y_{23}^{2f} + v_{31}^* y_{33}^{2f} \\ 0 & 0 & v_{12}^* y_{13}^{2f} + v_{22}^* y_{23}^{2f} + v_{32}^* y_{33}^{2f} \\ 0 & 0 & v_{13}^* y_{13}^{2f} + v_{23}^* y_{23}^{2f} + v_{33}^* y_{33}^{2f} \end{pmatrix}. \tag{73}$$

Since the coupling z^{1f} is diagonal, from the relation $z^{1f} = \cos\beta V_L^{f\dagger} y^{1f} + \sin\beta V_L^{f\dagger} y^{2f}$ and from the fact that if $(V_L^f y^{1f})_{ij} = 0$ then $(V_L^f y^{2f})_{ij} \neq 0$ and the opposite, it must be true that each of the contributions must be diagonal. From the expressions (73) we have

$$z_{ij}^{1f} = z_i^{1f}\delta_{ij} = \cos\beta(V_L^f y^{1f})_{ij},\ \text{for any}\ i\ \text{and}\ j = 1,\ 2.$$
$$z_{ij}^{1f} = z_i^{1f}\delta_{ij} = \sin\beta(V_L^f y^{2f})_{ij},\ \text{for any}\ i\ \text{and}\ j = 3. \tag{74}$$

That is to say, $(V_L^f y^{1f})_{ij}$ and $(V_L^f y^{2f})_{ij}$ are diagonal matrix with $(V_L^f y^{1f})_{33} = 0$ and $(V_L^f y^{2f})_{11} = (V_L^f y^{2f})_{22} = 0$. From these results, the Yukawa couplings of $\mathcal{H}_2$ with the physical fermions turn out to be diagonal:

$$z^{2f} = -\sin\beta(V_L^f y^{1f})_{ij} + \cos\beta(V_L^f y^{2f})_{ij} = -\tan\beta z_i^{1f}\delta_{ij}|_{i,j\in(1,2)} + \cot\beta z_i^{1f}\delta_{i3}.$$

In the last step we obtained the expressions for $(V_L^f y^{1f})_{ij}$ and $(V_L^f y^{2f})_{ij}$ from equation (74). In matrix form this result can be written as

$$z^{2f} = \begin{pmatrix} -\tan\beta z_1^{1f} & 0 & 0 \\ 0 & -\tan\beta z_2^{1f} & 0 \\ 0 & 0 & \cot\beta z_3^{1f} \end{pmatrix}. \tag{75}$$

This result is important because it shows that the coupling of the neutral scalars in the mass eigenstates of the SM fermions is diagonal. Therefore, our model does not present FCNC in the scalar sector. In most cases, the exact values of the matrix $y_{ij}^{\alpha f}$ are entirely unknown, and what we know are the diagonal couplings, $z_i = \frac{\sqrt{2}}{v}m_i^f$, where m_i^f is a diagonal matrix whose elements correspond to the fermion masses in the SM so that the Yukawa couplings will be given by

$$y_{ij}^{1f} = V_{Lik}^{f\dagger}\frac{\sqrt{2}}{v\cos\beta}m_k^{1f}\delta_{kj},\ 0 = m_3^{1f}\ \text{where}.$$

Here m^{1f} is a diagonal matrix with the first two eigenvalues equal to the masses of the particles in the SM and a third element equal to zero. We have a similar expression for the second term in equation (68)

$$y_{ij}^{2f} = V_{Lik}^{f\dagger}\frac{\sqrt{2}}{v\sin\beta}m_k^{2f}\delta_{kj},\ 0 = m_2^{2f} = m_1^{2f}\ \text{where}.$$

Here m^{2f} is a diagonal matrix with the first two eigenvalues equal to zero and a third element equal to the corresponding mass in the SM. On the other hand, the Yukawa couplings inducing flavor-changing charged currents can be written as shown below:

$$z^{2ud} = -\sin\beta[V_L^{u\dagger}V_L^d(V_L^{d\dagger}y^{1d}V_R^d)] + \cos\beta[V_L^{u\dagger}V_L^d(V_L^{d\dagger}y^{2d}V_R^d)],$$
$$z^{2du} = -\sin\beta[V_L^{d\dagger}V_L^u(V_L^{u\dagger}y^{1u}V_R^u)] + \cos\beta[V_L^{d\dagger}V_L^u(V_L^{u\dagger}y^{2u}V_R^u)],$$
$$z^{2ve} = -\sin\beta[V_L^{\nu\dagger}V_L^e(V_L^{e\dagger}y^{1e}V_R^e)] + \cos\beta[V_L^{\nu\dagger}V_L^e(V_L^{e\dagger}y^{2e}V_R^e)],$$
$$z^{2e\nu} = -\sin\beta[V_L^{e\dagger}V_L^\nu(V_L^{\nu\dagger}y^{1\nu}V_R^\nu)] + \cos\beta[V_L^{e\dagger}V_L^\nu(V_L^{\nu\dagger}y^{1\nu}V_R^\nu)].$$

Remembering that $V_{\text{CKM}} = V_L^{u\dagger}V_L^d \equiv V$ and $V_{\text{PMNS}} = V_L^{e\dagger}V_L^\nu \equiv U$, it is easy to see from equation (69) that

$$z^{2ud} = Vz^{2d}, \qquad z^{2du} = V^\dagger z^{2u}, \qquad z^{2ve} = U^\dagger z^{2e}, \qquad z^{2e\nu} = Uz^{2\nu}. \tag{76}$$

Appendix D. $Z-Z^{'}$ mixing

The $U(1)'$ charge assignments of the Higgs fields Q'_{Φ} in a specific model, generate the $\theta_{Z-Z'}$ mixing [61, 75]

$$\theta_{Z-Z'} = C\frac{g'}{g_1}\left(\frac{m_Z}{m_{Z'}}\right)^2 = -\frac{\sum_i t_{3i}Q'_{\Phi_i}v^2_{\Phi_i}}{\sum_i t^2_{3i}v_i^2}\frac{g'}{g_1}\left(\frac{m_Z}{m_{Z'}}\right)^2, \tag{77}$$

where t_{3i} is the third component of weak isospin of Φ_i, g' and $g_1(\sim 0.743)$ are the Z' and Z coupling strength constants, respectively and $m_{Z'}$ and m_Z its corresponding masses.

$$\begin{aligned}\theta_{Z-Z'} &= -2\left(x - z + \frac{v_1^2(y-x)}{v_{SM}^2}\right)\frac{1}{g_1}\left(\frac{m_Z}{m_{Z'}}\right)^2 \\ &= -2\left(y - z + \frac{v_2^2(x-y)}{v_{SM}^2}\right)\frac{1}{g_1}\left(\frac{m_Z}{m_{Z'}}\right)^2 \sim -\frac{2x}{g_1}\left(\frac{m_Z}{m_{Z'}}\right)^2,\end{aligned} \tag{78}$$

In the last step, we use the approximation $v_{\rm SM} \gtrsim v_2^2 \gg v_1^2$ and $x \gg z$. By imposing the condition $|\theta_{Z-Z'}| < 10^{-3}$ which, roughly speaking, is the upper limit of the $\theta_{Z-Z'}$ mixing for the leptophobic model in reference [61]. We impose this bound for our model since the couplings to the leptons are proportional to the coupling z, which, by collider constraints is less than 10^{-2} for Z' masses below 2 TeV where the $Z-Z'$ mixing constraints are strong. Under these considerations we obtain $\frac{2\,|\,x\,|}{g_1}\left(\frac{m_Z}{m_{Z'}}\right)^2 < 10^{-3}$, which is an almost model-independent result [61]. This is equivalent to

$$|x| < \left(\frac{m_{Z'}}{4.68\ \text{TeV}}\right)^2. \tag{79}$$

These constraints are very restrictive for Z' masses below 2 TeV as shown in figure 1.

ORCID iDs

Richard H Benavides https://orcid.org/0000-0003-2860-1572
Yithsbey Giraldo https://orcid.org/0000-0002-5348-8033
Eduardo Rojas https://orcid.org/0000-0002-7412-1345

References

[1] Donoghue J F, Golowich E and Holstein B R 2014 Dynamics of the Standard Model *Cambridge Monographs on Particle Physics, Nuclear Physics and Cosmology* 2 edn (Cambridge University Press) (https://doi.org/10.1017/CBO9780511524370)
[2] Nisati A and Sharma V 2017 *Discovery of the Higgs Boson* (World Scientific) (https://doi.org/10.1142/8595)
[3] Workman R L *et al* 2022 Review of particle physics *PTEP* **2022** 083C01
[4] Aad G *et al* 2016 Measurements of the Higgs boson production and decay rates and constraints on its couplings from a combined ATLAS and CMS analysis of the LHC pp collision data at $\sqrt{s} = 7$ and 8 TeV *J. High Energy Phys.* JHEP08(2016)045
[5] Ma E 1990 Hierarchical radiative quark and lepton mass matrices *Phys. Rev. Lett.* **64** 2866–9
[6] Langacker P 1981 Grand unified theories and proton decay *Phys. Rept.* **72** 185
[7] Dine M, Fischler W and Srednicki M 1981 A simple solution to the strong cp problem with a harmless axion *Phys. Lett.* B **104** 199–202

[8] Benavides R H, Forero D V, Muñoz L, Muñoz J M, Rico A and Tapia A 2023 Five texture zeros in the lepton sector and neutrino oscillations at DUNE *Phys. Rev.* D **107** 036008
[9] Alonso R, Gavela M B, Isidori G and Maiani L 2013 Neutrino mixing and masses from a minimum principle *J. High Energy Phys.* JHEP11(2013)187
[10] Mohapatra R N and Smirnov A Y 2006 Neutrino mass and new physics *Ann. Rev. Nucl. Part. Sci.* **56** 569–628
[11] Perlmutter S 2000 Supernovae, dark energy, and the accelerating universe: The Status of the cosmological parameters *Int. J. Mod. Phys.* A **15S1** 715–39
[12] Joyce A, Jain B, Khoury J and Trodden M 2015 Beyond the cosmological standard model *Phys. Rept.* **568** 1–98
[13] Golowich E and Pal P B 1990 Charge quantization from anomalies *Phys. Rev.* D **41** 3537–40
[14] Decamp D *et al* 1989 Determination of the number of light neutrino species *Phys. Lett.* B **231** 519–29
[15] Ellis J 2012 Outstanding questions: physics beyond the standard model *Phil. Trans. R. Soc. Lond.* A **370** 818–30
[16] Capozziello S and De Laurentis M 2011 Extended theories of gravity *Phys. Rept.* **509** 167–321
[17] Abdalla E *et al* 2022 Cosmology intertwined: a review of the particle physics, astrophysics, and cosmology associated with the cosmological tensions and anomalies *JHEAp* **34** 49–211
[18] Davidson A, Koca M and Wali K C 1979 $U(1)$ as the minimal horizontal gauge symmetry *Phys. Rev. Lett.* **43** 92
[19] Marshak R E and Mohapatra R N 1980 Quark-Lepton symmetry and B–L as the $U(1)$ generator of the electroweak symmetry group *Phys. Lett.* B **91** 222–4
[20] Ma E 2002 New $U(1)$ gauge symmetry of quarks and leptons *Mod. Phys. Lett.* A **17** 535–41
[21] Barr S M and Dorsner I 2005 The origin of a peculiar extra U *Phys. Rev.* D **72** 015011
[22] Adhikari R, Erler J and Ma E 2009 Seesaw neutrino mass and new $U(1)$ gauge symmetry *Phys. Lett.* B **672** 136–40
[23] Okada N and Orikasa Y 2012 Dark matter in the classically conformal B–L model *Phys. Rev.* D **85** 115006
[24] Langacker P and Plumacher M 2000 Flavor changing effects in theories with a heavy Z' boson with family nonuniversal couplings *Phys. Rev.* D **62** 013006
[25] Langacker P 2009 The Physics of Heavy Z' Gauge Bosons *Rev. Mod. Phys.* **81** 1199–228
[26] Crispim Romao M, King S F and Leontaris G K 2018 Non-universal Z' from fluxed GUTs *Phys. Lett.* B **782** 353–61
[27] Antusch S, Hohl C, King S F and Susic V 2018 Non-universal Z′ from SO(10) GUTs with vector-like family and the origin of neutrino masses *Nucl. Phys.* B **934** 578–605
[28] Pisano F and Pleitez V 1992 An $SU(3)$ x $U(1)$ model for electroweak interactions *Phys. Rev.* D **46** 410–7
[29] Frampton P H 1992 Chiral dilepton model and the flavor question *Phys. Rev. Lett.* **69** 2889–91
[30] Pleitez V 2021 Challenges for the 3-3-1 models *5th Colombian Meeting on High Energy Physics* p 12 hep-ph 2112.10888.
[31] Benavides R H, Giraldo Y, Muñoz L, Ponce W A and Rojas E 2022 Systematic study of the $SU(3)_c \otimes SU(3)_L \otimes U(1)_X$ local gauge symmetry *J. Phys.* G **49** 105007
[32] Suarez E, Benavides R H, Giraldo Y, Ponce W A and Rojas E 2024 Alternative 3-3-1 models with exotic electric charges *J. Phys.* G **51** 035004
[33] Benavides R, Muñoz L A, Ponce W A, Rodríguez O and Rojas E 2017 Minimal nonuniversal electroweak extensions of the standard model: A chiral multiparameter solution *Phys. Rev.* D **95** 115018
[34] Tang Y and Wu Y-L 2018 Flavor non-universal gauge interactions and anomalies in B-meson decays *Chin. Phys.* C **42** 033104
[35] Maji P, Nayek P and Sahoo S 2019 Implication of family non-universal Z' model to rare exclusive $b \to s(l\bar{l}, \nu\bar{\nu})$ transitions *PTEP* **2019** 033B06
[36] Garcìa-Duque C H, Muñoz J H, Quintero N and Rojas E 2021 Extra gauge bosons and lepton flavor universality violation in Υ and B meson decays *Phys. Rev.* D **103** 073003
[37] Athron P, Martinez R and Sierra C 2024 B meson anomalies and large $B^+ \to K^+ \nu\bar{\nu}$ in non-universal $U(1)'$ models. *J. High Energy Phys.* JHEP02(2024)121
[38] Kumar Alok A, Dighe A, Gangal S and Kumar J 2021 The role of non-universal Z couplings in explaining the Vus anomaly *Nucl. Phys.* B **971** 115538

[39] Alvarado J S, Mantilla S F, Martinez R, Ochoa F and Sierra C 2023 Gauged nonuniversal U(1)X model to study muon g-2 and B meson anomalies *Phys. Rev.* D **108** 095040
[40] Frank M, Hiçyilmaz Y, Mondal S, Özdal Özer and Ün C S 2021 Electron and muon magnetic moments and implications for dark matter and model characterisation in non-universal U(1)' supersymmetric models *J. High Energy Phys.* JHEP10(2021)063
[41] Greljo A, Stangl P, Eller Thomsen A and Zupan J 2022 On (g-2)$_\mu$ from gauged U(1)$_X$ *J. High Energy Phys.* JHEP07(2022)098
[42] Alok A K, Chundawat N R S and Kumar D 2022 Impact of $b \to s\ell\ell$ anomalies on rare charm decays in non-universal Z' models *Eur. Phys. J.* C **82** 30
[43] Aram Hayrapetyan et al. 2024 Search for a neutral gauge boson with nonuniversal fermion couplings in vector boson fusion processes in proton-proton collisions at $\sqrt{s} = 13$ TeV. 12 2024.
[44] Salvioni E, Strumia A, Villadoro G and Zwirner F 2010 Non-universal minimal Z' models: present bounds and early LHC reach *J. High Energy Phys.* JHEP03(2010)010
[45] Branco G C, Emmanuel-Costa D and Gonzalez Felipe R 2000 Texture zeros and weak basis transformations *Phys. Lett.* B **477** 147–55
[46] Gupta M and Ahuja G 2012 Flavor mixings and textures of the fermion mass matrices *Int. J. Mod. Phys.* A **27** 1230033
[47] Verma R 2013 Minimal weak basis textures and quark mixing data *J. Phys.* G **40** 125003
[48] Sharma S, Fakay P, Ahuja G and Gupta M 2015 Finding a unique texture for quark mass matrices *Phys. Rev.* D **91** 053004
[49] Emmanuel-Costa D and González Felipe R 2017 More about unphysical zeroes in quark mass matrices *Phys. Lett.* B **764** 150–6
[50] Benavides R H, Giraldo Y, Muñoz L, Ponce W A and Rojas E 2020 Five texture zeros for dirac neutrino mass matrices *J. Phys.* G **47** 115002
[51] Navas S *et al* 2024 Review of particle physics *Phys. Rev.* D **110** 030001
[52] Atwood D, Reina L and Soni A 1997 Phenomenology of two Higgs doublet models with flavor changing neutral currents *Phys. Rev.* D **55** 3156–76
[53] Aoki M, Kanemura S, Tsumura K and Yagyu K 2009 Models of Yukawa interaction in the two Higgs doublet model, and their collider phenomenology *Phys. Rev.* D **80** 015017
[54] Glashow S L and Weinberg S 1977 Natural conservation laws for neutral currents *Phys. Rev.* D **15** 1958
[55] Erler J, Langacker P, Munir S and Rojas E 2011 Z' Bosons at Colliders: a Bayesian Viewpoint *J. High Energy Phys.* JHEP11(2011)076
[56] Salazar C, Benavides R H, Ponce W A and Rojas E 2015 LHC Constraints on 3-3-1 Models *J. High Energy Phys.* JHEP07(2015)096
[57] Rojas E and Erler J 2015 Alternative Z′ bosons in E_6 *J. High Energy Phys.* JHEP10(2015)063
[58] Benavides R H, Muñoz L, Ponce W A, Rodrìguez O and Rojas E 2018 Electroweak couplings and LHC constraints on alternative Z′ models in E_6 *Int. J. Mod. Phys.* A **33** 1850206
[59] Aad G *et al* 2019 Search for high-mass dilepton resonances using 139 fb^{-1} of pp collision data collected at $\sqrt{s}$=13 TeV with the ATLAS detector *Phys. Lett.* B **796** 68–87
[60] Aaboud M *et al* 2018 Search for additional heavy neutral Higgs and gauge bosons in the ditau final state produced in 36 fb^{-1} of pp collisions at $\sqrt{s} = 13$ TeV with the ATLAS detector *J. High Energy Phys.* JHEP01(2018)055
[61] Erler J, Langacker P, Munir S and Rojas E 2009 Improved constraints on Z-prime Bosons from electroweak precision data *J. High Energy Phys.* JHEP08(2009)017
[62] Leike A 1994 Model independent Z' constraints at future e^+e^- colliders *Z. Phys.* C **62** 265–70
[63] Erler J 1999 Global fits to electroweak data using GAPP *Physics at Run II: QCD and Weak Boson Physics Workshop: 2nd General Meeting* p 6
[64] Sirunyan A M *et al* 2019 Search for a standard model-like Higgs boson in the mass range between 70 and 110 GeV in the diphoton final state in proton–proton collisions at $\sqrt{s}$= 8 and 13 TeV *Phys. Lett.* B **793** 320–47
[65] Aad G *et al* 2023 Search for a light charged Higgs boson in $t \to H^{\pm}b$ decays, with $H^{\pm} \to cb$, in the lepton+jets final state in proton–proton collisions at $\sqrt{s} = 13$ TeV with the ATLAS detector *J. High Energy Phys.* JHEP09(2023)004
[66] Arhrib A, Krab M and Semlali S 2024 Accommodating the LHC charged Higgs boson excess at 130 GeV in the general two-Higgs doublet model *J. Phys.* G **51** 115003

[67] Crivellin A, Fang Y, Fischer O, Bhattacharya S, Kumar M, Malwa E, Mellado B, Rapheeha N, Ruan X and Sha Q 2023 Accumulating evidence for the associated production of a new Higgs boson at the LHC *Phys. Rev.* D **108** 115031
[68] Banik S, Crivellin A, Iguro S and Kitahara T 2023 Asymmetric di-Higgs signals of the next-to-minimal 2HDM with a $U(1)$ symmetry *Phys. Rev.* D **108** 075011
[69] Sirunyan A M *et al* 2017 Measurements of properties of the Higgs boson decaying into the four-lepton final state in pp collisions at $\sqrt{s} = 13$ TeV *J. High Energy Phys.* JHEP11(2017)047
[70] Armen Tumasyan *et al.* 2024 Search for a new resonance decaying into two spin-0 bosons in a final state with two photons and two bottom quarks in proton-proton collisions at $\sqrt{\mathrm{s}} = 13$ TeV. *J. High Energy Phys.* JHEP05(2024)316
[71] Crivellin A and Mellado B 2024 Anomalies in particle physics and their implications for physics beyond the standard model *Nat. Rev. Phys.* **6** 294–309
[72] Aad G *et al* 2024 Search for a resonance decaying into a scalar particle and a Higgs boson in the final state with two bottom quarks and two photons in proton–proton collisions at $\sqrt{s} = 13$ TeV with the ATLAS detector *J. High Energy Phys.* JHEP11(2024)047
[73] Ponce W A, Giraldo Y and Sanchez L A 2003 Minimal scalar sector of 3-3-1 models without exotic electric charges *Phys. Rev.* D **67** 075001
[74] Georgi H and Nanopoulos D V 1979 Suppression of flavor changing effects from neutral spinless meson exchange in gauge theories *Phys. Lett.* B **82** 95–6
[75] Langacker P and Luo M 1992 Constraints on additional Z bosons *Phys. Rev.* D **45** 278–92